



National Library
of Canada

Bibliothèque nationale
du Canada

Canadian Theses Service

Service des thèses canadiennes

Ottawa, Canada
K1A 0N4

NOTICE

The quality of this microform is heavily dependent upon the quality of the original thesis submitted for microfilming. Every effort has been made to ensure the highest quality of reproduction possible.

If pages are missing, contact the university which granted the degree.

Some pages may have indistinct print especially if the original pages were typed with a poor typewriter ribbon or if the university sent us an inferior photocopy.

Reproduction in full or in part of this microform is governed by the Canadian Copyright Act, R.S.C. 1970, c. C-30, and subsequent amendments.

AVIS

La qualité de cette microforme dépend grandement de la qualité de la thèse soumise au microfilmage. Nous avons tout fait pour assurer une qualité supérieure de reproduction.

S'il manque des pages, veuillez communiquer avec l'université qui a conféré le grade.

La qualité d'impression de certaines pages peut laisser à désirer, surtout si les pages originales ont été dactylographiées à l'aide d'un ruban usé ou si l'université nous a fait parvenir une photocopie de qualité inférieure.

La reproduction, même partielle, de cette microforme est soumise à la Loi canadienne sur le droit d'auteur, SRC 1970, c. C-30, et ses amendements subséquents.

UNIVERSITY OF ALBERTA

**A NEW SET OF CODES AND CORRELATION SCHEME
FOR FIBRE-OPTIC CODE DIVISION MULTIPLE ACCESS**

BY



ASHUTOSH PANDE

A THESIS

SUBMITTED TO THE FACULTY OF GRADUATE STUDIES AND RESEARCH
IN PARTIAL FULFILMENT OF THE REQUIREMENTS FOR THE DEGREE OF
MASTER OF SCIENCE.

DEPARTMENT OF ELECTRICAL ENGINEERING

EDMONTON , ALBERTA

CANADA

SPRING 1991



National Library
of Canada

Bibliothèque nationale
du Canada

Canadian Theses Service Service des thèses canadiennes

Ottawa, Canada
K1A 0N4

The author has granted an irrevocable non-exclusive licence allowing the National Library of Canada to reproduce, loan, distribute or sell copies of his/her thesis by any means and in any form or format, making this thesis available to interested persons.

The author retains ownership of the copyright in his/her thesis. Neither the thesis nor substantial extracts from it may be printed or otherwise reproduced without his/her permission.

L'auteur a accordé une licence irrévocable et non exclusive permettant à la Bibliothèque nationale du Canada de reproduire, prêter, distribuer ou vendre des copies de sa thèse de quelque manière et sous quelque forme que ce soit pour mettre des exemplaires de cette thèse à la disposition des personnes intéressées.

L'auteur conserve la propriété du droit d'auteur qui protège sa thèse. Ni la thèse ni des extraits substantiels de celle-ci ne doivent être imprimés ou autrement reproduits sans son autorisation.

ISBN 0-315-66714-1

Canada

UNIVERSITY OF ALBERTA

RELEASE FORM

NAME OF AUTHOR : **ASHUTOSH PANDE**

TITLE OF THESIS : **A NEW SET OF CODES AND CORRELATION
SCHEME FOR FIBRE-OPTIC CODE DIVISION
MULTIPLE ACCESS**

DEGREE : **MASTER OF SCIENCE**

YEAR THIS DEGREE GRANTED : **SPRING 1991**

Permission is hereby granted to THE UNIVERSITY OF ALBERTA LIBRARY to reproduce single copies of this thesis and to lend or sell such copies for private, scholarly or scientific purposes only.

The author reserves other publication rights, and neither the thesis nor extensive extracts from it may be printed or otherwise reproduced without the author's written permission.



(Ashutosh Pande)

5 / 609 Malla Gorakhpur
Haldwani.
Dist : Naini Tal, U.P.
INDIA. 263139

Date : Dec 05 90

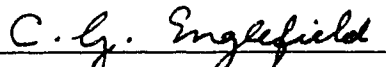
THE UNIVERSITY OF ALBERTA

FACULTY OF GRADUATE STUDIES AND RESEARCH

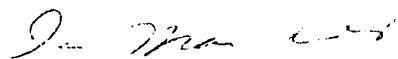
The undersigned certify that they have read, and recommend to the Faculty of Graduate Studies and Research for acceptance, a thesis entitled **A NEW SET OF CODES AND CORRELATION SCHEME FOR FIBRE-OPTIC CODE DIVISION MULTIPLE ACCESS** submitted by **Ashutosh Pande** in partial fulfillment of the requirements for the degree of **Master of Science**.



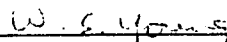
Dr. P. A. Goud, Co-Supervisor



Dr. C. G. Englefield, Co-Supervisor



Dr. R. I. MacDonald, Internal Examiner



Dr. W. S. Young, External Examiner

Date : 90 10 02

***To my parents, brother and sister,
For their love, support, and encouragement over the years.***

ABSTRACT

This thesis presents a multiple access technique, Fibre Optic Code Division Multiple Access (FO-CDMA), intended for high speed transmission on optical fibre local area networks. Present optical systems are of the intensity modulated direct detection type. Most codes for CDMA that have been developed are for electrical systems. Because optical power must always be positive, optical detectors can give only a unipolar output. These codes, therefore, are not optimum for use in optical networks.

In order to obtain bipolar signals at the receiver, an optical correlator using an optical switch is proposed, which will allow high speed signal processing. Based on this correlation method, several codes used for CDMA have been reviewed and a new set of codes, P-codes, has been generated. A mathematical equation for the generation of these codes has also been derived. The system capacity and the Bit Error Rate (BER) caused by interference from other signals, have been calculated. The results obtained from computer simulations indicate that a CDMA network, using n chip/bit P-codes and complementary correlation, can support n simultaneous users with a BER $< 10^{-9}$, provided dynamic detection is used.

An experimental system at a chip rate of 49.44 Mb/s and supporting 2 users was constructed. This system used an electronic correlator, thus limiting the channel bit rate; if an optical switch had been available, a much higher bit rate would have been possible. The system consisted of two transmitting stations, a 2x2 3 dB coupler, 1.5 km of single-mode fibre and a receiver. BER measurements performed on the system show that there was a 1.8 to 2.5 dB power penalty when the number of users was doubled. It was also observed

that, when dynamic detection was used, this power penalty was reduced to approximately 0.3 dB.

ACKNOWLEDGEMENT

I would like to express sincere thanks to my supervisors, Drs. P. A. Goud and C. G. Englefield, for their capable supervision, unwavering support, and their patience and encouragement throughout the completion of this project. I would also like to thank Dr. Jim McMullin for allowing me to set up the experimental system on his optical table.

It is my pleasure to thank Mr. Darrell Barabash for technical discussions and thanks are also due to the staff at the Alberta Telecommunications Research Centre, who have provided a pleasant working environment. In particular, I would like to acknowledge my colleagues, Mr. Russell Morris and Mr. Niranjan Vethanayagam, for helpful discussions and excellent suggestions.

For financial assistance, I express my gratitude to the Alberta Telecommunications Research Centre for their Graduate Scholarship, the Department of Electrical Engineering for the award of their Research and Teaching Assistantship and the University of Alberta for their Walter H. John's Graduate Award.

My appreciation is due to Dr. R. D. Mehta and his family, who have made Edmonton "home" to me for many years. I wish to thank my parents, my brother and sister, my teachers and friends, whose love and help have made it possible to complete this work in confidence and good spirit.

TABLE OF CONTENTS

1.	INTRODUCTION	1
1.1	Optical fibre communication systems.....	2
1.2	Types of coding.....	4
1.2.1	Source coding.....	4
1.2.2.	Error coding	5
1.2.3	Encryption	6
1.2.4	Spread spectrum modulation.....	6
1.3	Multiple user access techniques.....	7
1.3.1	Multiple access by time division.....	9
1.3.2	Multiple access by frequency division	9
1.3.3	Multiple access by code division	10
1.4	Spread spectrum modulation and CDMA.....	10
1.4.1	Code division multiple access.....	11
1.5	Advantages and disadvantages of CDMA over TDMA, FDMA and WDM.....	16
1.5.1	Advantages	16
1.6	Electrical and optical signal processing of codes.....	18
1.7	Network configuration for LANs	21
1.8	Thesis objectives and organization.....	22
1.8.1	Objectives.....	23
1.8.2	Organization of the thesis.....	25
2.	FIBRE OPTIC CODE DIVISION MULTIPLE ACCESS (FO-CDMA).....	27
2.1	FO-CDMA coding and decoding.....	27
2.1.1	Auto-correlation and cross-correlation	28
2.1.2	Desirability of optical processing.....	29
2.2	New method of correlation in optical fibre CDMA.....	30
2.3	Possible codes for FO-CDMA.....	32
2.3.1	M-sequence codes.....	34
2.3.2	Multilevel codes	35
2.3.3	Gold codes.....	36
2.4	New set of codes for FO-CDMA (P-codes).....	37
2.4.1	P-codes.....	38
2.4.2	Processing of P-codes.....	38
2.4.3	Generation of P-codes.....	40

3.	COMPUTER SIMULATION OF FO-CDMA USING P-CODES.....	45
3.1	Synchronous and asynchronous transmission.....	45
3.1.1	Synchronous transmission	45
3.1.2	Asynchronous transmission.....	46
3.2	Performance analysis of Gold codes	47
3.3.	Simulation results for P-codes	52
3.4	Calculation of system performance for P-codes.	56
3.4.1	Evaluation of the pdf for the interfering signal.....	61
3.4.2	Probability of error	69
4.	EXPERIMENTAL SYSTEM.....	73
4.1	Introduction	73
4.2	Transmitter	76
4.2.1	Clock generator.....	76
4.2.2.	Code generator.....	77
4.2.3.	Encoder	84
4.2.4	Laser driver and modulator circuit.....	86
4.3	Optical fibre couplers, links, attenuators and connections.....	91
4.3.1	Optical couplers, fibres and attenuators.....	91
4.3.2	Fibre connections	93
4.4	Receiver.....	94
4.4.1	Optical detector and preamplifier.....	95
4.4.2	Main Amplifier.....	95
4.4.3	Local code generator.....	95
4.4.4	Correlator and the integrate and dump filter.....	98
4.4.5	Comparator and decision circuit.....	102
4.4.6	Error detector	102
5.	EXPERIMENTAL RESULTS.....	105
5.1	System performance.....	105
5.1.1	Code generator.....	105
5.1.2	Encoder.....	108
5.1.3	Laser drive circuit.....	109
5.1.4	Detector output.....	110
5.1.5	Local code generator.....	111
5.1.6	Decoder correlator.....	112

5.1.7	Decoder decision unit.....	114
5.2	Bit error rate measurements	117
5.2.1	BER variation with the number of simultaneous users.	118
5.3	Power Spectra.....	120
6.	DISCUSSION AND CONCLUSION.....	124
	BIBLIOGRAPHY	129
	APPENDIX A ASYNCHRONOUS CORRELATION OF GOLD CODES.....	135
	APPENDIX B PROGRAM TO CALCULATE AUTO-CORRELATION.....	138
	APPENDIX C PROGRAM TO CALCULATE CROSS-CORRELATION.....	141
	APPENDIX D PROGRAM TO CALCULATE AUTO-CORRELATION FOR AN ASYNCHRONOUS TRANSMISSION MODE.....	144
	APPENDIX E PROGRAM TO CALCULATE THE CORRELATOR OUTPUT FOR ANY NUMBER OF USERS	146
	APPENDIX F PROGRAM TO FIND THE ORDER OF A SEQUENCE.....	149
	APPENDIX G CALIBRATION CURVES FOR THE LASER DIODES AND THE THERMISTOR, AND THE DATA SHEET FOR THE PHOTODIODE MODULE.....	151

LIST OF FIGURES

Fig. 1.1	Model of an optical fibre communication system.....	3
Fig. 1.2	Functional block of a communication link	5
Fig. 1.3	Various spreading techniques	12
Fig. 1.4	A typical spread spectrum communication system.....	13
Fig. 1.5	Illustration of code division multiple access.....	14
Fig. 1.6	Encoding of data bit with spreading sequence.....	14
Fig. 1.7	Illustration of auto- and cross-correlation of binary code sequences.....	15
Fig. 1.8	Network topologies.....	22
Fig. 2.1	Schematic of the proposed new correlation scheme.....	31
Fig. 2.2	(a) Linear code generator using p-ary shift register (b) Nonlinear code generator using p-ary shift register.....	33
Fig. 2.3	Autocorrelation trace of a maximal linear code.....	35
Fig. 2.4	Gold code sequence generator configuration.....	37
Fig. 2.5	[5,3] and [5,4,3,2] preferred m-sequence generators.....	41
Fig. 2.6	Schematic of a P-code generator.....	42
Fig. 3.1	Synchronous data slot transmission.....	46
Fig. 3.2	Asynchronous data slot transmission.	47
Fig. 3.3	Illustration of chip and ideal chip asynchronous.....	47
Fig. 3.4	General format of the cross-correlation output for Gold codes.....	49
Fig. 3.5	Outputs for the auto- and cross-correlation of code sequence 28 and 12.	50
Fig. 3.6	Upper and lower bound on the threshold of the received signal for Type-1 receive, with and without the Group-1 receiver code present.....	53
Fig. 3.7	Upper and lower bound on the threshold of the received signal for Type-2 receive, with and without the Group-2 receiver code present.....	54
Fig. 3.8	Upper and lower bounds for the channel power with increasing users.....	55
Fig. 3.9	Probability density function for the interference caused by varying number of users on a type 1 receiver.....	68

Fig. 3.10	Probability density function for the interference caused by varying number of users on a type 2 receiver	69
Fig. 3.11	Variation of the probability of error with the detection threshold for varying number of users.	70
Fig. 3.12	Variation of the bit error rate with the detection threshold for varying number of users.....	72
Fig. 4.1	Experimental layout of the FO-CDMA system.	74
Fig. 4.2	Block diagram of the code generator.....	77
Fig. 4.3	Schematic of the code generator.....	88
Fig. 4.4	Circuit schematic for the counter.....	80
Fig. 4.5	Cyclic shifting of codes	80
Fig. 4.6	Illustration of the 0 th , i = 24 th and the data clock.....	81
Fig. 4.7	Illustration of the dumped clock.....	82
Fig. 4.8	Block diagram of the code B generator	83
Fig. 4.9	Circuit schematic for the transmitter P-code generator.....	84
Fig. 4.10	Circuit diagram of the encoder.....	85
Fig. 4.11	Illustration of a '1010' coded data sequence and the reset pulse.....	86
Fig. 4.12	Laser diode modulation circuit for transmitter #1	88
Fig. 4.13	Laser diode modulation circuit for transmitter #2.....	88
Fig. 4.14	Widlar current mirror circuit.....	89
Fig. 4.15	Laser diode temperature control circuit.....	91
Fig. 4.16	Location of the fibre-to-fibre connections made in the experimental system	94
Fig. 4.17	Block diagram of the receiver section.....	94
Fig. 4.18	Circuit for the receiver local code generator.....	97
Fig. 4.19	A 32 bit P-code sequence generator using four 8 bit.....	98
Fig. 4.20	Circuit diagram of the electronic correlator.....	99
Fig. 4.21	Schematic of the comparator and hold circuit.....	103
Fig. 5.1	Illustration of the 32 nd pulse, the i = 24 th pulse and the data clock	106
Fig. 5.2	Illustration of the dumped clock obtained at the output of the P-code generator	106

Fig. 5.3	Illustration of the P-code sequence, the data clock and the i^{th} pulse	107
Fig. 5.4	P-code sequences for transmitter #1 and #2.....	107
Fig. 5.5	A NRZ '1010' data sequences and the coded data.....	108
Fig. 5.6	Encoded output for a $2^{15}-1$ PRBS data signal.....	109
Fig. 5.7	Modulating signal at the laser driver for Tx #1	109
Fig. 5.8	Modulating signal at the laser driver for Tx #2	110
Fig. 5.9	NRZ '11011110' sequence received at the output of the amplifier with only one transmitter 'ON'	111
Fig. 5.10	Illustration of the signal received at the output of the amplifier with both transmitters 'ON'; one transmitter sent a '1111' word while the other transmitted a 9 bit word pattern.....	112
Fig. 5.11	Illustration of the P-code generated at the transmitter	112
Fig. 5.12	Illustration of the received '1111' NRZ data and the local P-code sequence.....	114
Fig. 5.13	Cross-correlated output for the signals in Fig. 5.12.....	114
Fig. 5.14	Integrated and dumped waveform for a 15 bit word.....	115
Fig. 5.15	Eye pattern obtained for a 9 bit PRBS	116
Fig. 5.16	Regenerated output for cross-correlation (at low power).....	117
Fig. 5.17	Regenerated output for cross-correlation (at high power)	117
Fig. 5.18	BER measurements for P-codes for the following cases.....	119
Fig. 5.19	Variation of BER with the power of the jamming transmitter.....	120
Fig. 5.20	Spectra of the 1.544 Mb/s PRBS transmitted data	121
Fig. 5.21	Spectrum of the 49.408 Mb/s $2^{15}-1$ PRBS coded data	121
Fig. 5.22	Spectrum of the data at the output of the amplifier.....	122
Fig. 5.23	Spectrum of the data at the output of the correlator	123
Fig. 5.24	Spectrum of the data at the output of the decision circuit.....	123
Fig. F.1	Laser output power characteristics, as a function of the bias current for NORTHERN TELECOM PBH-4317-32 LD	151
Fig. F.2	Laser output power characteristics, as a function of the bias current for LASER DIODE INC. 1300-09632 LD	152
Fig. F.3	Temperature vs. resistance curves obtained for the thermistor ..	153

LIST OF TABLES

Table 1.1	Properties of various coding techniques.....	8
Table 2.1	Truth table for the correlator.....	32
Table 2.2	P-code sequences generated from preferred m-sequences.....	43
Table 2.3	Properties of Group 1 and Group 2 type codes.....	44
Table 3.1	Truth table for standard optical correlation	48
Table 3.2	Group 1 and Group 2 code sequences.	54
Table F.1	Data sheet for the RCA type C30986QC-02 photodetector module.....	154

LIST OF ABBREVIATIONS

ACI	Adjacent Channel Interference
BEF	Bandwidth Expansion Factor
BER	Bit Error Rate
BW	Bandwidth
CATV	Cable Television
CDMA	Code Division Multiple Access
CSMA / CD	Carrier Sense Multiple Access / Collision Detection
dB	DeciBels
DS CDMA	Direct Sequence Code Division Multiple Access
ECL	Emitter Coupled Logic
FDMA	Frequency Division Multiple Access
FO-CDMA	Fibre-Optic Code Division Multiple Access
GHz	Giga Hertz
IC	Integrated Circuit
IM-DD	Intensity Modulated - Direct Detection
ISDN	Integrated Services Digital Network
LANs	Local Area Networks
LD	Laser Diodes
Mb/s	Megabits per second
MBd	Megabaud
MHz	Mega Hertz
NRZ	Non Return to Zero
OOK	On Off Keying
PDF	Probability Density Function
Pdf	Probability density function
PE	Probability of Error
PRBS	Pseudo-Random Bit Sequence
PSD	Power Spectral Density
RZ	Return to Zero
TDMA	Time Division Multiple Access
TTL	Transistor Transistor Logic
VMOSFET	V groove Metal Oxide Semiconductor Field Effect Transistors
WDM	Wavelength Division Multiplexing

LIST OF SYMBOLS

$\{A\}$	M-sequence generated by a [5,3] generator
$A_j^{(n)}$	j^{th} chip of the n^{th} m-sequence generated by a [5,3] generator
$\{B\}$	M-sequence generated by a [5,4,3,2] generator
$B_j^{(n)}$	j^{th} chip of the n^{th} m-sequence generated by a [5,4,3,2] generator
$b_n^{(m)}$	m^{th} data bit of the n^{th} user
$b_n(t)$	Binary data signal of the n^{th} user
$P_n(t)$	P-code for the n^{th} user
$b_l^{(n)}$	n^{th} users data sequence
$C_j^{(n)}$	j^{th} chip of the n^{th} P-code sequence
A_{C_l}	Number of combinations of l units in a group of A units
$\{c_i\}$	Local code of the receiver
F	Total length of the code sequence
G_1	Gold code sequence #1
$ I $	Uniformly distributed interference
$I_n^{(1)}$	Interference of the n^{th} user on receiver #1
I_1	Total interference at the output of receiver #1
K	Weight of the code
M	Mean of the interference of the n^{th} user on receiver #1
M_{I_1}	Mean of the total interference in receiver #1

M_{I+1}	Mean of the interference of the n^{th} user on receiver #1 when the interference is +1
M_{I-1}	Mean of the interference of the n^{th} user on receiver #1 when the interference is -1
N	Number of simultaneous users
$\overline{P_1(t)}$	Complement of the P-code for receiver #1
$P_T(t)$	Rectangular pulse of duration T
$P(A)$	Probability of 'A' group 1 users transmitting
$P_{I,A}$	Probability of an interference I being caused when A group 1 users are transmitting
$P(I_A)$	Probability of an interference I being caused by A group 1 users
$P_{I_1}(I_1)$	Probability of the interference being equal to I_1
P_{T_c}	Chip waveform of period T_c
$\Pr(x=y)$	Probability of x being equal to y
P_e	Probability of error
p	Probability of the interference being equal to +1
q	Probability of the interference being equal to 0
r	Probability of the interference being equal to -1
$r(t)$	Signal at the front end of the receiver
$S_n(t)$	n^{th} baseband signal at the O/P of the n^{th} optical encoder
S_n	n^{th} users optical intensity
$\{s_x\}$	Signal received at the correlator

T_c	Time period of a chip
T	Time period of a data bit
X	One half of the weight of the Gold code sequence
$Z_{x,x}^{(i)}$	Auto-correlation product for the sequence 'x' with the i shifted version of itself
$Z_{x,y}^{(i)}$	Cross-correlation product for the sequence 'x' with the i shifted version of the code sequence 'y'
Z_1	Output of the integrate and dump filter
$\delta(x)$	Dirac delta function
λ_a	Value of the auto-correlation sidelobe
λ_c	Value of the cross-correlation
$\sigma_{I_1}^2$	Variance of the total interference in receiver #1
σ^2	Variance of the total interference of the n^{th} user on receiver #1
$\sigma_{I_1,+1}^2$	Variance of the interference of the n^{th} user on receiver #1 when the interference is +1
$\sigma_{I_1,-1}^2$	Variance of the interference of the n^{th} user on receiver #1 when the interference is -1
Ψ	Constant of integration for the integrate and dump filter

CHAPTER 1

INTRODUCTION

Due to their high channel capacity, very low attenuation per unit length, very low volume and weight, and noise immunity to electromagnetic sources, single mode fibres are rapidly replacing co-axial cables for transporting information in telecommunication systems. Further, due to the need for a network that will enable subscribers to send and receive all forms of information including voice, video and data with the ease and flexibility of placing today's telephone call, ISDN (Integrated Services Digital Network) is evolving.

Although long haul optical fibre systems have become the dominant medium, the technology for short range high speed optical networks is struggling to become commercially competitive. Optical fibres have found acceptance in local area networks (LANs) as the physical transport medium, but conventional media access protocols such as Carrier Sense Multiple Access with Collision Detection (CSMA/CD) and ALOHA are not optimal for high speed services. These protocols are designed to handle low traffic loads and relatively low signal rates (10 MBd). When they are used at higher speeds or at higher traffic loads, the number of collisions encountered increases, requiring retransmission of an increasing percentage of the signals. This, in turn, causes an increase in the waiting time for each user. The system then becomes slow and hence this type of signalling cannot benefit from the large bandwidth available in an optical fibre channel.

Spread spectrum multiplexing techniques, which have been investigated extensively in the context of satellite and mobile communication [1] [2], offer

several potential advantages over CSMA/CD and ALOHA multiple access schemes [3], for use in LANs.

System performance for a spread spectrum multiplexing system depends on the number of simultaneous users, which may be smaller than the total number of users actually subscribing to the network. Code Division Multiple Access (CDMA), which is a spread spectrum technique, permits multiple users to access the channel simultaneously with no waiting time. Thus CDMA eliminates the time delay inherent in other access schemes (e.g. CSMA/CD), where each user waits for the channel to become idle before gaining access. As stated earlier, an increase in traffic intensity or transmission distance increases the incidence of collision between packets in CSMA/CD. This causes the waiting time to increase with CSMA/CD but has no effect on a CDMA system. Thus CDMA offers the potential for efficient use of the fibre bandwidth, with improved system performance and multi user access.

1.1 Optical fibre communication systems

Networks using optical fibres to transmit voice, video, and data, have been offered by vendors. These systems, usually available as local area networks, can improve the communication inside a high-use area such as in most office buildings, industrial facilities, university campuses, and military bases [4].

In any communication system, there are two primary communication resources: transmitted power and channel bandwidth. A general system design objective is to use these two resources as efficiently as possible. In most communication channels, one resource may be considered more important than the other. We therefore classify communication systems as being either

power limited or bandwidth limited. An optical communication system in a LAN is a power limited channel although its bandwidth may be limited by the associated electronics.

Figure 1.1 shows the block diagram of an optical fibre communication system. The optical system, like any other communication system, consists of three major parts: (1) the transmitter, (2) the communication channel, and (3) the receiver. The main purpose of the transmitter is to modify the message signal into a form suitable for transmission over the channel. This modification is achieved by means of either or both of the following processes: modulation and coding.

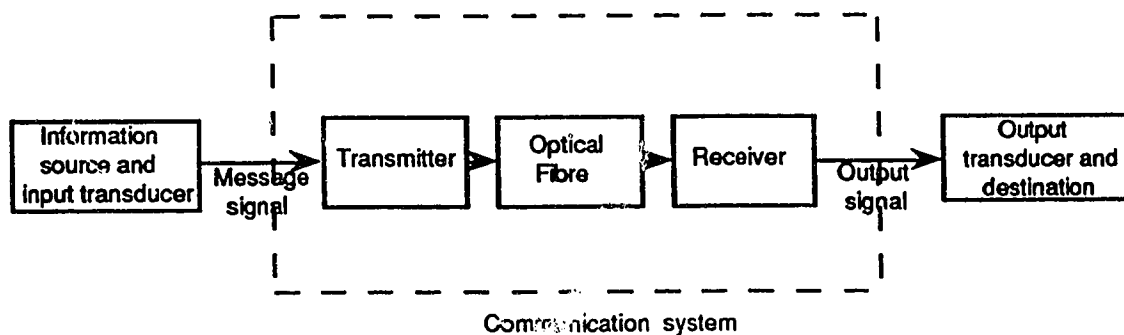


Fig. 1.1 Model of an optical fibre communication system

In propagating through the optical fibre channel, the transmitted signal is distorted due to nonlinearities and/or imperfections in the frequency response of the fibre. Other sources of degradation are noise and interference picked up by the signal during the course of transmission through the channel. Noise and distortion are the two basic problems in the design of a communication system. Usually, the transmitter and receiver are carefully designed so as to minimize the effects of noise and distortion on the quality of reception.

The main purpose of the receiver is to recreate the original message signal from the degraded version of the transmitted signal after propagation through the channel. This reproduction is accomplished by using demodulation and/or decoding, which are the reverse of the processes used in the transmitter. Due to the unavoidable presence of noise and distortion in the received signal, the receiver cannot replicate the original message signal exactly. The resulting degradation in overall system performance is influenced by the type of modulation or coding scheme used.

1.2 Types of coding

Coding is the translation of the user-provided information bits (source bits) to the transmitted data symbols (coded symbols). A communication channel can be divided into coding blocks, as shown in Figure 1.2, on the basis of their individual function. It is clear from the figure that there are four main types of coding that data may undergo before being finally transmitted. In various systems, the importance of each of the functional blocks will be different.

1.2.1 Source coding

The ever-growing demand for the transmission of data necessitates the more efficient use of existing transmission facilities. Data compression is the branch of communications that deals with the problem of representing a source of information with as few bits as possible, while preserving a certain degree of fidelity. A source coding or waveform coding system is a scheme that operates on source data to remove redundancies so that only those values essential to the reproduction of the signal are retained. Thus the overall idea is to transform the original symbol space to a symbol space that requires a minimum channel capacity. This is achieved by making the length of each symbol inversely

proportional to its relative probability of occurrence or by requiring the input data stream to have minimum entropy. Examples of such codes are the Huffman codes.

1.2.2. Error coding

The previous coding technique is used for controlling the spectrum of the transmitted signal. The objective of error coding is to trade information rate capacity for information error rejection. Error detection capability can be achieved in a system by using certain codes. The process of error coding deals with the addition to the transmitted symbols a set of symbols which do not carry information, but which are derived from the non-redundant set of symbols in such a way that they can detect and also correct errors in the information carrying symbols.

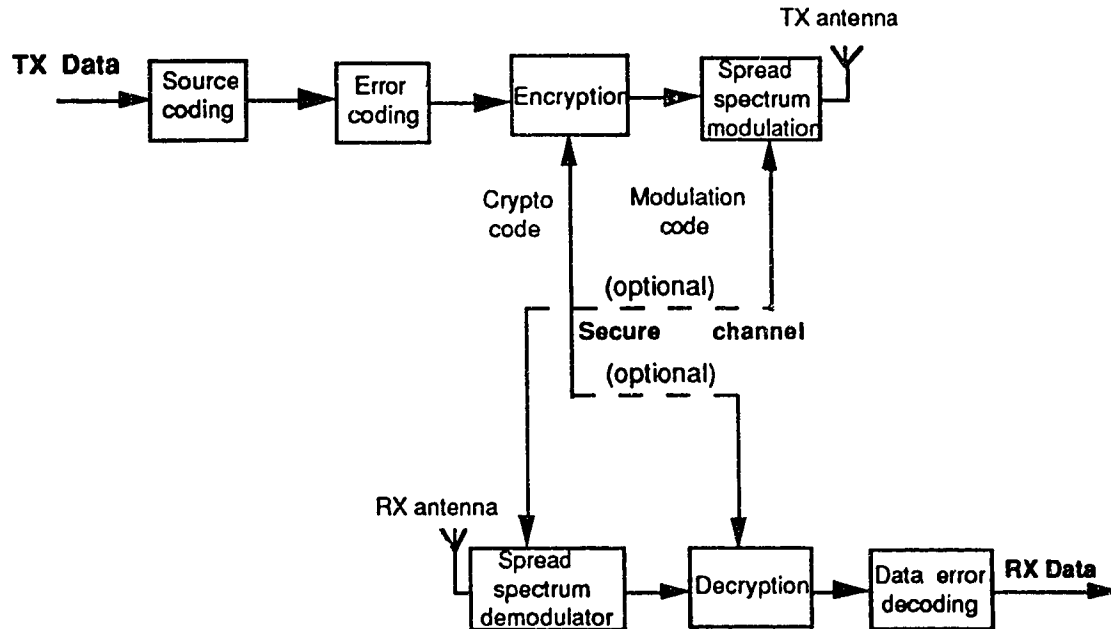


Fig. 1.2 Functional block of a communication link

Thus an error encoder (also called the channel coder) is designed specifically for one of these purposes:

- (i) *Error detection* ; to increase reliability by causing the retransmission of the blocks of data until they are correctly received.
- (ii) *Error correction* ; by using the redundancy to correct transmission errors.
- (iii) *Error prevention* ; by reducing the probability of error [5].

1.2.3 Encryption

Codes can also be used to increase the security of the channel. The objective of encryption is to deny unauthorized access to the communication channel. It is the process of converting the data stream into another data stream in such a way that the time and cost associated with the decoding of the scrambled data will be very much higher for an unauthorized receiver than for the intended receiver.

The coded stream $e(t)$ can be represented as:

$$e(t) = F[b(t)]$$

where F is the algorithm for coding and $b(t)$ is the input data stream.

1.2.4 Spread spectrum modulation

The use of all the coding techniques discussed above is appropriate on sharply bandlimited channels, or on channels with increasing crosstalk at higher frequencies.

Under certain circumstances the bandwidth required for transmission is deliberately increased. There are several reasons for doing this, including countering jamming and interference in military communications, countering intersymbol interference due to multipath distortion, and separating users

sharing a common communication medium (multiple access networks). A common technique for increasing the bandwidth is spread spectrum. A useful definition of spread spectrum is [6]:

Spread spectrum is a means of transmission in which the signal occupies a bandwidth in excess of the minimum necessary to send the information; the band spread is accomplished by means of a code that is independent of the data; synchronized reception with the same code at the receiver is used for despreading and subsequent data recovery.

Thus the requirement in spread spectrum modulation is to realize a modulator capable of generating a waveform with an information rate that is higher than that of the data flow. This is done in order to achieve a dramatic increase in transmission properties and system capability. This can be achieved by replacing a single bit stream with a coded waveform. The more complicated and well designed the code (pseudorandom code), the better and more secure will be the communication.

Table 1.1 shows the various types of coding techniques generally used and the advantages derived from them. Depending on the requirements for a particular channel and network, some or all of the schemes can be used at the same time.

1.3 Multiple user access techniques

One of the key issues that must be resolved when realizing a digital communication system network is how to provide access to a single transmission medium for two or more (typically many more) users.

Table 1.1 Properties of various coding techniques [44], *adapted*

	Source coding	Error coding	Encryption	RF modulation	Spread spectrum modulation
Data source optimization	●				
Error detection		●			
Error correction		●			
TX security unregarded channel coding			●		
Band allocation				●	●
Protection against unauthorized reception (eavesdropping)			●		●
Protection against unauthorized transmission (authentication)			●		●
Protection against interference (jamming)					●
Protection against detection of radiation					●
Data error reduction for a given spectral density power					●
Optimization to transmission medium (multipath fading)					●

This technique, in which two or more users share a common channel, is known as multiple access. Important practical applications of multiple access techniques include:

- (i) *Full Duplex data transmission on a single medium.* An important application of this is data transmission on the subscriber loop, between the central office and customer's premises, where only a single wire pair is available for both directions of transmission.
- (ii) *Multiple channels sharing a common high-speed transmission link.* By building very high speed transmission links using, for example, coaxial cable or optical fibre, and then sharing that link over many users, economies of scale are realized. The cost of the transmission link, when divided by the number of users, can be very much lower than the cost of an equivalent lower speed link. The

process of sharing many channels on a single high speed link is called multiplexing.

(iii) *To provide access between any user and any other user without a switch.*

Thus, when one user broadcasts to the other only the user for which the communication is intended pays attention. This type of *multiple access* is often exploited in local area networks within a customer's premises, and in satellite networks in the context of a wide geographical area.

All of these multiple access techniques require that the messages corresponding to different users be separated in such a fashion so that they do not interfere with one another. This is accomplished by making the messages orthogonal in space. Orthogonality of two or more signals can be achieved in several ways:

- (i) The message can be separated in *time*, insuring that the different users transmit at different times.
- (ii) The message can be separated in *frequency*, insuring that the different users use different frequency bands.
- (iii) The messages can be transmitted at the same time and at the same frequency, but made orthogonal by some other means. Usually this is done by *code division*, in which the users transmit signals which are made to be orthogonal through the use of specially designed codes.

1.3.1 Multiple access by time division.

Multiple access by time division is the most common method of separating channels. This technique has many variations, the most common of which are listed below.

- (i) Point - to - Point Link Access

- (ii) Time Division Multiple Access (TDMA)
- (iii) Time - Compression Multiplexing
- (iv) Packetizing
- (v) Packet Switching Multiple Access

1.3.2 Multiple access by frequency division

The separation of many users on a common medium in analog transmission invariably uses frequency division. Frequency division multiple access (FDMA) can also be used for digital transmission, where independent data streams are transmitted in non-overlapping frequency bands. Frequency division is very simple, in that the transmitters sharing the medium have output power spectra in non-overlapping bands.

1.3.3 Multiple access by code division

Separation of signals in time or frequency are relatively simple ways of ensuring that the signals will be orthogonal. However, code division multiple access (CDMA) is useful on channels which have other characteristics suitable for spread-spectrum, such as time varying multipath distortion or hostile jamming. Code division multiplexing is achieved by choosing 2BT, RZ, orthogonal waveforms, where each occupies a total bandwidth B and the total time T , and assigning one of the waveforms to each user to use as its isolated pulse for transmission with bit interval T . Since each isolated pulse has a bandwidth much greater than the minimum $1/2T$ required for this bit interval, in effect each user is using spread spectrum transmission.

1.4 Spread spectrum modulation and CDMA

Spread spectrum has long been used in secure military communication systems [7]. More recently, a number of commercial applications have arisen,

and the technique is sufficiently useful to be employed in power limited channels. Spread spectrum signalling enables multiplexing of a number of users for point-to-point or multi-point communication on various channels [1, 8-10].

Spread spectrum can be achieved by various techniques. These are illustrated in Figure 1.3 and are :

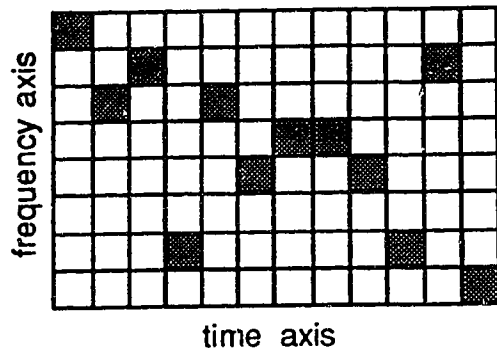
- (i) *One frequency hopper*: only one frequency slot is activated at a time and the code selects the frequency.
- (ii) *Multifrequency hopper*: a number of frequencies are activated at one time.
- (iii) *Time hopper*: only the time axis is considered and an uncertainty in the time of arrival rather than the frequency is allowed.
- (iv) *Direct sequence system (multitime hopper)*: a set of time slots can be set and thus a spread of frequency over the full frequency band is achieved.
- (v) *Generalized coding*: no restriction on the structure of the code.

The shaded areas in Figure 1.3 shows the time and frequency slots used by a particular technique. Figure 1.4 shows a communication system employing spread spectrum techniques. As can be observed from the figure the modulator, timing recovery and demodulator units are the main components in such a system.

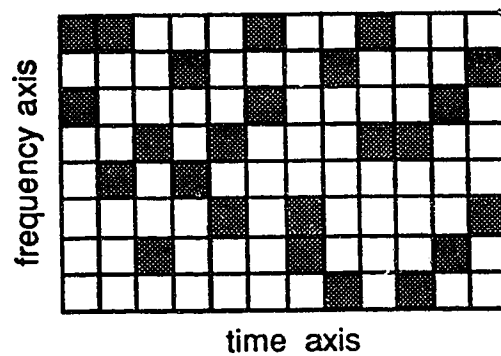
1.4.1 Code division multiple access

Code Division Multiple Access (CDMA) is a spread spectrum technique in which the transmitted data bit is coded with the spreading function of the intended receiver, as illustrated in Figure 1.5. Thus, since the receiver code is used as a spreading function, the spreading function also serves as a message

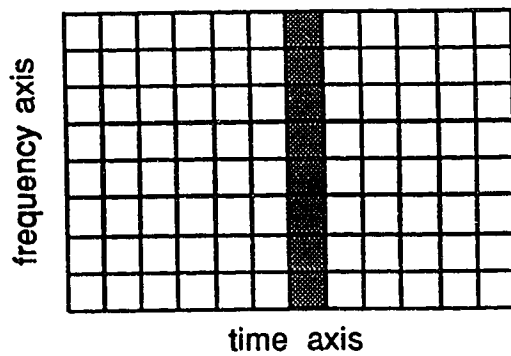
addressing function. In a CDMA system all members can communicate at the same carrier frequency, although it is not strictly necessary. Usually there is a common data rate $R_d = 1/T_d$ and a common spreading code chip rate $R_c = 1/T_c$.



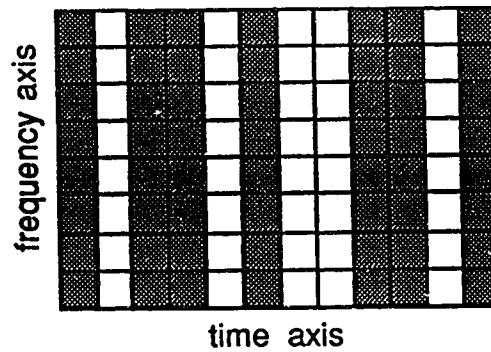
**One - frequency hopper
coding scheme**



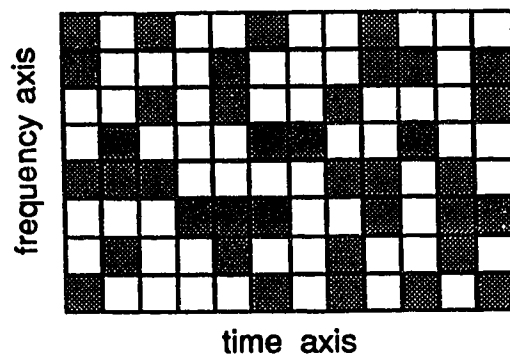
**Multifrequency hopper
(Two frequency case)**



Time hopper



Direct sequence system



Generalized coding scheme

Fig. 1.3 Various spreading techniques

The coding process is achieved by modulating the data bit with the CDMA code of the intended receiver (Figure 1.6). At the receiver, matched filters (correlators) are used to extract the individual spreading function from the message. The decoding process in a matched filter is that of correlation and integration. The receiver will at any time give an output which is proportional to the correlation of the input signal with that of the receiver local code.

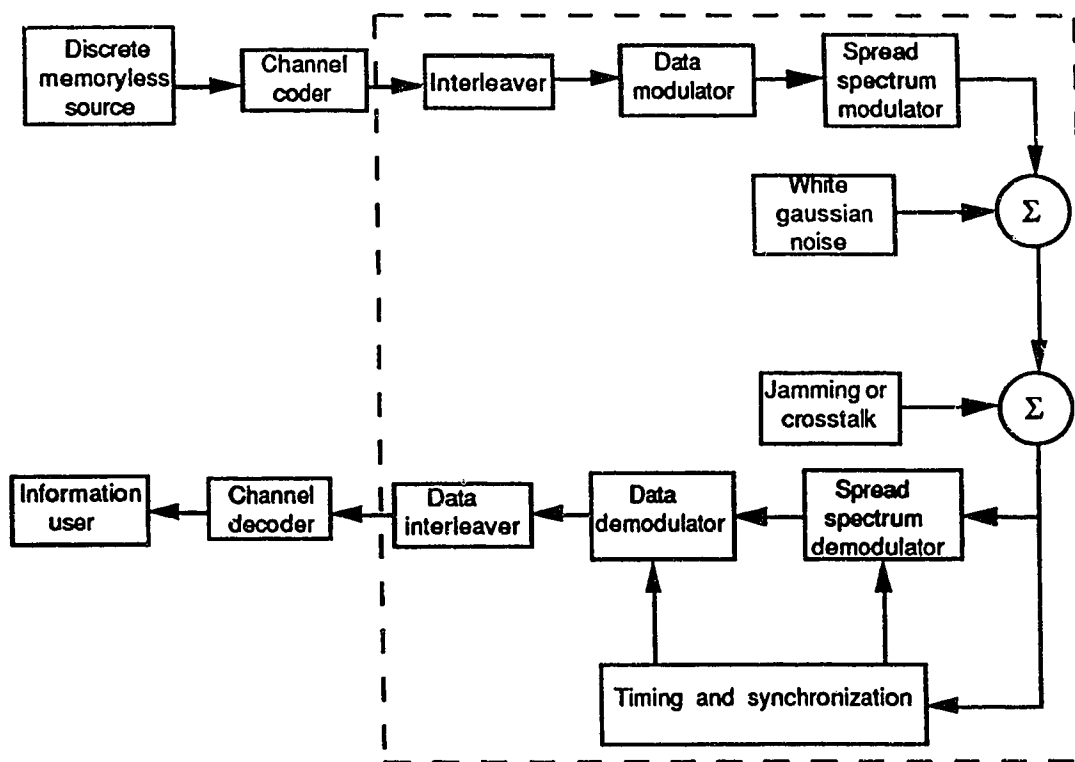


Fig. 1.4 A typical spread spectrum communication system

Figure 1.5 shows the spectra of the transmitted signal in various stages of a CDMA network. Fig. 1.5 (a) presents the spectrum of the data being transmitted in channels 1 to 5 at a different central frequency. The effect of coding on the spectrum of the data stream can be seen in spectra (b) to (f). Each shows the spread of the spectrum for channels 1 to 5. Spectrum (g) displays

channel 3 after despreading; i.e., correlation. As can be seen, the original spectrum of the data in channel 3 is regenerated.

Encoding of a data bit by the code, in a CDMA system, is achieved in two different ways. In some CDMA systems, a data bit, '1', is coded with the code sequence and a data bit, '0', is coded with the inverse of the code. In other systems, like the one used in this thesis, a data bit, '1', is coded with the code sequence and a data bit, '0', is sent as is. A data bit, '1', and a data bit after being encoded, are represented in Figure 1.6.

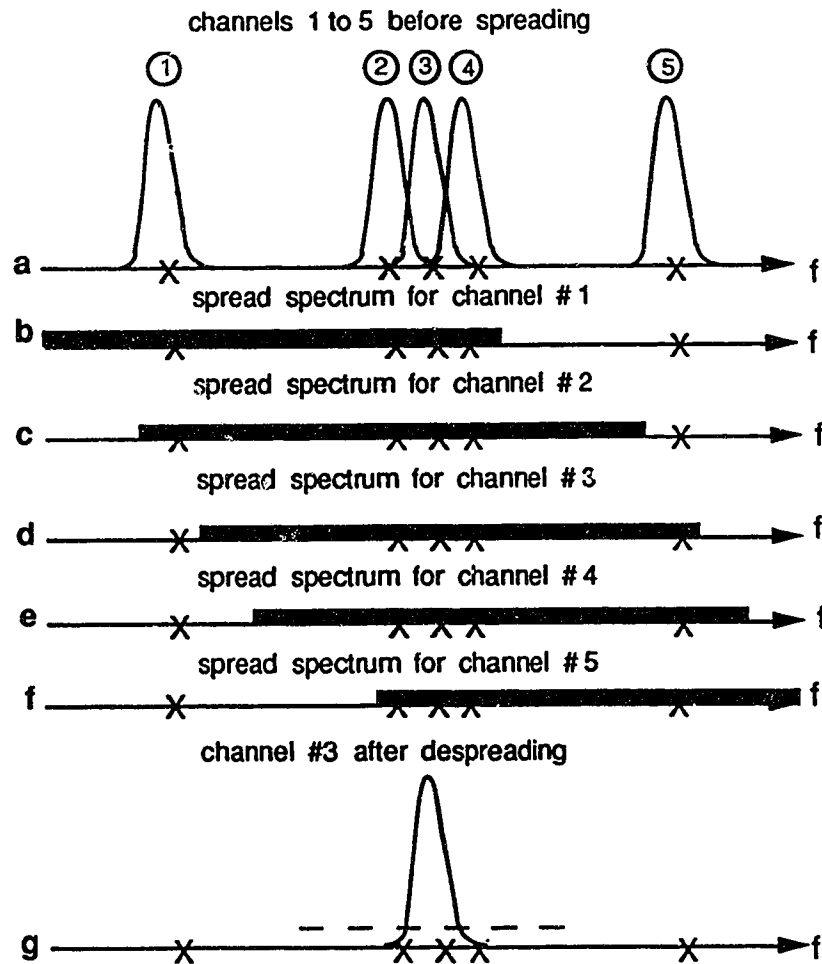


Fig. 1.5 Illustration of code division multiple access.

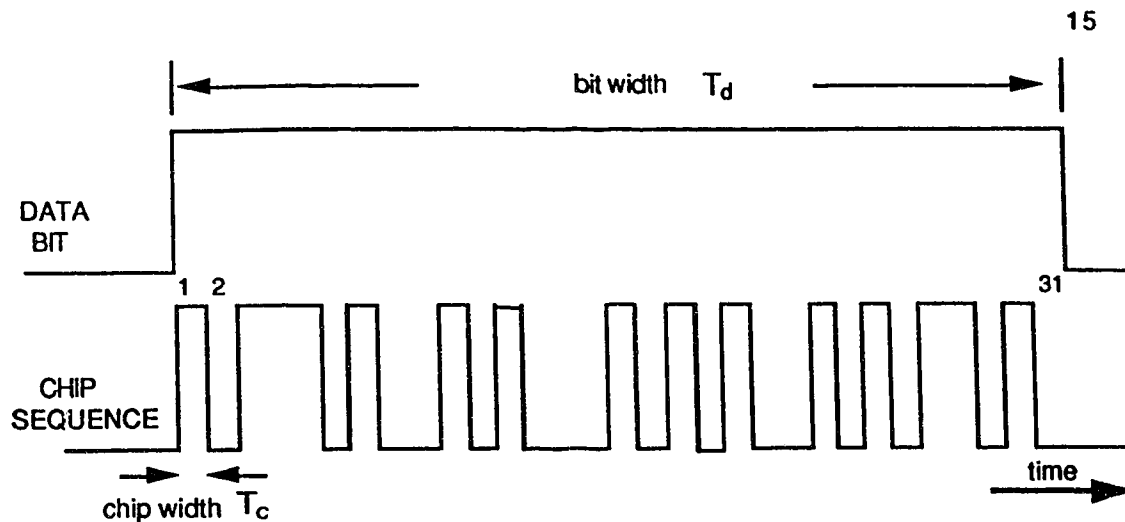


Fig. 1.6 Encoding of data bit with spreading sequence

The two main properties of interest in a CDMA communication system are its auto-correlation and cross-correlation. The correlation properties of the code sequences used in spread spectrum communication depend on the code type, length, chip rate, and even the chip by chip structure of the code being used. Auto-correlation refers to the degree of correspondence between a code and a phase shifted replica of itself. Cross-correlation on the other hand is the measure of agreement between two different codes. Figure 1.7 illustrates the difference between auto-correlation and cross-correlation.

Fibre-optic code division multiple access (FO-CDMA) is a scheme that takes advantage of excess bandwidth in single-mode fibres to map low information rate electrical or optical signals into very high rate optical pulse sequences for the purpose of achieving random communication access among many users.

FO-CDMA transmission has several advantages in an optical fibre local area network:

(1) It offers potentially high speed. The high bit rate allows for great flexibility in terms of the type of service that a station can provide.

(2) It allows each bursty user to share the entire transmission channel (this occurs quite often in local area networks) by providing asynchronous access to each user, so that it makes more efficient use of the channel.

(3) It allows new users to be easily added to the network by simply connecting them to the channel using a passive optical coupler.

(4) It provides multi-user simultaneous access to the channel with no waiting time; therefore, there is no need for the user to wait for the right frame slot (as in TDMA), or to wait until the channel is idle (as in CSMA) to gain access.

(5) Forward error correction is more effective when it is used with CDMA than when it is used with FDMA [12].

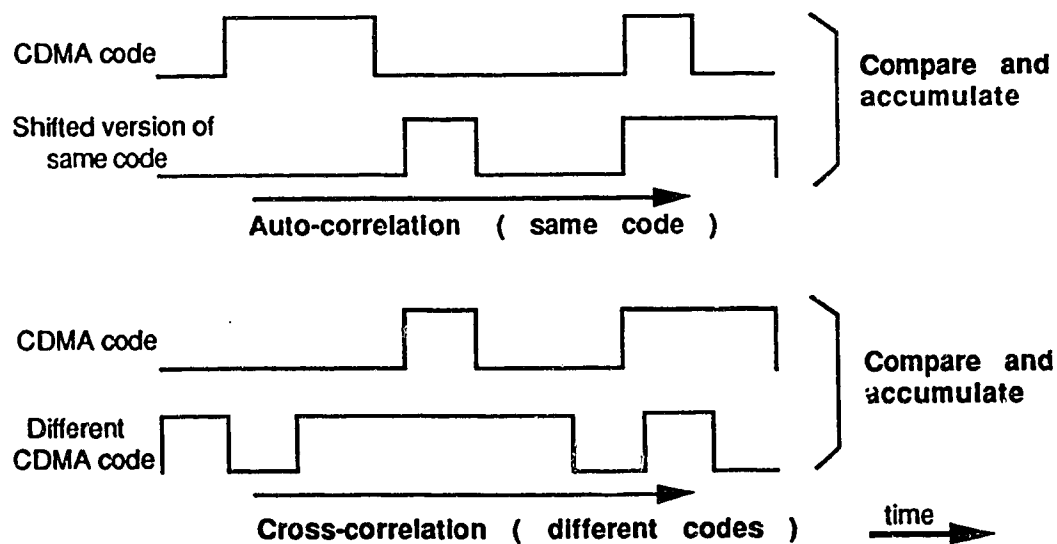


Fig. 1.7 Illustration of auto- and cross-correlation of binary code sequences

1.5 Advantages and disadvantages of CDMA over TDMA, FDMA and WDM.

Code division multiple access offers many advantages over other multi-access techniques such as TDMA, FDMA and WDM. On the other hand, CDMA has some inherent disadvantages, such that it has not been widely accepted as the sole multi-user access technique. Some of the advantages and disadvantages of CDMA are presented below.

1.5.1 Advantages of CDMA

(i) *Sharing of bandwidth* : New schemes of band allocation can be derived using CDMA techniques. Thus, code multiplexing can be utilized to stack a number of channels within the same frequency band.

(ii) *Asynchronous access to users* : CDMA provides asynchronous access to each user. In asynchronous systems the user does not have to wait for the channel to be clear before gaining access to the network. This avoids timing problems and also provides multi user access. In LANs where traffic is bursty, asynchronous multiplexing schemes are more suitable than synchronous multiplexing schemes (TDMA), which dedicate a portion of the channel to each user.

(iii) *Ideally no waiting time* : This facilitates simultaneous access to the channel to many users with no waiting time. Thus CDMA eliminates the time delay inherent in other access schemes where the user waits for the channel to become idle before gaining access.

(iv) *Waiting time not dependent on traffic intensity* : In schemes like WDM, FDM and TDM, as the traffic intensity increases, the frequency of collisions between packets increases. This causes waiting time to increase with transmission distance. This is not the case with CDMA.

(v) *Privacy*: Unauthorized listening is discouraged by making it impossible to receive the signal without knowing the code.

(vi) *No carrier drift*: Frequency division multiplexing in an optical band can be severely impaired by the supersensitivity of carrier frequency to physical perturbations. This phenomenon does not affect CDMA systems adversely. Thus CDMA systems suffer less from Adjacent Channel Interference (ACI).

1.5.2 Disadvantages of CDMA

(i) *Complexity*: The spread spectrum approach involves complexity. However, with the continuing advances in microprocessor technology, this complexity does not seem overwhelming.

(ii) *Increasing bandwidth (BW) but decreasing power spectral density (PSD)*: CDMA has a disadvantage in that it requires a large bandwidth. Thus it is not suitable for band limited systems. Fibre systems, having potentially very large bandwidth, offer the best medium for the use of CDMA in LANs.

(iii) *Limited number of users*: A major drawback of CDMA systems is that they allow a limited number of simultaneous users. The efficiency of a CDMA system, as far as supporting multiple users is concerned, is expressed by the bandwidth expansion per channel. The bandwidth expansion factor (BEF) is defined as the number of chips per bit, while the bandwidth expansion per channel is simply the ratio of the BEF to the total number of simultaneous channels supported by that code. A bandwidth expansion per channel of one defines a highly efficient system.

1.6 Electrical and optical signal processing of codes

Due to the lack of mature integrated optical components at the present time (optical amplifiers etc.), many key signal processing functions such as

regeneration, multiplexing, demultiplexing, filtering, etc. are carried out electronically. In a regenerator, for example, a stream of optical pulses must first be converted to an electrical signal for any desired signal processing, converted back to optical signals and then transported in single-mode fibre to the next destination. This process of optical to electrical and electrical to optical conversion for signal processing puts a limit on how much fibre bandwidth can be used because of the limited speed of electronic signal processing. It can be said that the bandwidth limitation in a fibre network is primarily due to the optoelectronic interfaces and electronic signal processing, rather than the capacity of the fibre.

One way to increase the signal processing speed is by using optical devices [12] [13] (e.g. optical directional couplers, single-mode fibre delay lines, etc.) for the high speed part of the signal processing. The other advantage derived by using optical devices in optical networks for the purpose of regeneration, multiplexing, filtering etc, is the reduction of the unnecessary photon-electron-photon conversion, since photons are the primary carriers of information. Due to these advantages, it is believed that optical components, once fully developed and integrated, will offer much higher speeds for optical signal processing than do their electronic counterparts. Therefore a very desirable feature of optical communication systems would be the ability to perform signal processing functions optically.

Thus, at the receiver in a Direct Sequence CDMA (DS CDMA) system, there are two basic ways to process the received signal so as to decode the received data (i.e. to despread the spectrum). These two methods are electrical and optical signal processing.

Today's systems are normally incoherent systems of the Intensity Modulated-Direct Detection (IM-DD) type, and are thus modelled as positive systems [14]. A positive system is defined as one that cannot manipulate its signals to add to zero and whose output is always greater than zero. There will be a marked difference between the properties of a code in the electrical domain and the same code (i.e. you cannot send a negative amount of power in an optical system) in the optical domain in a IM-DD system [15]. A recent paper by MacDonald [16] presents a way of overcoming this difficulty. According to this paper an effective negative signal was obtained by using an array of detector diodes, some of which contributed a positive current to the output in the normal way, and some of which were connected to subtract from the output current.

Over the past few years, several papers have described incoherent optical transmission using CDMA. Systems using electrical processing and Gold codes have been reported [17, 18, 27]. Systems using optical processing and new CDMA sequences, which were designed specifically for this kind of processing, have also been reported [19-26, 49-57]. These schemes take advantage of the large available bandwidth in single mode fibres by mapping low information rate electrical or optical signal into very high rate optical pulse sequences (signature sequences) to achieve random access communication.

In this project, CDMA using optical processing has been investigated and a new correlation scheme has been defined. Since traditional codes are not suitable for positive signal processing, a new set of codes have been developed. The advantages of using optical processing includes better system performance (faster data rate and more efficient bandwidth usage) as compared to systems using electrical processing.

1.7 Network configuration for LANs

Several definitions have been given for a local area network (LAN). The IEEE802 Committee has defined a LAN as follows: “ A Local Network is a data communication system which allows a number of independent devices to communicate with each other” [34]. Connectivity is a central concept in local area networks, meaning that any device on the LAN may be addressed by any other user or terminal as an individual connection.

There are a variety of ways in which networks might be organized, and most networks are in a constant state of change and growth. It is possible for a single communications system to provide communications for two or more concurrently operating computer networks. A few of the several characteristic network configurations are : point-to-point; multi-point; star(centralized); ring (distributed); bus structure (distributed); and hierarchical (distributed). Figure 2.9 contains diagrammatic representations of the various network configurations or topologies.

The topology that has been chosen for this project is a star network in which all the users are connected to a central node (master). Thus, a signal from any transmitter is received by all the other stations. This accounts for the drawback of such networks, in that they are power inefficient. The drawbacks arising due to the high power requirement of these networks can be overcome by having high power transmitter and/or highly sensitive receivers. The second option, of using a highly sensitive receiver, was implemented in our project.

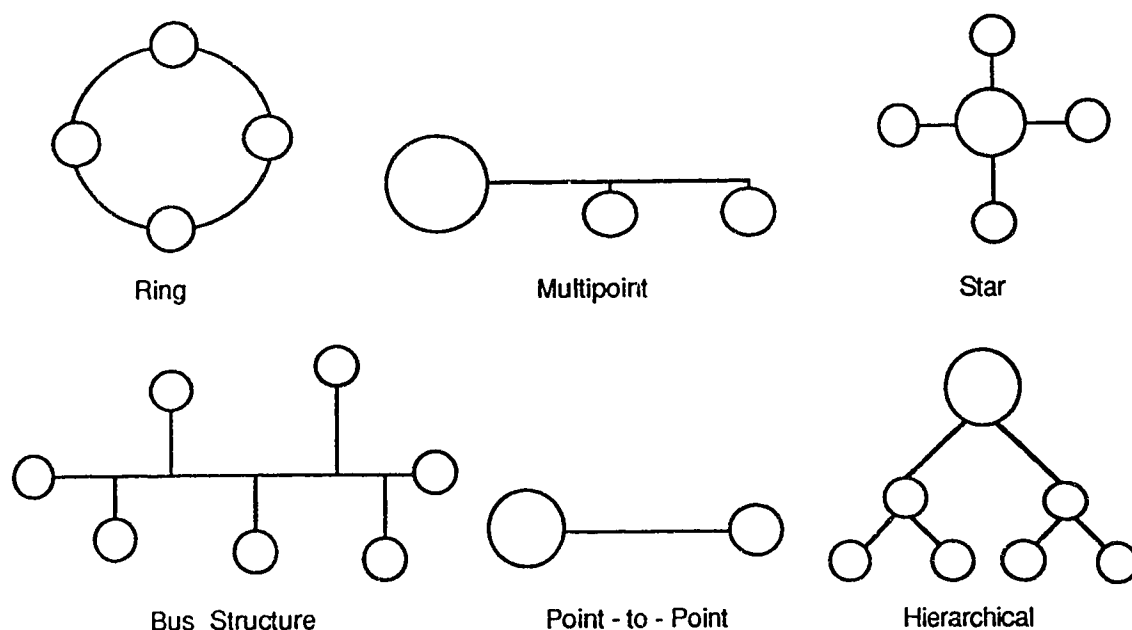


Fig. 1.8 Network topologies

1.8 Thesis Objectives and Organization

As has been discussed earlier, much work is being done in the field of multiplexing signals and then detecting them optically. The main difficulty in using Code Division Multiple Access with all-optical processing is the unipolar nature of the signal; this means that completely orthogonal codes cannot be achieved in an IM-DD system.

Various codes have already been suggested for optical CDMA, which have auto-correlation side lobes and a cross-correlation peak less than some maximum value. The main drawback of these codes is that they require a large bandwidth (e.g., prime sequence codes require a chip rate of K^2 / bit , where K is the number of users, although they generate a cross-correlation below 2 units of intensity). Recently, a new class of codes has been reported [16] which gives small auto-correlation sidelobes, and which limits the cross-correlation peaks to

1/2 the auto-correlation peak, while requiring a smaller bandwidth. This scheme is transmitter synchronous and can be used effectively only for broadcasting.

1.8.1 Objectives

While it is very desirable that a local area network have the ability to handle a large number of subscribers, practical difficulties need to be surmounted. By using spread spectrum techniques and optical processing, we can overcome some of these problems. Optical processing, although not a common technique, is gaining acceptance, and once the technology of other optical processing components, e.g. optical amplifiers, optical switches, etc., is more mature, it could well replace conventional electronic circuitry for demultiplexing incoming data.

This thesis project involves both a theoretical and an experimental component. Taking the properties and drawbacks of some of the standard codes (e.g., Gold, m-sequence, multilevel, etc.) into consideration, the main objectives of the research can be stated as follows:

- (i) To design a CDMA system that has signal conversion, from optical to electrical, only after signal processing.
- (ii) To devise a coding scheme for optical CDMA that is suitable for LANs.
- (iii) To build an optical communication network using CDMA that is capable of performing signal processing optically.

Thus, the central idea of the thesis is to develop new ways of using optical processing for the purpose of:

- (i) Increased network flexibility.
- (ii) Decreased access cost.

(iii) Decentralization of the system.

The following theoretical (1-5) and experimental steps (6-9) have been taken in order to achieve the above objectives:

- (1) A new correlation scheme for optically processing the received signal was devised.
- (2) An investigation into the properties of various existing codes, using the new correlation scheme, was carried out and a new set of codes was designed, starting from m-sequences, to be used as the address codes in CDMA.
- (3) A theoretical analysis of the transmitting pattern for the new address codes was conducted, to obtain the maximal number of stations that can be supported by the system for a given chip rate.
- (4) A computer simulation of the system Bit Error Rate (BER) caused by the interference of other users and for the channel capacity for a given system BER has been presented.
- (5) Computer simulations for transmission under a varying number of users have been performed.
- (6) An experimental system was set up, comprising of the code sequence generator, encoders, lasers and modulators, fibre link and coupler, photo-detector and decoder.
- (7) Experimental measurements of system BER, channel capacity, the near-far problem, and the signal spectrum, were obtained under the conditions of single station transmission as well as of multi-user environments.
- (8) A comparison between the computer simulation and experimental results has been made.

- (9) An analysis, discussion of the results, and conclusions have been presented.

1.8.2 Organization of the thesis

The first chapter has been devoted to the description of optical fibre systems, types of coding schemes, and multi-user access techniques. Concepts of spread spectrum modulation and their applications to state-of-the art communication systems have been presented. Advantages of CDMA over WDM, TDM, and FDM have been cited and a comparison is made between optical and electrical processing of a received codeword in a spread spectrum system.

Chapter 2 deals with a theoretical investigation of the properties of various codes. Auto- and cross-correlation concepts have been discussed, followed by the properties required by a code for possible use as a spreading sequence. Finally, the properties and generation procedure for a new set of codes, called P-codes, have been defined.

Chapter 3 discusses the simulation results of interference noise and system BER. A comparison of performance of P-codes with Gold codes in a FO-CDMA network is made. Development of the probability density function (pdf) for P-codes is discussed and the relationship of the BER, the length of code and the number of users is illustrated. Dynamic detection of the received signal for better correlation is discussed and upper and lower bounds are derived. Computer simulations for several different transmission conditions are demonstrated.

Chapters 4 and 5 deal with the second stage of the project; i.e., the experimental system operation and measurement. Chapter 4 describes the

design and construction of each part of the experimental system, which consists of two transmitters, optical star coupler, the fibre channel, and a receiver. Operation of the system and the problems encountered in the design of the circuits and the system are described.

The performance of the different parts of the system and the experimental results are discussed in Chapter 5. System transmission properties have been measured and calculated. Signal waveforms, transmission errors and the variation of the decision threshold for different groups of users has been illustrated. The change in the BER caused by increasing the number of simultaneous users and by a variation in the transmitted signal power has also been measured and illustrated. The power spectrum of the data and of the coded data has been measured in order to illustrate the concept of bandwidth spreading in CDMA.

The results and conclusions of this thesis, together with the possible areas of application of this thesis work, are given in Chapter 6. Possible future research topics in optical fibre CDMA are defined.

The various programs used to define the various codes, their correlation and their BER in single-user and multi-user access environments are given in Appendices A, B, C, D, E and F. Data sheets for the lasers and the pin photodiode form part of the Appendix G.

CHAPTER 2

FIBRE OPTIC CODE DIVISION MULTIPLE ACCESS (FO-CDMA)

In a CDMA system, each station i has its own unique code or signature sequence, x_i . This code x_i is made up of N "chips", $a_1, a_2 \dots a_N$, where each chip can have a value of 0 or 1, depending on the code type. A binary data bit is thus divided into N chips, so that the transmitted symbol rate is N times the bit rate; hence a large increase in the bandwidth is required for transmission. When a station j wants to transmit data to station i , it sends the code x_i if the data is a '1'. For a data bit of '0' the transmitted sequence depends on the type of the code used. In many applications e.g. the m-sequence code and the Gold codes, the complement of x_i is transmitted. In an optical code, a data "0" is often represented by no transmission. At the receiver, each decoder correlates out the undesired stations by using the relative orthogonality of the address codes and regenerates the intended data.

2.1 FO-CDMA coding and decoding

Central to the potential success of any code division multiple access (CDMA) scheme, whether electrical or optical, is the choice of the signature sequences to be used by each receiver. Good measures of the performance of the scheme are the correlation coefficients, auto-correlation and cross-correlation, of the various sequences. The correlation properties of the code sequences used in spread spectrum communications depend on the code type, length, chip-rate, and even the chip-by-chip structure of the particular code being used.

2.1.1 Auto-correlation and cross-correlation

The following two properties need to be satisfied while constructing sequences for CDMA :

(i) **Auto-correlation property** : Auto-correlation in the context of coding refers to the degree of correspondence between a code and a phase-shifted replica of itself. Auto-correlation plots show the number of agreements minus the number of disagreements for the overall length of the two codes being compared, as the codes assumes every shift in the field of interest. Such a plot can be generated easily using computer simulation.

For any periodic sequence $x=(x_n)$ with length F and weight K in the set, we define the auto-correlation, $|Z_{x,x}^{(i)}|$, as:

$$|Z_{x,x}^{(i)}| = \sum_{n=0}^{F-1} x_n x_{n+i} = \begin{cases} K & \text{for } i = 0 \\ \lambda_a & \text{for } 1 \leq i \leq F-1 \end{cases}$$

The length of a code (F) is defined as the total number of '0's and '1's in the code and the weight of a code (K) is defined as the total number of '1's in the code.

(ii) **Cross-correlation property** : Cross-correlation is a measure of the agreement between two different codes and is not as well behaved as the auto-correlation. The effect of a high degree of correlation between an undesired received code and a receiver reference code word is an increase in the receiver's bit error rate. When a large number of transmitters, using different codes, are to share a frequency band the code sequences must be carefully chosen to avoid interference between users. For each pair of periodic

sequences $x = (x_n)$ and $y = (y_n)$, with length F and weight K , we define the cross-correlation, $|Z_{x,y}^{(i)}|$, as :

$$|Z_{x,y}^{(i)}| = \sum_{n=0}^{F-1} x_n y_{n+i} = \begin{cases} \lambda_c & \text{for } 1 \leq i \leq F-1 \end{cases}$$

These two properties form the prime basis for the selection of a set of codes for CDMA. The codes are selected in such a way that they are orthogonal. Strictly orthogonal codes having $\lambda_a = \lambda_c = 0$ are preferred as codes for CDMA. The orthogonality of the codes increases the signal and decreases the interference, at the receiver, thus improving the error rate performance of the system [6]. Orthogonal systems eliminate the near-far problem that arises when a near transmitter (shorter propagation distance) produces more receiver power than a desired transmitter located further away, even though both transmit with the same power. However, orthogonal CDMA systems do induce specific limitations on the system. The orthogonal signal raises the general noise level of the system and hence reduces the range for a given transmitted power.

In a FO-CDMA network, optical signals are always unipolar and hence strict orthogonality cannot be achieved. This necessitates modification of the auto-correlation and cross-correlation requirements for the codes that are to be used in a FO-CDMA network. We define a sequence x_n to be pseudo-orthogonal with respect to its shifted version x_{n+i} if λ_a takes on its minimum value, and two sequences are considered pseudo-orthogonal if λ_c takes on a minimum value.

2.1.2 Desirability of optical processing

The bandwidth of an optical fibres communication systems is limited by the speed of the electronic switching and signal processing elements. This

bandwidth limitation can be extended greatly by performing the signal processing optically rather than electronically. By performing the processing of the signal optically (rather than electronically) two benefits result [29].

First, optical processing removes the speed limitation of ordinary electronic processing and eliminates the bottleneck at the opto-electronic interface. Whereas electronic processing is limited to tens of MHz in silicon and a few GHz in gallium arsenide, optical processing can be performed at hundreds of GHz.

Second, optical processing provides excess bandwidth at no extra cost. Thus, replacing electronic processing by optical processing raises the capacity of the entire LAN to that of the optical fibre itself. Hence more users can be accommodated in the channel as compared with the number of users accommodated using electronic processing.

Thus, it is advantageous to employ optical processing of the received CDMA signal in a local area network.

2.2 New method of correlation in optical fibre CDMA

Today's systems are normally of the Intensity Modulated-Direct Detection type, and are thus modelled as positive systems [14]. In an optical system one cannot send a negative amount of power; such a system is termed a positive system. A positive system is defined as one that cannot manipulate its signals to add up to zero. Hence, there is a marked difference between the properties of a code in the electrical domain and the same code in the optical domain [15]. A recent paper [16] presents a way of overcoming this difficulty. In this paper, a method to obtain an effective negative signal using an array of detector diodes,

some of which contributed a positive current to the output in the normal way and some of which are connected to subtract current from the output current, is presented.

As illustrated in Figure 2.1, in this thesis the use of two detector diodes, for the + and - operations, together with an optical switch for directing the code-word chips to the appropriate diode is proposed. All the power is sent to the positively biased photodiode when the chip in the target code is a '1' and to the negatively biased photodiode when the chip in the target code is a '0'. The overall photocurrent per chip interval from this device thus corresponds to the correlation of the received signal with the local code. The truth table of such a correlator is shown in Table 2.1. The overall output of the two diodes is sent to an integrate and dump filter. The integrated output is dumped at the end of each data period, thus resulting in a bit rate which is generally orders of magnitude lower than the chip rate.

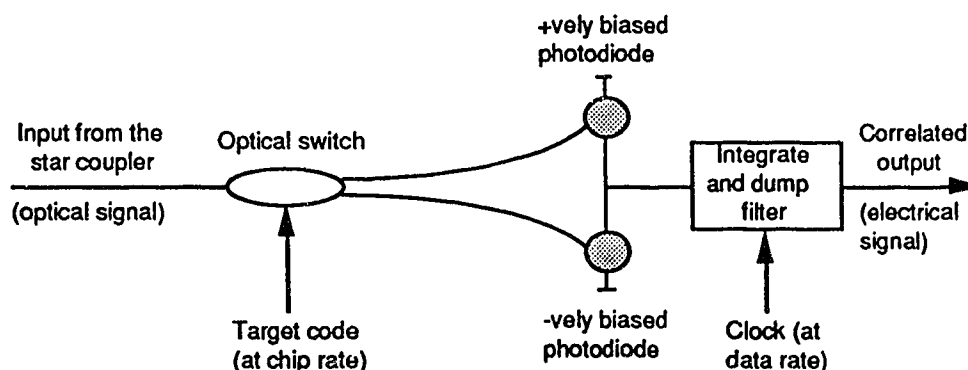


Fig. 2.1 Schematic of the proposed new correlation scheme.

An advantage of this correlation mechanism is that the local code is introduced instantaneously by means of the bias to the optical switch. Thus, the system can be operated at a higher bit rate. Another advantage of the scheme is

that there is no electrical interference on the data stream. Hence, a better signal to noise ratio is obtained at the receiver.

Table 2.1 Truth table for the correlator

Received signal	Target code sequence	Output of correlator
0	0	0
0	1	0
1	0	-1
1	1	1

2.3 Possible codes for FO-CDMA

The importance of the code sequence to the performance of a spread spectrum communication or ranging system is difficult to overemphasize, since the type of code used, its chip rate, and its length, set bounds on the performance of the system. The code sequence used in CDMA should have the following properties:

- (1) be easy to generate,
- (2) be statistically pseudo-random,
- (3) have a high auto-correlation as well as a low cross-correlation, and
- (4) should be such that it is easy for the receiver to synchronize with the desired signal.

Codes in general can be classified into two groups, linear and non-linear. Figure 2.2 illustrates a block diagram for the generation of linear and non-linear codes. Non-linear codes are used where high message security is

desired and thus find very little application in CDMA applications. Linear codes, on the other hand, are suitable for interference rejection, ranging, and other spread spectrum applications, but are not very effective for securing a transmission system. Thus, linear codes are frequently used in CDMA systems.

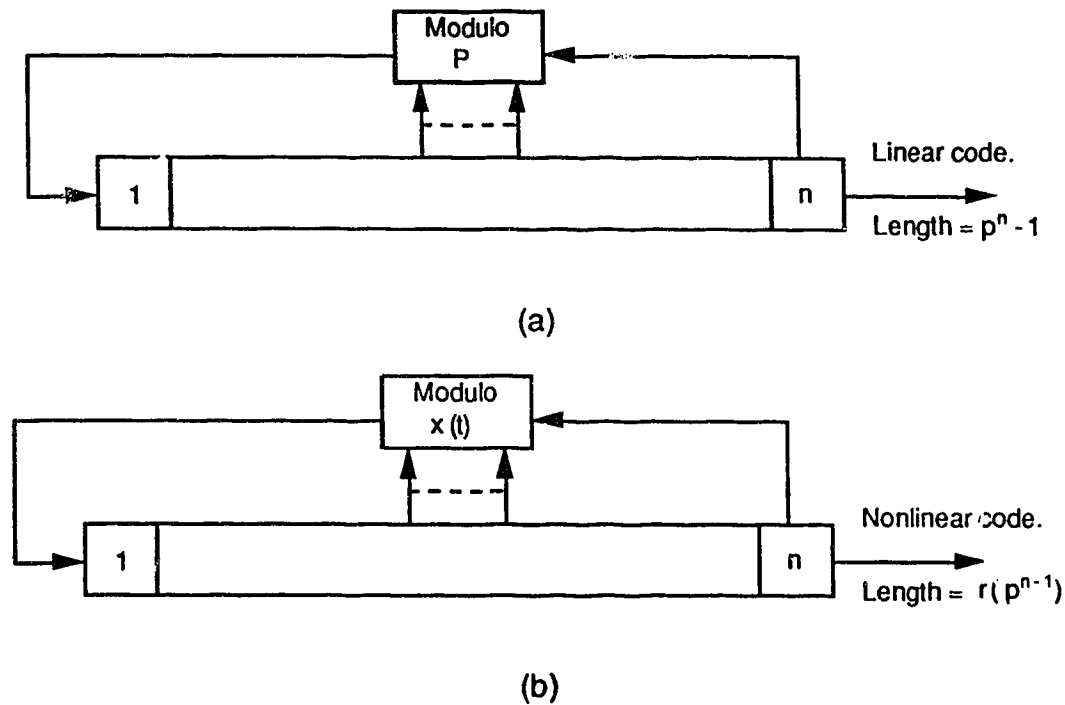


Fig. 2.2 (a) Linear code generator using p-ary shift register

(b) Nonlinear code generator using p-ary shift register

Various linear optical codes with low auto-correlation wings and small cross-correlation products, along with a high auto-correlation peak, have been proposed for incoherent optical systems [16] [19] [23]. A major drawback of these codes is that they have a high bandwidth expansion factor. Balanced codes, such as the m-sequence or Gold codes, where the number of '1's is within 1 of the number of '0's, are more bandwidth efficient. Therefore it is very advantageous to use a balanced code in CDMA optical LANs.

2.3.1 M-sequence codes

Maximal linear code sequences (often called m-sequences or pn codes) are, by definition, the longest codes that can be generated by a given shift register or a delay element of a given length. A shift register sequence generator consists of a shift register working in conjunction with an appropriate logic, which feeds back a logical combination of the state of two or more of its stages to its input. The maximum length of the sequence generated by a n stage shift register is $2^n - 1$ chips

Properties which make the maximal code sequences the most frequently used codes in CDMA systems are summarized below [8] :

1. The number of ones in a code sequence is equal to the number of zeros in the code, within one chip. For a 31-chip code there are 16 ones and 15 zeros or 15 ones and 16 zeros.
2. The statistical distribution of ones and zeros is well defined and is always the same.
3. The auto-correlation of a maximal linear code is such that for all values of phase shift the correlation value is -1, except for the 0 ± 1 chip phase shift area (Figure 2.3) in which correlation varies linearly from the -1 value to $2^n - 1$ (the sequence length).
4. A modulo-2 addition of a maximal linear code with a phase-shifted replica of itself results in another code with a phase shift different from either of the originals. This property gives us a way to produce *composite sequences* which have different properties from m-sequences.
5. Every possible state of a given n -stage generator exists at some time during the generation of a complete code cycle. Each state exists for one and

only one clock interval. The exception is that the all-zero state does not normally occur and cannot be allowed to occur. If all the stages of the generator go to an all zero state, the feedback will also be a zero and thus the output sequence will always remain zero.

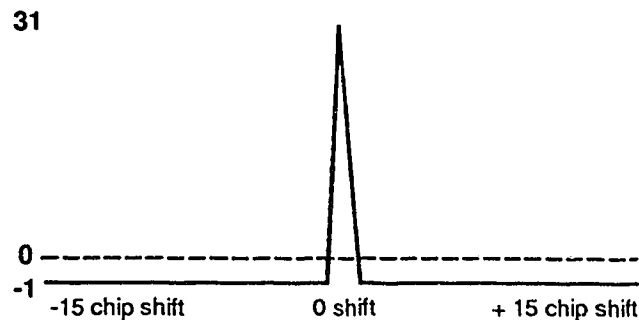


Fig. 2.3 Autocorrelation trace of a maximal linear code

Maximal linear code sequences are unexcelled for general use in communications. Other codes can do no better than equal their performance. When used in an asynchronous network, certain m-sequences will interfere very strongly with each other. Those sequences exhibiting the minimum possible cross-correlation peak in a synchronous network are referred to as preferred m-sequences [30]. Usually CDMA requires a large number of assignable addresses. Since there are only a few preferred m-sequences (3 for $N=32$) it is not practical to use a set of preferred m-sequences for CDMA, when a large number of address sequences is needed and the network is asynchronous.

2.3.2 Multi-level codes

Multi-level sequences are sometimes utilized for data encoding in CDMA [31][32]. If the interference level is low enough, it is better to use more than two

levels for the pulse heights. With a choice of four levels each pulse represents a symbol from an alphabet with $q=4$ symbols. If the bits are combined according to the scheme $00=0$, $01=1$, $10=2$, $11=3$, then the original message 11010010 is represented by 3102. The rate of transmission of information is doubled, since each pulse represents $\log_2 q = 2$ bits [33]. Thus a higher than normal data rate can be achieved by transmitting the data information using multi-level symbols. The cost paid for this increased information rate is an increase in the transmission error rate, since for a given average power the various levels are more closely spaced.

2.3.3 Gold codes

Gold codes are a set of composite codes constructed from a combination of linear maximal sequences. These codes are generated by modulo-2 addition of a pair of maximal linear sequences as shown in Figure 2.4. The code sequences are added chip-by-chip, using a binary (modulo-2) adder. Although, Gold codes are constructed from maximal codes they are not maximal but instead possess special correlation properties. These codes allow the construction of families of 2^n-1 codes from pairs of n -stage shift registers in which all codes have well-defined correlation characteristics. Thus, Gold code sequence generators are useful because of the large number of codes they supply, although they require only one pair of feedback tap sets.

In addition to their advantage in generating a large number of codes, Gold codes may be chosen so that for a set of codes available from a given generator, the cross-correlation between the codes is uniform and bounded. Thus, Gold codes are useful where a number of code-division-multiplexed signals are to be used.

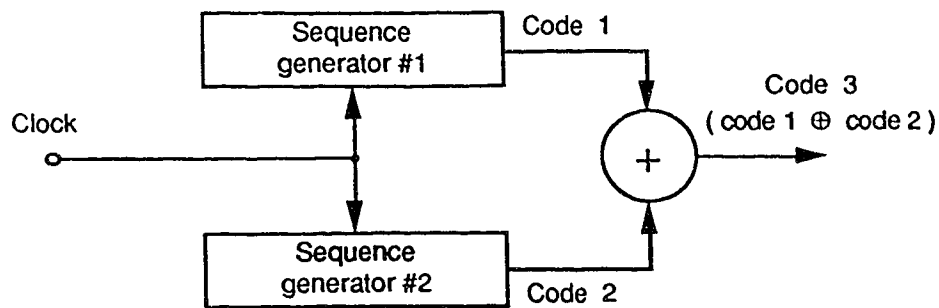


Fig. 2.4 Gold code sequence generator configuration.

Although Gold codes are quite suitable for CDMA with electrical processing [18], their properties for optical processing are not very useful in a FO-CDMA network.

2.4 New set of codes for FO-CDMA (P-codes)

In this thesis a new correlation technique employing an optical switch for correlation has been defined in Section 2.2. The codes defined in Section 2.3, being designed for standard correlation processes, cannot be used to obtain an optimum system performance in a network using the above correlation scheme. To work successfully with such a correlation scheme, a new set of composite codes, "P-codes", has been found and generated.

P-codes have the property that, when used in a synchronous system with a correlator as defined in Section 2.2, they give an auto-correlation peak equal to the weight of the code (K), and a cross correlation which, in principle, could be zero. Like Gold codes, P-codes have the advantage that a large number of codes, $2^n - 1$, can be generated from a n -stage shift register. These codes have a bandwidth expansion factor of $2^n - 1$ and thus a bandwidth expansion per channel of 1.

2.4.1 P-codes

We define the P-code as a $(F, K, \lambda_a, \lambda_c)$ family of (0,1) sequences, of length $F = 2^n - 1$ and weight $K = 2^{n-1} - 1$ or 2^{n-1} with auto-correlation and cross-correlation constraints $\lambda_a = \pm 1$ and $\lambda_c = \pm 1$. We generate the P-codes using two preferred m-sequences $\{A\}$ and $\{B\}$, each of length F , by cyclically shifting sequence $\{A\}$ one chip at a time, but inverting some of the resulting sequences according to the elements of $\{B\}$.

Thus the P-code can be represented as the periodic sequence :

$$P_n(t) = \sum C_j^{(n)} P_{T_c}(t - jT_c) , \quad (2.1)$$

$$\text{where } P_{T_c} = \begin{cases} 1 & \text{for } 0 \leq t \leq T_c \\ 0 & \text{elsewhere} \end{cases} .$$

$C_j^{(n)} = C_j$ is the j^{th} chip of an m-sequence with period $F = T/T_c$, where T is the period of a binary data bit and T_c is the period of a chip. Due to the periodicity of the sequence,

$$C_{j+F}^{(n)} = C_j^{(n)} = C_j . \quad (2.2)$$

Mathematically, we may write a set of P-codes as

$$\{C_n\} = \{A\}^n \oplus B(n) \quad (2.3)$$

where n takes on the values 1 through F . $\{A\}^n$ indicates that $\{A\}$ must be shifted cyclically by n chips, and $B(n)$ is the n^{th} element of $\{B\}$.

2.4.2 Processing of P-codes

The codes that have been proposed in this thesis use the correlation method shown in Figure 2.1; i.e., any signal that occurs in the '0' chips of a receiver's code-word is subtracted from the total signal received in the '1' chips

of the receiver code-word, and is synchronous. Thus the output of the receiver, at the end of the bit period can be written as :

$$v_o = \{s\} \cdot \{c\} - \{s\} \cdot \{\bar{c}\} = s.c - s.\bar{c} \quad (2.4)$$

When only one transmitter is considered, the received signal s_1 is identical to c_1 , since $s_1.\bar{c}_1 = c_1.\bar{c}_1 = 0$, and $v_o = s_1.c_1 = K$, the weight of the code or the number of 1's in the code-word c_1 . If we consider a second signal s_2 arriving at Receiver 1 the interference, V_i , can be written as,

$$v_i = s_2.c_1 - s_2.\bar{c}_1 \quad (2.5)$$

Since the P-codes, as generated in Section 2.4.1, have an odd value of F , the weight K of the P-codes is either $(F+1)/2$ or $(F-1)/2$. Thus the weight is either even or odd. For the case where K is even, the output can be zero if the binary '1's in s_2 occur so that half of them are aligned with the '1's in c_1 . Then the other '1's in s_2 must fall on the '0's of c_1 which are the '1's of \bar{c}_1 . Therefore, for a code of weight K , we can have

$$\begin{aligned} v_i &= s_2.c_1 - s_2.\bar{c}_1 \\ &= \frac{K}{2} - \frac{K}{2} = 0. \end{aligned} \quad (2.6)$$

When the P-code has an odd value of weight 'K', we can have two possible cases:

Case 1. One more chip is aligned to the '1's of C_1 than the '0's of C_1 and the output is given by $v_i = s_2.c_1 - s_2.\bar{c}_1 = \left(\frac{K+1}{2}\right) - \left(\frac{K-1}{2}\right) = +1$ (2.7)

Case 2. One more chip is aligned to the '0's of C_1 than the '1's of C_1 and the output is given by $v_i = s_2.c_1 - s_2.\bar{c}_1 = \left(\frac{K-1}{2}\right) - \left(\frac{K+1}{2}\right) = -1$. (2.8)

Therefore, in general, for each interfering transmission, $v_i = s_n (c_1 - \bar{c}_1) = \pm 1$. As the number of interfering signals ($s_2, \dots s_n$) increases, the value of the received interference changes. Generalizing equation (6), we have

$$v_i = \sum_{n=2}^N s_n (c_1 - \bar{c}_1) . \quad (2.9)$$

However, maximum interference is obtained when we have $N = F$ simultaneous users and it is given by

$$v_{i_{\max}} = \left| \sum_{n=2}^F s_n (c_1 - \bar{c}_1) \right| = K. \quad (2.10)$$

Thus the total interference can go up to a maximum of 'K' when all the users are transmitting simultaneously.

2.4.3 Generation of P-codes.

As stated before, P-codes can be generated using two preferred m-sequences {A} and {B}, each of length F, by cyclically shifting sequence {A} one chip at a time, but inverting some of the resulting sequences according to the elements of {B}.

M-sequences can be generated by using delay lines or digital shift registers. When using shift registers, the output of the register is fed back into the input after being mixed with the tapped outputs of some predefined stages of the register. The tapped stages are assigned by the preferred m-sequence selected. Any preferred sequence can be used for the generation of P-codes and is defined as [a,b,..n], where a, b, .. n represent the tapped stages. For a 32 bit code there are only three preferred m-sequences. The two we have

chosen can be expressed as $[5,3]$ and $[5,4,3,2]$. The m-sequence generators for the above are shown in Figure 2.5. The symbol, \oplus , in Figure 2.5 represents the modulo 2 addition of the outputs from the tapped stages. For a 32 bit (2^n , $n=5$) m-sequence generator a 5 bit shift register is used, and the stages are numbered 1,2, .. 5 in the figure.

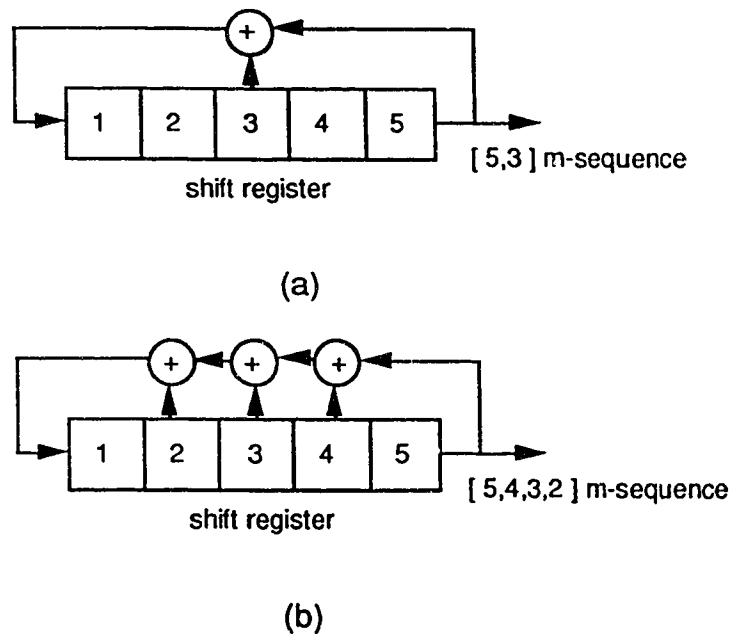


Fig. 2.5 $[5,3]$ and $[5,4,3,2]$ preferred m-sequence generators

We refer the codes generated from the $[5,4,3,2]$ and $[5,3]$ combination as codes A and B, respectively. The code sequences generated can thus be written as :

Code A: 1 1 1 1 1 0 0 1 0 0 1 1 0 0 0 0 1 0 1 1 0 1 0 1 0 0 0 1 1 1 0

Code B: 1 1 1 1 1 0 0 0 1 1 0 1 1 1 0 1 0 1 0 0 0 0 1 0 0 1 0 1 1 0 0

P-code sequence # n , P_n , is formed from the m-sequences by cyclically shifting code A according to the number of the code, n , minus one; i.e. $n-1$, and then modulo 2 adding the resulting sequence with the value of the chip corresponding to the P-code number (n), in code B. Since the value of a chip

can be a '0' or a '1'. the modulo 2 addition is equivalent to inverting the chips in the resulting sequence if the chip corresponding to the code number in code B is a '1'.

Figure 2.6 shows a way of generating P-codes from the preferred m-sequences for the case when $n=5$. The number of chips in a $n=5$ P-code sequence is $2^5-1=31$. The following are the operations performed for the generation of P-code, code number 5, using a 5 bit shift register :

- (1) Code A : 1 1 1 1 1 0 0 1 0 0 1 1 0 0 0 0 1 0 1 1 0 1 0 1 0 0 0 0 1 1 1 0
- (2) Code B : 1 1 1 1 1 0 0 0 1 1 0 1 1 1 0 1 0 1 0 0 0 0 1 0 0 1 0 1 1 0 0
- (3) Code A : 1 0 0 1 0 0 1 1 0 0 0 0 1 0 1 1 0 1 0 1 0 0 0 1 1 1 0 1 1 1 1
shifted by 4
- (4) 5th chip in code B is a 1, and thus code C (code A shifted by 4) is inverted, thus the 5th P-code sequence is :
- (5) 0 1 1 0 1 1 0 0 1 1 1 1 0 1 0 0 1 0 1 0 1 1 1 0 0 0 1 0 0 0 0

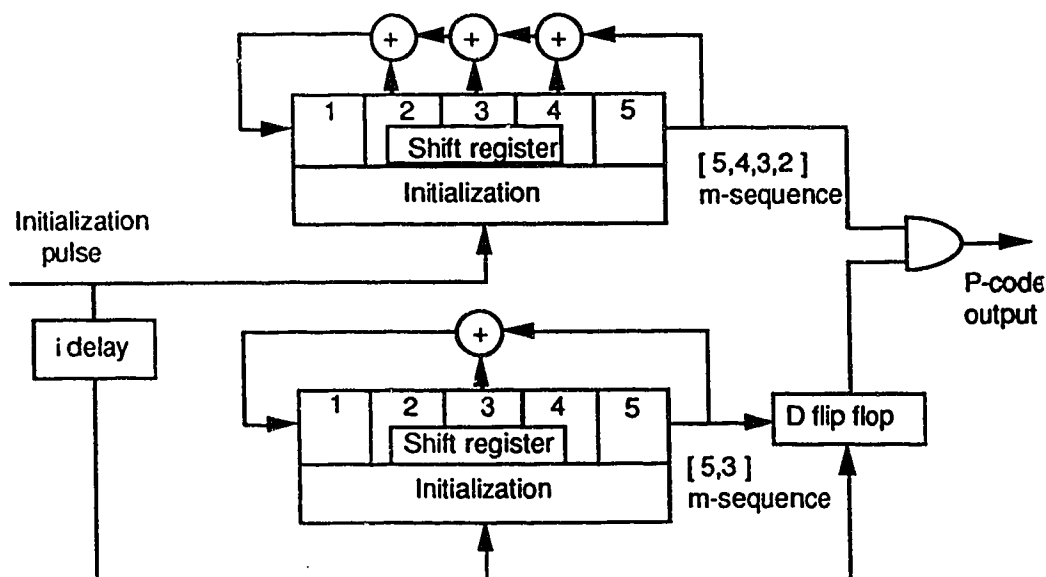


Fig. 2.6 Schematic of a P-code generator

The corresponding P-codes generated from the above codes are shown in Table 2.2.

Table 2.2 P-code sequences generated from preferred m-sequences

Code A: 1 1 1 1 1 0 0 1 0 0 1 1 0 0 0 0 1 0 1 1 0 1 0 1 0 0 0 1 1 1 0
 Code B:

	P-code sequences																																	
↓																																		
1	0	0	0	0	0	1	1	0	1	1	0	0	1	1	1	0	1	0	0	1	0	1	0	1	1	1	0	0	0	1				
1	0	0	0	0	1	1	0	1	1	0	0	1	1	1	1	0	1	0	0	1	0	1	0	1	1	1	0	0	0	1	0			
1	0	0	0	1	1	0	1	1	0	0	1	1	1	1	0	1	0	1	0	0	1	0	1	0	1	1	1	0	0	0	1	0		
1	0	0	1	1	0	1	1	0	0	1	1	1	1	0	1	0	0	1	0	1	0	1	1	1	1	0	0	0	1	0	0	0		
1	0	1	1	0	1	0	0	1	1	1	1	0	1	0	0	1	0	1	0	1	0	1	1	1	0	0	0	1	0	0	0	0		
0	0	0	1	0	0	1	1	0	0	0	0	1	0	1	1	0	1	0	1	0	0	0	1	1	1	0	1	1	1	1	1	1		
0	0	1	0	0	1	1	0	0	0	1	0	1	1	0	1	0	1	0	1	0	0	0	1	1	1	0	1	1	1	1	1	0		
0	0	1	0	0	1	1	0	0	0	1	0	1	1	0	1	0	1	0	1	0	0	0	1	1	1	0	1	1	1	1	1	0		
1	1	1	0	0	1	1	1	0	1	0	0	1	0	1	0	1	1	1	0	0	0	1	0	0	0	0	0	0	0	1	1	0		
1	1	0	0	1	1	1	1	0	1	0	0	1	0	1	0	1	1	1	0	0	0	1	0	0	0	0	0	0	1	1	0	1		
0	1	1	0	0	0	0	1	0	1	1	0	1	0	1	0	1	0	0	0	1	1	1	0	1	1	1	1	1	0	0	1	0	0	
1	0	1	1	1	1	0	1	0	0	1	0	1	0	1	0	1	1	1	0	0	0	1	0	0	0	0	0	1	1	0	1	1	0	
1	1	1	1	1	0	1	0	0	1	0	1	0	1	1	1	0	0	0	1	0	0	0	0	0	0	0	1	1	0	1	1	0	0	1
0	0	0	1	0	1	1	0	1	0	1	0	0	0	1	1	1	0	1	1	1	1	1	1	1	1	0	0	1	0	0	1	1	0	0
1	1	0	1	0	0	1	0	1	0	1	1	1	0	0	0	1	0	0	0	0	0	0	0	0	1	1	0	1	1	0	0	1	1	1
0	1	0	1	0	0	1	0	1	0	1	1	1	0	1	1	1	1	1	0	0	1	0	0	1	1	0	0	0	0	1	0	1	1	0
0	0	1	0	1	0	0	0	1	1	1	0	1	1	1	1	1	0	0	1	0	0	1	0	0	1	1	0	0	0	0	1	0	1	1
0	1	0	1	0	0	0	1	1	1	0	1	1	1	1	1	0	0	1	0	0	1	1	0	0	0	0	0	0	1	0	1	1	0	0
1	1	0	1	1	1	0	0	0	1	0	0	0	0	0	1	1	0	1	1	0	0	1	1	0	0	1	1	1	0	1	0	0	1	0
0	1	0	0	0	1	1	1	1	0	1	1	1	1	1	0	0	1	0	0	1	1	0	0	0	0	0	1	0	1	1	0	1	0	1
1	1	1	0	0	0	1	0	0	0	0	1	1	0	1	1	0	1	1	0	0	1	1	1	1	0	1	0	0	1	0	1	0	1	0
0	0	1	1	1	0	1	1	1	0	0	1	1	0	1	1	0	0	1	1	1	0	1	0	0	1	0	1	0	1	1	0	1	1	0
0	1	0	1	1	1	1	1	0	0	1	0	0	1	1	0	0	0	0	1	0	1	1	0	1	0	1	0	1	0	0	0	1	1	1
0	0	1	1	1	1	0	0	1	0	0	1	1	0	0	1	1	0	0	0	0	1	0	1	1	0	1	0	0	0	1	1	1	1	1

The P-code sequences listed above can be numbered from code #1 (P1) to code #31 (P31), depending on the value of the chip of code B that was used for generation. It is observed that P-codes sequences can be divided into two

distinct groups. These are referred to as the group 1 P-codes or the group 2 P-codes. Users having a local code that is a group 1 code are referred to as group 1 users. The same holds true for group 2 users. It is observed that the weight of the code can be used to decide the group of the code. Codes having a weight of 15 fall under group 1 P-codes while those with a weight of 16 fall under group 2 P-codes category. It can be seen that the codes having a weight of 16 when correlated, as defined in Section 2.4.2, with a receiver code of weight 16 or a receiver with a local code of weight 15 would give an output of 0. At the same time a code of weight 15 when correlated with a receiver code of weight 15 gives an output of -1, while a code of weight 15 when correlated with a receiver code of weight 16 gives an output of +1. This is shown in Table 2.3.

Table 2.3 Properties of Group 1 and Group 2 type codes

Received signal	Target code sequence	Output of correlator
Group 1 code	Group 1 code	- 1
Group 1 code	Group 2 code	1
Group 2 code	Group 1 code	0
Group 2 code	Group 2 code	0

CHAPTER 3

COMPUTER SIMULATION OF FO-CDMA USING P-CODES

In order to determine the key properties of the P-codes, a computer simulation was carried out. This chapter describes the simulation results obtained. The two transmission patterns commonly encountered in CDMA systems, namely: data slot synchronous and data slot asynchronous, are also discussed. This is followed by an analysis of Gold codes as a possible set of codes for the correlation scheme mentioned in Section 2.2. P-codes are introduced and simulation results obtained for the system, employing these codes for the transmission of data, are discussed. It is shown that P-codes perform well in a synchronous system when the new optical correlation scheme is used. It is also shown that, ideally, if a dynamic detection threshold is used at the receiver, then error free transmission can be realized. Finally, the system performance of the P-codes for synchronous transmission is determined by deriving an expression for the probability density function of the interference caused at a receiver. The probability of error and the bit error rate for the codes are calculated from the pdf.

3.1 Synchronous and asynchronous data slot transmission

3.1.1 Synchronous data slot transmission

In synchronous data slot transmission, all the stations in the network are synchronized not only to the chip bits but also to the data slots, as shown in Figure 3.1. Each station has access to the network at any time. There is a small waiting time, but this is never more than the time required for the transmission of a single data bit. The performance of a synchronous system is far better than

that of an asynchronous system, although the design of such a system involves greater complexity.

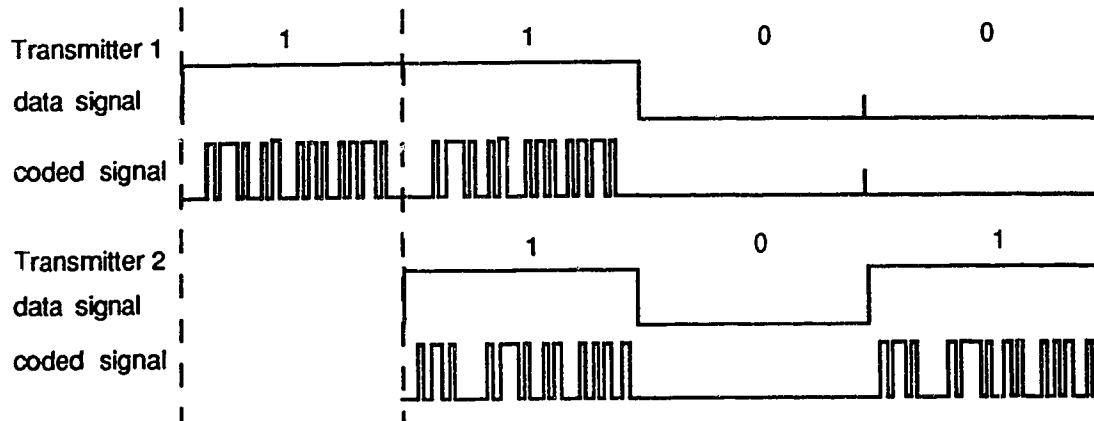


Fig. 3.1 Synchronous data slot transmission

3.1.2 Asynchronous data slot transmission

Asynchronous data slot transmission, also referred to as asynchronous transmission, is depicted in Figure 3.2. In asynchronous transmission each station gains access to the network, with no waiting time, hence the beginning of each data interval for the various transmitters is not coincident. Thus, the coded signals are data bit asynchronous although they may or may not be asynchronous with respect to the chip bits. An asynchronous transmission that is synchronous with respect to the chips is known as “ideal chip asynchronous”. Chip asynchronous transmission refers to the situation where the transmission is asynchronous with respect to the chips. The difference between chip asynchronous and ideal chip asynchronous transmission is illustrated in Fig 3.3: transmitter 2 is chip asynchronous with respect to the transmitter 1, whereas transmitter 3 is ideal chip asynchronous with respect to transmitter 1.

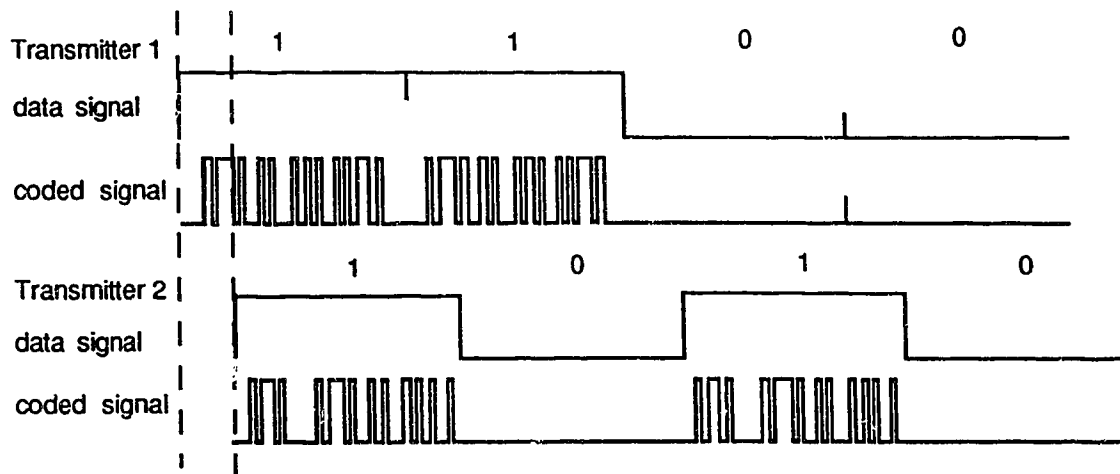


Fig. 3.2 Asynchronous data slot transmission.

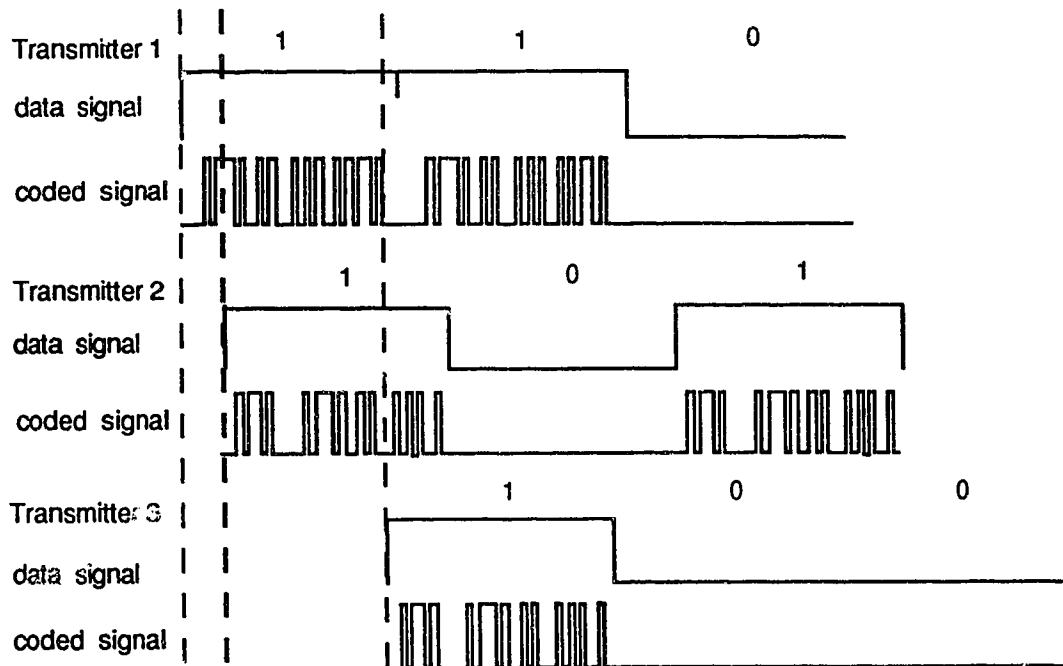


Fig. 3.3 Illustration of chip asynchronous and ideal chip asynchronous transmission.

3.2 Performance analysis of Gold codes

The possibility of using Gold codes as the preferred set of codes for FO-CDMA has been examined. An analysis of the correlation of Gold codes using standard optical correlation has been performed. The truth table used to define

standard optical correlation is shown in Table 3.1. Results obtained from the calculation show that, although Gold codes possess advantages when used with conventional correlation schemes, they are not very useful in a FO-CDMA system. It is observed that Gold codes, when correlated optically in a synchronous system, exhibit certain unique features. Simulation results show that the maximum value of the cross-correlation and the maximum auto-correlation side lobe of any Gold code sequence of length $N=31$ with any other Gold code, correlated one code at a time, is as shown in Figure 3.4. It can be seen that the cross-correlation product and the auto-correlation sidelobes follow a certain pattern. Referring to the figure, the value 'X' is equal to half the weight of the target code, i.e., the local code of the receiver. Since Gold codes of length 31 can have a weight of 12, 16 or 20, 'X' can take values equal to 6, 8 or 10.

Table 3.1 Truth table for standard optical correlation

Received signal	Target code sequence	Output of correlator
0	0	0
0	1	0
1	0	0
1	1	1

To illustrate the above observation, the cross-correlation of Gold code sequence 28, G28, with Gold code sequence G1 to G27 and G29 to G33 along with the auto-correlation of sequence G28, are considered. The Gold code sequence G28 has a weight of 12 and hence the value of 'X' in Fig.3.4 is '6'. Thus, the maximum value of the cross-correlation of code G4 and G8 with G28 is 'X-2', i.e. 4 and 'X+2', i.e. 8, respectively. The value of the maximum auto-correlation side-wing is equal to 'X-2', i.e., 4. However, the auto-correlation

peak, being equal to the weight of the code for the optical correlation scheme used, is at ' $2X$ '. Alternatively, it is observed that a weight of '8' (2^{n-2}) when added to the auto-correlation side lobe maxima of the code yields the peak auto-correlation of the code.

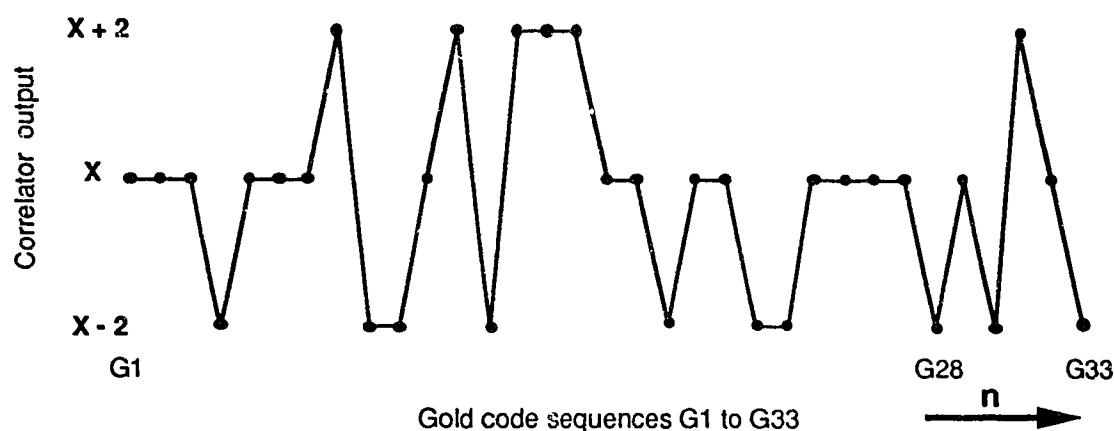
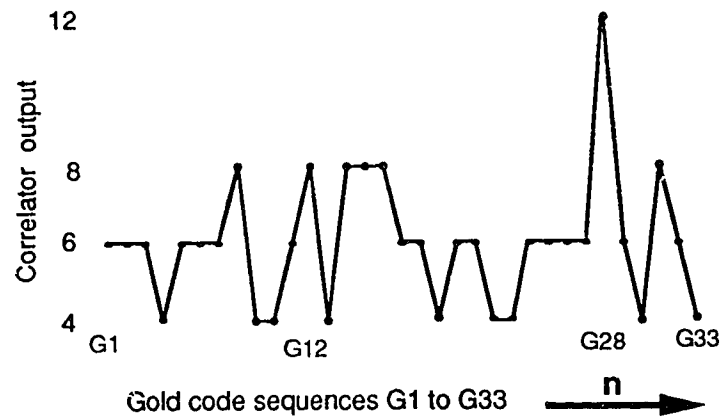
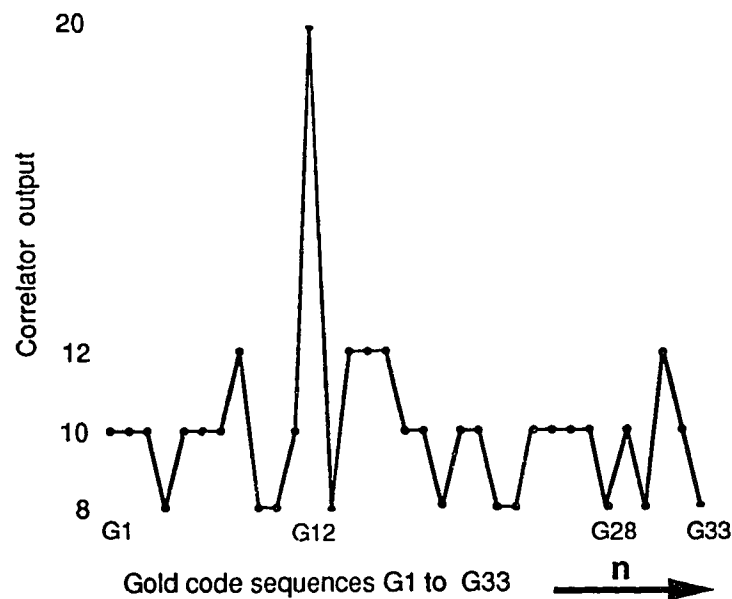


Fig. 3.4 General format of the cross-correlation output for Gold codes

Figure 3.5 (a) and (b) show the peak auto-correlation and the maximum cross-correlation outputs of the correlator for Gold code sequences G28 and G12 respectively with other sequences, for the case of two simultaneous bit synchronized users. As stated earlier, the code sequence G28 has a weight of 12 and hence the value of ' X ' is 6. The value obtained for the cross-correlation of sequence number 28 from Figure 3.4 is seen to be $X-2 = 4$. Thus the auto-correlation for code 28 is $(X-2)+8 = 12$, the weight of the code. However, for the code sequence G12, the value of ' X ' is equal to 10 and the auto-correlation is equal to ' $2X$ ', i.e., 20. This value is the same as that which would be obtained if we were to add eight to the value of the auto-correlation side lobe maximum, i.e. 12.



(a)



(b)

Fig. 3.5 Maximum auto- and cross-correlation outputs obtained for the Gold code sequences (a) G28 and (b) G12 with codes G1 to G33, correlated one code at a time

Comparing the results obtained for the sequences 28 and 12 we see that the auto-correlation peak at the receivers having a local code with a weight of 12 is '12', whereas, the maximum cross-correlation obtained in the receivers having a local code of weight 20 is also '12'. Thus, the decision circuit designed for the receivers having a local code with a weight of 12 cannot be used in

those receivers having a local code with a weight of 20, as this will lead to a false detection of the signal at the receiver. Hence, different receivers are required for the three different types of Gold code sequences; i.e., those receivers having a local code with a weight of 12, 16 and 20, respectively.

From these simulations, it is seen that a synchronous CDMA system using $N=31$ Gold codes for station identification and spreading can accommodate 31 simultaneous users. However, since the value of the maximum cross-correlation peaks and of the auto-correlation side-wing are nearly the same as that of the auto-correlation peak, there is a high probability of a false detection of the signal. As the number of users increases, the probability of error increases and the system performance deteriorates drastically; thus the use of Gold codes in optical CDMA is clearly not the best choice.

At the same time, simulation results have shown that a maximum of four simultaneous users can be supported in an asynchronous network using Gold codes and employing optical correlation (Appendix A). It was observed that there were some constraints as to which four users could gain access to the channel at a particular time. The users can be divided into 4 distinct groups, according to their Gold code number. Users with Gold code sequence G1, G2, G3, G4 and G5 can be placed in one group while users with sequences G6, G7 and G8 constitute the second group. The other two groups are made up of users with sequences G14, G16, G18 and G21, G22, G24, G25, G27, G30 respectively. One user from each group can access the channel at a particular time while other users in that group will have to wait (for the user on the line to hang-up) in order to gain access to the channel. For example, when the user with code sequence G1 is on the line, users with sequences G2, G3, G4 and G5

cannot gain access to the channel. At the same time, one of the users in groups 2 to 4 can access the channel and transmit / receive the data. Thus the use of Gold codes in an asynchronous CDMA network cannot be justified.

3.3. Simulation results for P-codes

P-codes have already been introduced in Chapter 2. As has been pointed out, P-codes have a weight of 2^{n-1} or $2^{n-1}-1$, depending on whether the codes are Group 1 or Group 2 codes, where n is the order of the code and the total number of P-code sequences is $2^n - 1$. Simulation results for P-codes have shown that a CDMA system using a 2^{n-1} chip P-code can accommodate 2^{n-1} simultaneous users, provided optical correlation is used. The correlation outputs are generated in accordance with Table 2.1. Simulation programs developed for the analysis of P-codes are listed in Appendices B - F.

Simulations were also performed to study the auto-correlation and cross-correlation properties of the P-codes. From the simulation results, it is inferred that the difference between the auto-correlation peak and the maximum cross-correlation for group 1 and group 2 users is always equal to the weight of the code.

It has been observed during simulations that the P-codes show some unique and interesting properties. These properties are the combined result of the codes and of the correlation scheme that is used. We see that the receivers for the two different groups of codes, group 1 and group 2, have different behaviors. While the lower bound for the correlator output, for receivers having a local code falling in group 1 (Type 1 receiver) decreases for each additional user, the upper bound for a receiver having a local code falling in group 2 (Type 2 receiver) increases with an increase in the number of users. This property of

the codes can be used to achieve the selective addressing facility and security against illegal reception. A user in Group 1 cannot receive the message from a Group 2 user, even if the local code is changed to be the same as the other user's code, because the receiver design required to detect the signal is different. This can be seen in Figures 3.6 and 3.7. As can be seen from the figures P-codes follow a very open upper and lower bound, i.e., there is a perceivable difference in the upper and lower bounds for the codes, with and without the intended user code being transmitted.

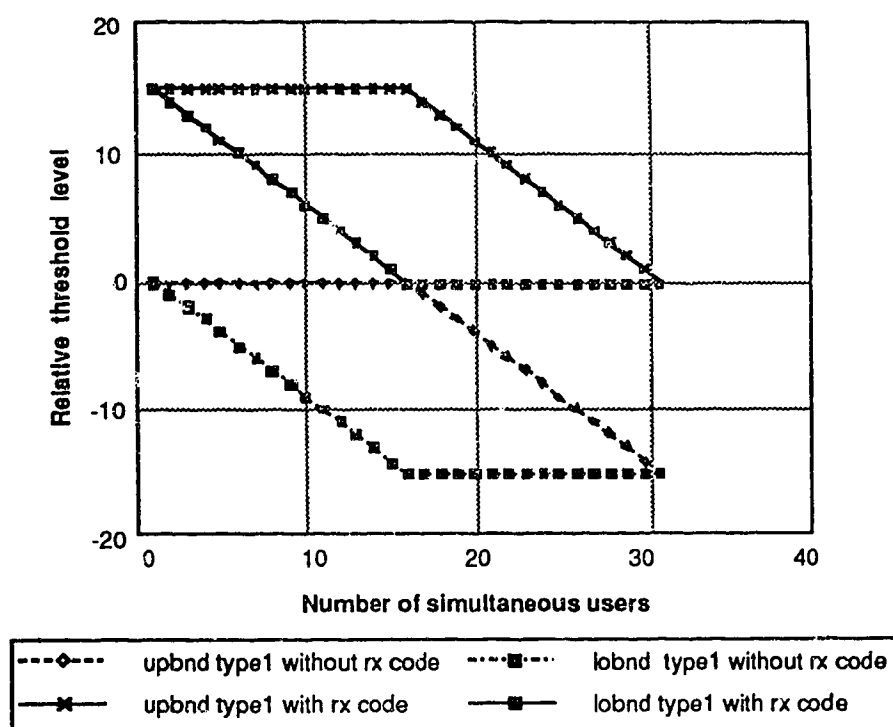


Fig. 3.6 Upper and lower bounds on the threshold of the received signal for Type-1 receiver, with and without the Group-1 receiver code present.

For a $n=5$, P-code generator using the 5, 3 and 5, 4, 3, 2 m-sequence generators, we can divide the 31 P-codes generated into two groups as shown in Table 3.2.

Table 3.2 Group 1 and Group 2 P-code sequences.

Group 1 P-code sequences are: 1 2 3 4 5 9 10 12 13 14 16 18 23 26 28 29

Group 2 P-code sequences are: 6 7 8 11 15 17 19 20 21 22 24 25 27 30 31

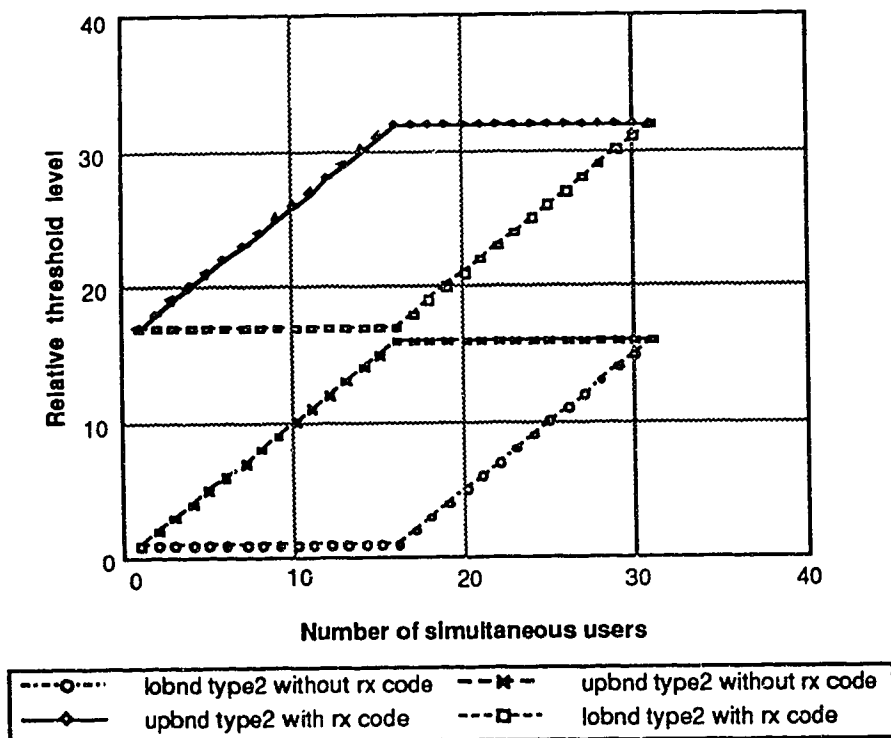


Fig. 3.7 Upper and lower bounds on the threshold of the received signal for Type-2 receiver, with and without the Group-2 receiver code present

Simulation results show that the total number of users supported by P-codes in a synchronous network is equal to $2^n - 1$. It can be inferred from the upper and lower bounds obtained for the codes that this can be achieved with almost no error provided that dynamic detection is used. In dynamic detection the detection threshold is adjusted according to the total number of users in the channel. Dynamic detection in a FO-CDMA network can be achieved based on the following concept. As the number of users increases in the channel, the total

laser power in the channel increases. This is true because the variation of the power with the change in the number of users, assuming that all the power from each user is coupled into a star coupler, is proportional to the number of chips in the signal. Thus, by detecting the total power in the channel, an estimate of the total number of users is readily achieved. Figure 3.8 shows the relationship between the upper and lower bounds of the total power in the system and the number of simultaneous users.

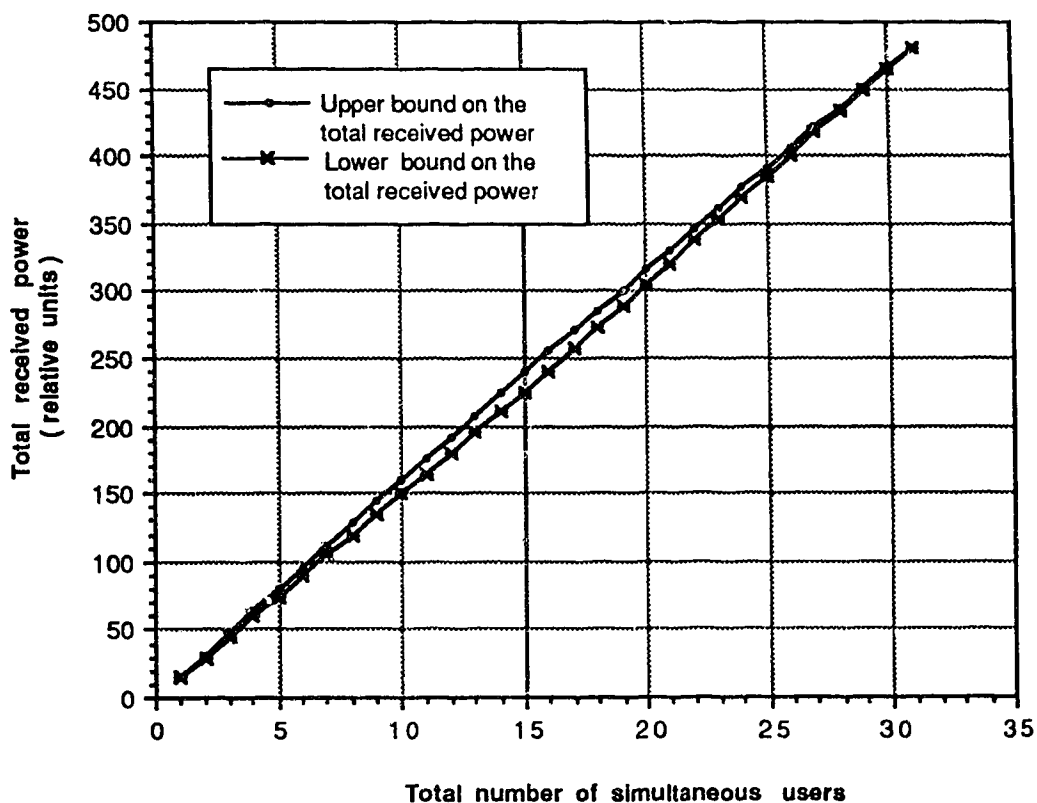


Fig. 3.8 Upper and lower bounds for the channel power with increasing users

Once an estimate of the total number of users in the channel has been made, the detection threshold can be set according to the bounds obtained for the codes. An alternative method to achieve dynamic detection is to feed the detected output from the preamplifier to a decision threshold setting circuit [46].

A simulation was also carried out to study the asynchronous transmission of signals using P-codes as signature sequences. It was seen that a total of two users, one from each group defined earlier, can be supported in an asynchronous CDMA network using P-codes. This result is true since the P-codes are primarily derived from two preferred m-sequences. Thus P-codes can be used as signature sequences in a CDMA network for multi user access only in synchronous networks.

3.4 Calculation of system performance for P-codes.

In order to calculate the system performance for P-codes, we need to develop an expression for the probability density function, the probability of error and the BER for the correlator output.

The following assumptions are made in the evaluation of the system performance [3], namely:

- (1) A lossless, distortionless and noiseless electrical-to-optical signal conversion, and vice versa. It is assumed that the system performance deteriorates only due to the increasing number of users. The effects of noise and splicing losses on the system performance are not considered.
- (2) An incoherent laser light source is used for the electro-optic conversion; the opto-electronic conversion is also incoherent.
- (3) All transmitters produce the same average effective power at any user's receiver, so that no transmitter can overwhelm the others.
- (4) All transmitters operate at the same bit rate and use the same signal format.
- (5) Communication between the n^{th} transmitter and the j^{th} receiver is continuous.

From the above assumptions, we can express the n^{th} transmitted baseband signal, $S_n(t)$, at the output of the n^{th} optical encoder as :

$$S_n(t) = S_n b_n(t) P_n(t) \quad (3.1)$$

where S_n is the n^{th} user optical intensity, $b_n(t)$ is the binary data signal and $P_n(t)$ is the P-code of the n^{th} receiver.

Assuming continuous communication, the n^{th} user's binary data signal $b_n(t)$ is given by :

$$b_n(t) = \sum_{l=-\infty}^{\infty} b_l^{(n)} P_T(t - lT) \quad (3.2)$$

where $b_l^{(n)} = b_l^{(n)}$ is the n^{th} user's data sequence taking the value 0 or 1 (OOK) for each l , with equal probability, and $P_T(t)$ is the rectangular pulse of duration T which starts at $t = 0$.

Also, $P_n(t)$, the n^{th} user's P-code or signature sequence is given by :

$$P_n(t) = \sum_{j=-\infty}^{\infty} C_j^{(n)} p_{T_c}(t - jT_c) \quad (3.3)$$

where $p_{T_c} \equiv \begin{cases} 1 & 0 \leq t \leq T_c \\ 0 & \text{elsewhere} \end{cases}$ is defined as the chip waveform, and $C_j = C_j^{(n)}$ is the j^{th} periodic sequence of binary optical pulse (0,1) with period F .

$$\text{Thus, } C_{j+F}^{(n)} = C_j^{(n)} \quad (3.4)$$

Also,

$$C_j^{(n)} = [A_{(n-1+j) \bmod F}^{(n)} \oplus B_{n_j}^{(n)}] \quad (3.5)$$

where, A and B are the m-sequences from which the P-code is generated.

But $B_{n_j}^{(n)} = B_n^{(n)}$, therefore,

$$C_j^{(n)} = [A_{(n-1+j) \bmod F}^{(n)} \oplus B_n^{(n)}] \quad (3.6)$$

The chip time $T_c = T/N$ where T is the period of a bit thus the bandwidth of $P_n(t)$ is N times that of $b_n(t)$.

Two cases are possible in a multiple access transmission system:

- 1) Transmitters are not synchronous.
- 2) Transmitters and receivers are time synchronous in the sense that the received data from all transmitters arrives in synchronism at the receiver.

For the first case, the received signal $r(t)$ at the front end of the receiver is of the form,

$$r(t) = \sum S_n(t - \tau_n) \text{ , where } \tau_n \text{ is the delay associated with the } n^{\text{th}} \text{ signal (3.7)}$$

Substituting equation 3.1 in equation 3.7 we have,

$$r(t) = \sum b_n(t - \tau_n) P_n(t - \tau_n) \text{ , assuming } S_n = 1 \text{ } 1 \leq n \leq N \text{ . (3.8)}$$

In the second case, assuming perfect synchronization, we have

$$r(t) = \sum_{n=1}^N S_n(t) \text{ (3.9)}$$

Therefore, from equation 3.1 and equation 3.9 we get,

$$r(t) = \sum_{n=1}^N b_n(t) P_n(t) \text{ , assuming that the intensity } S_n = 1, 1 \leq n \leq N \text{ (3.10)}$$

In this thesis work only case two is considered and an expression for the interference at the output of the integrate and dump filter is derived. The signal, Z_1 , at the output of the integrate and dump filter of receiver #1 at a time T , considering that the desired user signal is denoted by $n=1$, can be written as,

$$Z_1 = \frac{1}{T_c} \int_0^T r(t) [P_1(t) - \overline{P_1(t)}] dt \text{ (3.11)}$$

where, $P_1(t)$ is the P-code sequence of user 1 and where $\overline{P_1(t)}$ is the complement of $P_1(t)$. Substituting equations 3.10 and 3.3 into equation 3.11, Z_1 can be written as:

$$Z_1 = \frac{1}{T_c} \int_0^T \sum_{n=1}^N b_n(t) P_n(t) \left[\sum_{j=-\infty}^{\infty} C_j^{(1)} p_{T_c}(t-jT_c) - \sum_{j=-\infty}^{\infty} \overline{C_j^{(1)} p_{T_c}(t-jT_c)} \right] dt \quad (3.12)$$

Z_1 can be expressed as a function of the P-codes in order to derive an expression for the pdf. Thus, we have :

$$Z_1 = \frac{1}{T_c} \int_0^T \left[\sum_{n=1}^N \sum_{l=-\infty}^{\infty} b_l^{(n)} P_T(t-lT) \sum_{j=-\infty}^{\infty} C_j^{(n)} P_{T_c}(t-jT_c) \right] \left[\sum_{j=-\infty}^{\infty} C_j^{(1)} P_{T_c}(t-jT_c) - \sum_{j=-\infty}^{\infty} \overline{C_j^{(1)} P_{T_c}(t-jT_c)} \right] dt \quad (3.13)$$

Substituting equation 3.4 into equation 3.13 we get ,

$$Z_1 = \frac{1}{T_c} \int_0^T \left[\sum_{n=1}^N \sum_{l=-\infty}^{\infty} b_l^{(n)} P_T(t-lT) \sum_{j=-\infty}^{\infty} C_j^{(n)} P_{T_c}(t-jT_c) \right] \left[\sum_{j=-\infty}^{\infty} P_{T_c}(t-jT_c) (A_{j \bmod F}^{(1)} \oplus B_{1j}^{(1)}) - \sum_{j=-\infty}^{\infty} \overline{P_{T_c}(t-jT_c)} (\overline{A_{j \bmod F}^{(1)} \oplus B_{1j}^{(1)}}) \right] dt \quad (3.14)$$

Assuming a perfectly synchronous system, the case we are interested in, the expression for the output of the integrate and dump filter can be written as,

$$Z_1 = \frac{1}{T_c} \int_0^T \left[\sum_{n=1}^N \sum_{l=-\infty}^{\infty} b_l^{(n)} P_T(t-lT) \sum_{j=-\infty}^{\infty} (A_{(n-1+j)}^{(n)} \oplus B_n^{(n)}) P_{T_c}(t-jT_c) \right] \left[P_{T_c}(t-jT_c) (A_{j \bmod F}^{(1)} \oplus B_{1j}^{(1)}) - \overline{P_{T_c}(t-jT_c)} (\overline{A_{j \bmod F}^{(1)} \oplus B_{1j}^{(1)}}) \right] dt \quad (3.15)$$

For analysis the above equation can be broken up into two terms, namely the required signal $b_m^{(n)}$ and the interference signal I_n , where $b_m^{(n)}$ is the m^{th} data bit of the n^{th} user, which can take two values, 0 or 1, with equal probability. Therefore we can represent equation 3.15 as

$$Z_1 = b_0^{(1)} K + \sum_{n=2}^N I_n^{(1)} \quad (3.16)$$

$$\text{or } Z_1 = b_0^{(1)} K + I_1 \quad ; \quad \text{where } K \text{ is the weight of the code.} \quad (3.17)$$

The interference or crosstalk, I_1 , arising at the output of the integrate and dump filter of user 1, using equation 3.11, can be expressed as:

$$I_1 = \frac{1}{T_c} \int_0^T I_1(t) [P_1(t) - \overline{P_1(t)}] dt \quad (3.18)$$

where

$$I_1(t) = \sum_{n=2}^N S_n(t). \quad (3.19)$$

Therefore, the interference can be written as:

$$I_1 = \sum_{j=0}^{F-1} V_j^{(1)} [C_j^{(1)} - \overline{C_j^{(1)}}] \quad (3.20)$$

where, $V_j^{(1)}$ is defined as

$$V_j^{(1)} = \frac{1}{T_c} \int_{jT_c}^{(j+1)T_c} I_1(t) dt. \quad (3.21)$$

However, since $\overline{C_j^{(1)}} = 1 - C_j^{(1)}$, we can write equation 3.20 as:

$$I_1 = \sum_{j=0}^{F-1} V_j^{(1)} [2C_j^{(1)} - 1]. \quad (3.22)$$

Substituting equations 3.21 and 3.1 in equation 3.22 and taking Ψ as the constant of integration we get,

$$I_1 = \Psi \sum_{j=0}^{F-1} \sum_{n=2}^N b_0^{(n)} \cdot C_j^{(n)} \cdot [2C_j^{(1)} - 1]. \quad (3.23)$$

The undesired signal I_1 is composed of $(n-1)$ interference signals $I^{(1)}_n$, where each $I^{(1)}_n$ is a random variable with mean $M^{(1)}_n$ and variance $\sigma_{I^{(1)}_n}^2$.

Since all the interference signals are distributed random variables, the mean and variance of interfering signal I_1 , for $2 \leq n \leq N$, can be written as:

$$M_{I_1} = \sum_{n=2}^N M_{I^{(1)}_n} \quad (3.24)$$

$$\sigma_{I_1}^2 = \sum_{n=2}^N \sigma_{I^{(1)}_n}^2. \quad (3.25)$$

3.4.1 Evaluation of the pdf for the interfering signal

To evaluate the pdf for the interfering signal I_1 , which is the main source of error in the receiver, we require the pdf associated with each $I^{(1)}_n$ for $2 \leq n \leq N$. Since there are N users and the interference $I^{(j)}_n$ at the output of the r^{th} receiver contains $(N-1)$ interference terms and also

$$I^{(j)}_n = I^{(n)}_r \quad \text{for all } 1 \leq n \text{ and } n \neq j, \quad (3.26)$$

a total of $N(N-1)/2$ pdfs will be required to find the exact probability density function of the interference. Since the exact calculation of the interference pdf is lengthy, we will evaluate here only the upper and lower bound for the pdf. This is in no way going to affect the operation of the FO-CDMA system since the system is designed for a synchronous case which is the lower bound for the pdf.

From simulation results it has been observed that for P-codes the interference caused by a particular code on a receiver is dependent on two factors:

- (1) Group number of the code, i.e., whether the transmitted code is a group 1 or a group 2 code.
- (2) Type of the receiver, i.e., depending on whether the local code of the receiver is a group 1 code or a group 2 code the receiver is classed as a type 1 or type 2 receiver.

It has already been listed in Table 2.3 that a group 1 code produces an interference of -1 when it is correlated in a type 1 receiver and an interference of +1 when it is correlated in a type 2 receiver. It has also been stated that a group 2 code does not produce any interference in any of the receivers. Thus we see that, for a particular type of receiver, there can be only two types of interferences that can be caused by any other code, i.e., an interference of -1 and 0 for a type 1 receiver and an interference of +1 and 0 for a type 2 receiver. In a type 1 receiver, as the interference increases, the value of the auto-correlation peak goes on decreasing causing the auto-correlation peak to come closer to the set threshold and the system performance deteriorates. Thus it is necessary to treat the negative interference in a type 1 receiver in the same way as positive interference as far as its influence on the system performance is considered, i.e., as a source of error.

We can define a generalized interference pattern with a probability density function expressed as :

$$P_I(I) = q \delta(I) + p \delta(I - 1) + r \delta(I + 1) + (1 - p - q - r) |T| \quad (3.27)$$

where I is a random variable associated with the above generalized interference pattern, and

$$q \equiv \Pr(I = 0), p \equiv \Pr(I = 1), r \equiv \Pr(I = -1) \text{ and } 1 - p - q - r \equiv \Pr(0 \leq |I| \leq 1).$$

However, depending on the type of the receiver being a (type 1 or a type 2) the value of 'p' or 'r' is equal to zero.

Considering a type 2 receiver the mean, M_I , and variance, σ_I^2 , for the random variable I can be written as,

$$M_I = E(I) = 0 \cdot \Pr(I=0) + 1 \cdot \Pr(I=1) + \int_0^1 I \cdot \Pr(0 < |I| < 1) dI \quad (3.28)$$

$$M_{I+1} = 0 + p + \frac{(1-p-q)}{2} = \frac{1+p-q}{2} \quad (3.29)$$

and,

$$\sigma_I^2 = E(I^2) - E^2(I) \quad (3.30)$$

$$E(I^2) = 0 + 1^2 \cdot p + \int_0^1 I^2 \cdot \Pr(0 < |I| < 1) dI \quad (3.31)$$

$$= 2 \cdot \frac{1^3}{3} \cdot \Pr(0 < |I| < 1) = p + \frac{1}{3} \cdot (1-p-q) = \frac{1+2p-q}{3} \quad (3.32)$$

Therefore,

$$\sigma_{I+1}^2 = q\left(\frac{1}{6} - \frac{q}{4}\right) + \frac{pq}{2} + p\left(\frac{1}{6} - \frac{p}{4}\right) + \frac{1}{12} \quad (3.33)$$

Similar analysis for the mean and the variance for a type 1 receiver yields the following expressions:

$$M_{I-1} = 0 + r + \frac{(1-r-q)}{2} = \frac{q-r-1}{2} \quad (3.34)$$

$$\sigma_{I-1}^2 = q\left(\frac{1}{6} - \frac{q}{4}\right) + \frac{rq}{2} + r\left(\frac{1}{6} - \frac{r}{4}\right) + \frac{1}{12} \quad (3.35)$$

Although we assume the system to be ideal and operating in synchronism in order to be able to support the maximum number of users, for purposes of complete analysis [9] we define the two extreme cases to derive the bounds. The two cases which set the bound (Figures 3.1 and 3.2) are :

- (A) *Chip synchronous*; i.e., assume that relative chips are in the same time slot. Thus, the shifts between any two chips of two transmitting stations is a multiple of the chip widths.
- (B) *Chip asynchronous*; i.e., assume that the relative position of chips are random. Thus, the shifts between any chip of the two transmitters is a fraction of the chip width.

The lower bound of the probability of error per bit is given by the results derived from case A and the upper bound is given by case B [3]. Thus,

$$P_e(\text{case A}) \leq P_e(\text{exact}) \leq P_e(\text{case B}) \quad (3.36)$$

Since P-codes work well in a synchronous system, an expression for the probability density function of the interfering signal for case A, with reference to the type of the receiver used for detection, is discussed.

Case A-1: Probability density function for the interference caused by signals on a type 1 receiver for the chip synchronous case

The interference caused by signals on a type 1 receiver, I_1 , is the sum of $N-1$ distributed random variables, $I_n^{(1)}$, which follows a binomial distribution.

From table 2.3 we see that the interference caused by the n^{th} user code on a type 1 receiver is either a '0' or a '-1'. An interference of '-1' is caused by a data '1' being transmitted with a group 1 code. The probability of $I_n^{(1)}$, interference of the n^{th} user on the 1st user, being a '-1' is denoted by r and is given by the expression,

$$r = \Pr(b_0^{(n)} = 1) \cdot \Pr(n^{\text{th}} \text{ user transmitted code is a group 1 code}) \quad (3.37)$$

where $b_0^{(n)}$ corresponds to the zeroth data of the n^{th} user which takes two values, 1 or 0, with equal probability.

There are $2^{n-1} - 1$ ($= K$) P-codes in group 1 out of a total of $2^n - 1$ ($= F$) P-codes that are supported by the system (Section 2.4.1). Thus, the probability of a group 1 code being transmitted by the n^{th} user is given by K/F .

$$\text{Therefore, } \Pr(\text{ } n^{\text{th}} \text{ user transmitted code is a group 1 code}) = \frac{K}{F} \quad (3.38)$$

and

$$\Pr(b_0^{(n)} = 1) = \frac{1}{2}. \quad (3.39)$$

Substituting equations 3.38 and 3.39 in equation 3.37 we have,

$$r = \frac{K}{2F} \quad (3.40)$$

The interference is a zero when either a '0' is transmitted or a data bit '1' is transmitted with a group 1 code. Thus, q , the probability of the interference being a '0' is given by the expression

$$q = \Pr(b_0^{(n)} = 0) + \Pr(b_0^{(n)} = 1) \cdot \Pr(\text{ } n^{\text{th}} \text{ user transmitted code is a group 2 code}) \quad (3.41)$$

Since there are $F-K$ group 2 P-codes out of a total of F P-codes, the probability of a group 2 code being transmitted is given by

$$\Pr(\text{ } n^{\text{th}} \text{ user transmitted code is a group 2 code}) = \frac{F-K}{F} \quad (3.42)$$

and the probability of the interference being a '0' is given by

$$q = \frac{1}{2} + \frac{1}{2} \cdot \left(\frac{F-K}{F} \right) = 1 - \frac{K}{2F} \quad (3.43)$$

Substituting the value of r and q from equations 3.40 and 3.43 in equation 3.27 along with the value for p and $|I|$ as a zero, the probability density function for $I_n^{(1)}$, is defined as :

$$P_{I_n^{(1)} | I_n^{(1)}} = \left(\frac{K}{2F} \right) \delta(I_n^{(1)} + 1) + \left(1 - \frac{K}{2F} \right) \delta(I_n^{(1)}) \quad (3.44)$$

For a case where there are more than one interfering user, the pdf of the interference can be found using similar analysis. However, since two transmitters cannot transmit to the same receiver, the transmitters that are accessing the channel must all be transmitting different codewords. For this condition, the total amount of interference at any particular receiver may be easily determined.

For $N-1$ interfering users, A of which are of the group 1 type and the remaining $N-1-A$ are of the group 2 type, the interference caused by $N-1$ users, I_1 , is the sum of the $N-1$ random variables $I_n^{(1)}$. Since the receiver is a type 1 receiver, the number of group 1 users that can access the channel is $K-1$ and hence, for full duplex transmission, the probability of ' A ' group 1 users being present among the $N-1$ users, where $A = 0, 1, 2, \dots, N-1$ for $N-1 \leq K-1$ and $0, 1, 2, \dots, K-1$ for $N-1 > K-1$, can be written as:

$$P(A) = \frac{{}^{K-1}C_A * {}^{F-K}C_{(N-1)-A}}{{}^{F-1}C_{(N-1)}} \quad (3.45)$$

Out of the A group 1 users transmitting at a particular instance, not all users transmit a data bit '1'. Depending on the number of group 1 users transmitting a data '1' and the fact that the interference I caused by a group 1 user in a group 1 receiver is negative, the interference ranges from 0 to $-A$. The probability that an interference I is caused at the receiver, when A group 1 users are accessing the channel, is given by the equation

$$P_{I,A} = \left[\frac{1}{2} \right]^A * {}^AC_I \quad (3.46)$$

The probability that 'A' number of group 1 users transmit and cause an interference I is denoted by $P(I_A)$, which is given by the equation,

$$P(I_A) = P_{I,A} * P(A). \quad (3.47)$$

From equation 3.45 and 3.46 we have,

$$P(I_A) = \sum_{I=0}^A \left[\frac{1}{2} \right]^A * A C_I * \frac{K-1 C_A * F-K C_{(N-1)-A}}{F-1 C_{(N-1)}} \delta(I_A + I) \quad (3.48)$$

The probability that the interference is I_1 is given by the sum of the probability of the interference I_A caused by the group 1 users, for $A = 0, 1, 2, \dots, N-1$ for $N-1 \leq K$ and $0, 1, 2, \dots, K$ for $N-1 > K$. Thus the probability density function of the interference I_1 caused at receiver #1 is given by :

$$P_{I_1}(I_1) = \sum_{A=0}^{N-1} \sum_{I=0}^A \left[\frac{1}{2} \right]^A * A C_I * \frac{K-1 C_A * F-K C_{(N-1)-A}}{F-1 C_{(N-1)}} \delta(I_1 + A) \delta(I_A + I) \quad \text{for } N-1 \leq K \quad (3.49)$$

and

$$P_{I_1}(I_1) = \sum_{A=N-16}^K \sum_{I=0}^A \left[\frac{1}{2} \right]^A * A C_I * \frac{K-1 C_A * F-K C_{(N-1)-A}}{F-1 C_{(N-1)}} \delta(I_1 + A) \delta(I_A + I) \quad \text{for } N-1 > K \quad (3.50)$$

Thus it can be seen that the pdf of the interference varies with the number of users. Figure 3.9 shows the pdf of the varying interference caused at a type 1 receiver when the number of users is 5, 10, 15, 20, 25 and 30.

Case A-2: Probability density function for the interference caused by signals on a type 2 receiver for the chip synchronous case

The analysis of the pdf for the interference caused in a type 2 receiver is the same as that for a type 1 receiver except for the fact that in a type 2 case, the

value of r , the probability that the interference is a '-1' becomes zero and the value of p , the probability that the interference is a '+1', is $K/2F$.

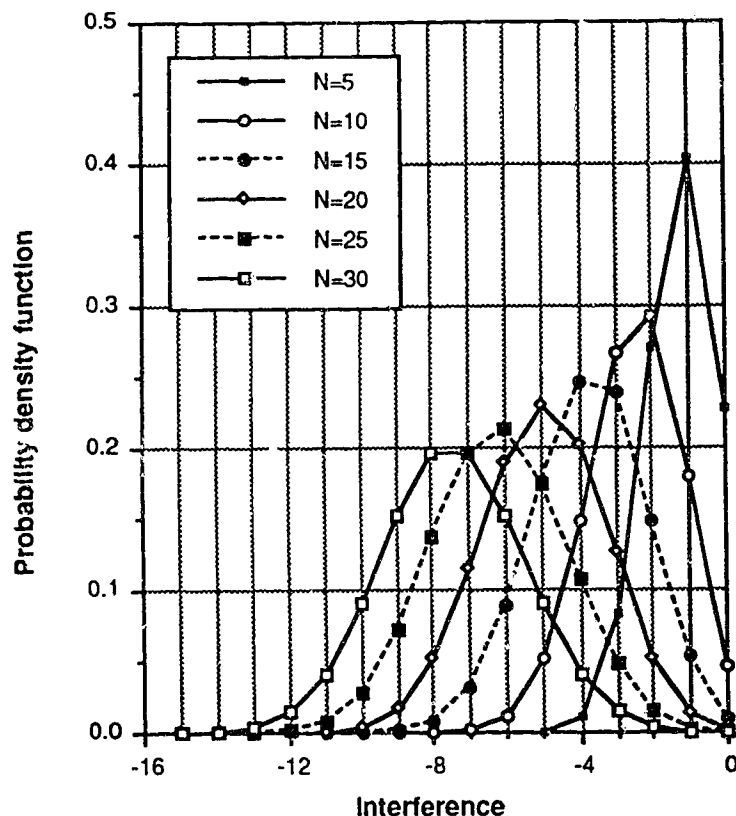


Fig. 3.9 Probability density function for the interference caused by varying number of users on a type 1 receiver.

The value of the probability density function for $I_n^{(1)}$, can be defined as :

$$P_{I_n^{(1)}}(I_n^{(1)}) = \left(\frac{K}{2F}\right) \delta(I_n^{(1)} - 1) + \left(1 - \frac{K}{2F}\right) \delta(I_n^{(1)}) \quad (3.51)$$

The pdf for the interference caused at a receiver by N transmitters is calculated by applying the same analysis as is used for the Case A-1 and is shown in Figure 3.10. Since the receiver is a type 2 receiver, the number of group 1 and group 2 codes that can cause an interference is K and $F-K-1$

respectively. It is seen that the interference caused at the receiver is positive and is given by:

$$P_{I_1}(I_1) = \sum_{A=0}^{N-1} \sum_{l=0}^A \left[\frac{1}{2} \right]^{A-A} C_l \cdot \frac{K C_A \cdot F - K-1 C_{(N-1)-A} \delta(I_1 - A) \delta(I_A - l)}{F-1 C_{(N-1)}} \quad \text{for } N-1 \leq K \quad (3.52)$$

and

$$P_{I_1}(I_1) = \sum_{A=N-1}^K \sum_{l=0}^A \left[\frac{1}{2} \right]^{A-A} C_l \cdot \frac{K C_A \cdot F - K-1 C_{(N-1)-A} \delta(I_1 - A) \delta(I_A - l)}{F-1 C_{(N-1)}} \quad \text{for } N-1 > K \quad (3.53)$$

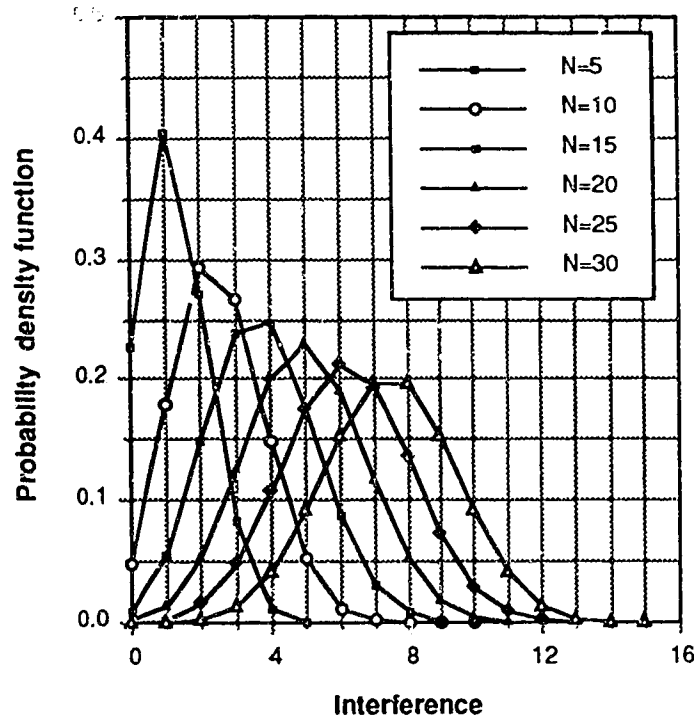


Fig. 3.10 Probability density function for the interference caused by varying number of users on a type 2 receiver.

3.4.2 Probability of error

The probability of error per bit (P_e) is defined as the average probability of error, and is given by :

$$P_e = P \left(Z_1 \geq Th / b_0^{(1)} = 0 \right) \cdot P \left(b_0^{(1)} = 0 \right) + P \left(Z_1 < Th / b_0^{(1)} = 1 \right) \cdot P \left(b_0^{(1)} = 1 \right) \quad (3.54)$$

where Th is the threshold level in the detector.

The second term of the above equation is a zero for $0 \leq Th \leq K$, because:

$$\Pr(Z_1 < Th / b_0^{(1)} = 1) = \Pr(K - Th + I_1 < 0) = \Pr(\eta < 0) \quad (3.55)$$

where $\eta = K - Th + I_1$ and is non-negative. Therefore, the probability of error when $b_0^{(1)} = 1$ is zero. Thus the exact probability of error per bit is given by :

$$P_e = P(Z_1 \geq Th / b_0^{(1)} = 0) \cdot P(b_0^{(1)} = 0) \quad (3.56)$$

or,

$$P_e = \frac{1}{2} \int_{Th}^{\infty} P_{I_1}(I_1) dI_1 \quad (3.57)$$

where,

$$I_1 = \sum_{n=2}^N I_n. \quad (3.58)$$

For the chip synchronous case, and at a type 1 receiver, substituting equation 3.45 to equation 3.57, the probability of error can be expressed as ,

$$PE = \frac{1}{2} \cdot \sum_{A=th}^{N-1} \sum_{l=0}^A \left[\frac{1}{2} \right]^A \cdot A_{C_l} \cdot \frac{K-1 C_A \cdot F-K C_{(N-1)-A}}{F-1 C_{(N-1)}} \quad \text{for } N-1 \leq K \quad (3.59)$$

and

$$PE = \frac{1}{2} \cdot \sum_{\substack{A=th \\ (A > N-16)}}^K \sum_{l=0}^A \left[\frac{1}{2} \right]^A \cdot A_{C_l} \cdot \frac{K-1 C_A \cdot F-K C_{(N-1)-A}}{F-1 C_{(N-1)}} \quad \text{for } N-1 > K \quad (3.60)$$

The probability of error for a synchronous case and at a type 2 receiver is given by:

$$PE = \frac{1}{2} \cdot \sum_{A=th}^{N-1} \sum_{l=0}^A \left[\frac{1}{2} \right]^A \cdot A_{C_l} \cdot \frac{K C_A \cdot F-K-1 C_{(N-1)-A}}{F-1 C_{(N-1)}} \quad \text{for } N-1 \leq K \quad (3.61)$$

and

$$PE = \frac{1}{2} * \sum_{\substack{A=th \\ (A > N-16)}}^K \sum_{l=0}^A \left[\frac{1}{2} \right]^A * A C_l * \frac{K C_A * F - K - 1 C_{(N-1)} - A}{F - 1 C_{(N-1)}} \quad (3.62)$$

for $N-1 > K$

The probability of error and the bit error rate results obtained from the simulations are shown in Figure 3.11 and 3.12 respectively.

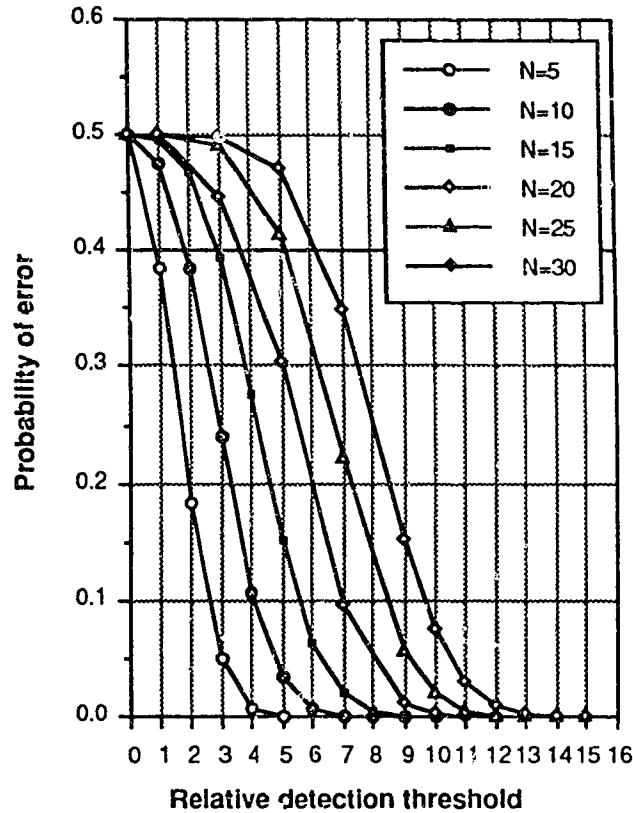


Fig. 3.11 Variation of the probability of error with the detection threshold for varying number of users.

It is seen from Figure 3.12 that a BER of 10^{-9} can be maintained provided that the detection threshold is varied as the number of users increases. The BER falls to zero after the threshold value of 15 since the maximum interference caused at the receiver by other users is equal to 15. Thus, using a dynamic detection mechanism and P-codes as CDMA sequences, error free communication can be achieved. Hence, from simulation results, we can

conclude that it is possible to achieve an error rate close to zero in a FO-CDMA system using P-codes for spreading even with a large number of simultaneous users .

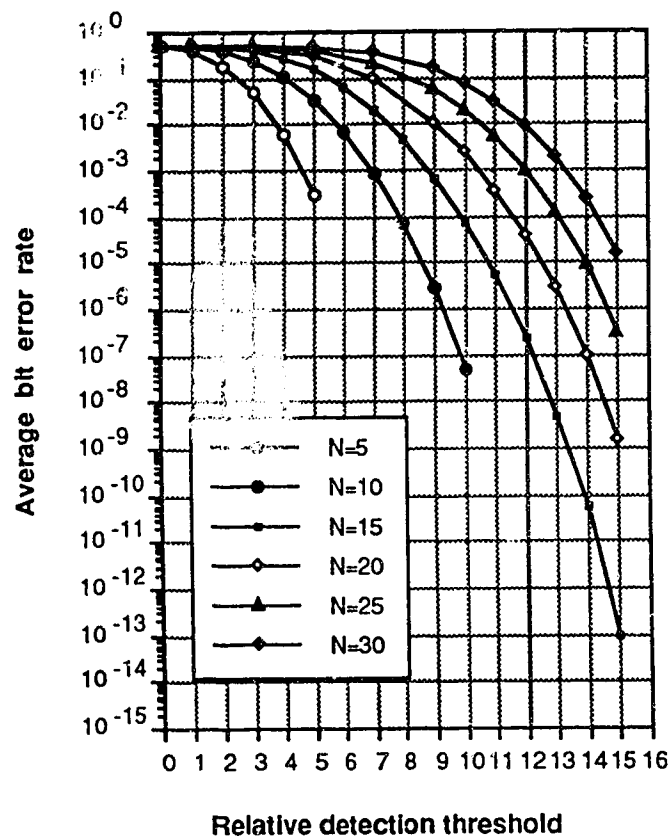


Fig. 3.12 Variation of the bit error rate with the detection threshold for a varying number of users.

CHAPTER 4

EXPERIMENTAL SYSTEM

In this chapter, the experimental system that was set up to test FO-CDMA using P-codes is described. The experimental system permits two simultaneous users to gain access to the channel, using a star configuration. Figure 4.1 shows the block diagram of the experimental system. It consists of two transmitting stations, a 2X2 optical coupler, an optical fibre channel, an optical attenuator and a receiving station. Upgrading of the system to allow a higher number of users can be achieved by replacing the 2X2 coupler with an nXn coupler, where n is the number of users.

4.1 Introduction

Each transmitting station of the FO-CDMA link contains a clock generator, a P-code generator, an encoder and a laser transmitter. The clock, operating at the chip rate, is generated by a HP-8116 A Pulse/Function generator. The HP-3780 A Pattern / Error Detector is used as a data generator and also as an error detector. The receiving station consists of a PIN detector and preamplifier, followed by a main amplifier and a correlator. The correlator contains the local P-code generator, a comparator and a data clock phase shifter.

The operation of the system can be described as follows: RZ clock pulses, at a rate of 49.4 Mbits/s, are generated by the HP 8116 A pulse generator. These clock pulses, at the chip rate, are also referred to as the system clock. The system clock is fed into the code generator which houses the 32 and 1 chip counter along with the code generator. A countdown circuit within the P-code generator generates the RZ data clock at a rate equal to the system

clock divided by 32, i.e., 1.54375 Mb/s. At the same time two trigger pulses, namely the 32nd and i^{th} pulses, are generated in the counter circuit. The i^{th} pulse triggers the P-code generator to generate the P-code of the intended receiver while the 32nd pulse is used as a trigger and synchronization pulse. The data clock and the system clock, along with the two pulses are distributed to other parts of the code generator and the encoder unit. The data clock is also supplied to the HP-3780 A Pattern generator/Error detector as an external clock for the data generator.

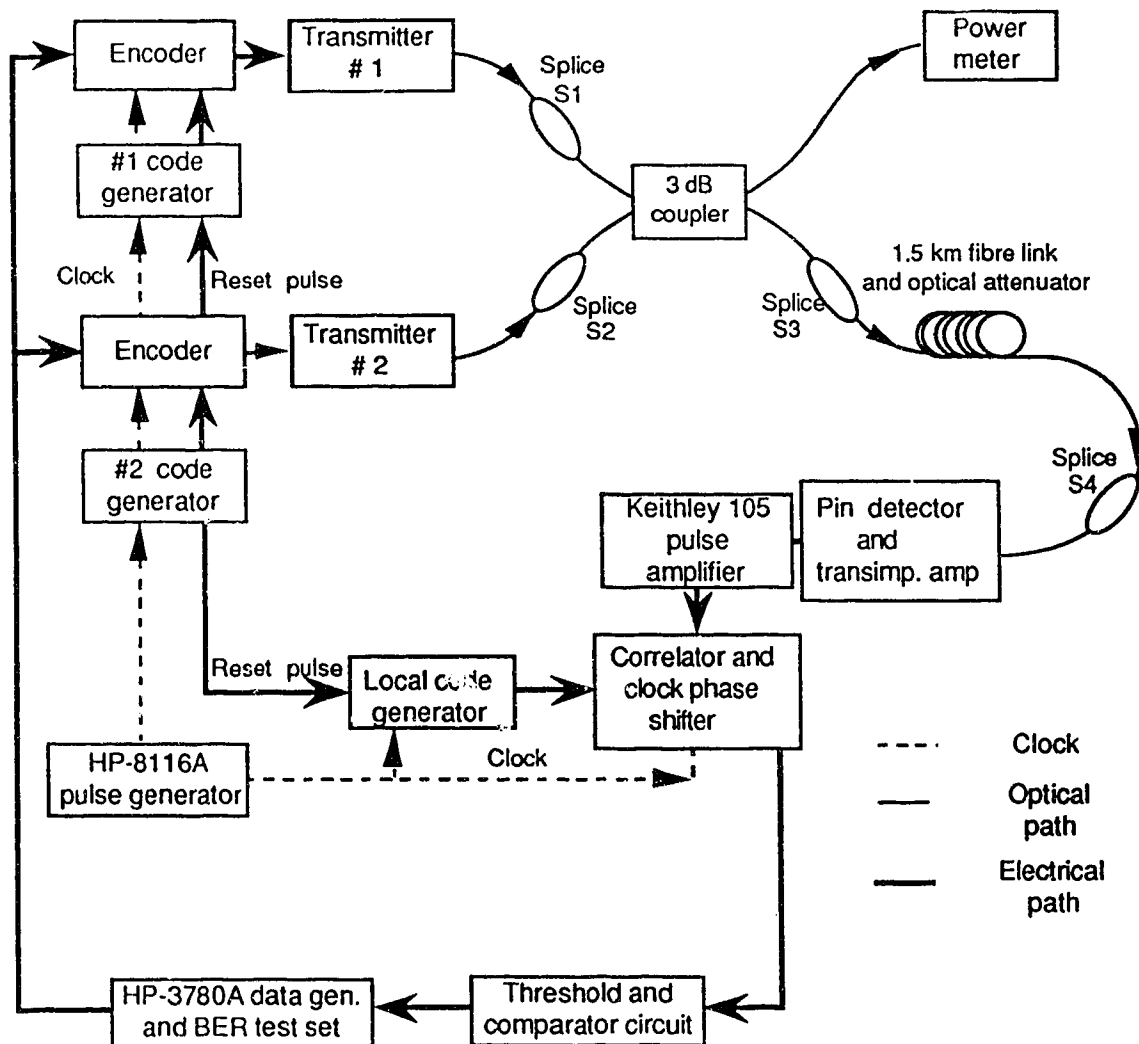


Fig. 4.1 Experimental layout of the FO-CDMA system.

Data generated by the pattern generator is coupled into the encoder, where it is modulated with the P-code coming from the P-code generator. The data stream is encoded by multiplying the data stream by the code. Multiplication was chosen so that the data bit '1' could be encoded with the P-code while the data bit '0' could stay as a zero. The output of the encoder, the coded data stream, is coupled to the laser modulator circuitry of the laser transmitter. Current flowing through the laser is modulated by the coded data and the varying optical output from the laser is coupled into one of the inputs of the 2X2 optical coupler. The other input of the coupler is spliced to the laser pigtail of the other transmitter.

One of the two output pigtails of the coupler is spliced to a 1.5 km length of single mode fibre whose other end of the single mode fibre is spliced to the pin detector. The other output of the coupler is connected to a power meter to monitor the total power in the channel. Optical attenuation is provided in front of the detector by introducing micro bends into the single mode fibre. This is done so as to prevent saturation of the detector and pre-amplifier. The detected signal is amplified 20 db by a Keithley 105 pulse amplifier and the amplified output is applied to the correlator.

For convenience, the data clock generated at the transmitter is fed to the local signal generator at the receiver. The local P-code sequence at the output of the local code generator, is phase shifted so as to be synchronous with the received coded data. The local P-code sequence, in synchronization with the received signal, is applied to the correlator. In the correlator, a correlation between the received coded data, the output from the amplifier, and the local P-code sequence is made on a chip by chip basis. The output of the correlator is sent to an integrate and dump filter. Here the signal is integrated for 31 chip

intervals using a capacitor and then dumped during the 32nd time slot. The dumped voltage is compared with the preset detection threshold voltage in the comparator and a decision is made as to whether the transmitted data bit is a '1' or a '0'. This regenerated signal is stored for one data period in the D flip-flop.

The output from the D flip-flop is coupled into the HP-3780 A Pattern generator. Here, a measurement of the bit error rate is made in order to monitor the performance of the system.

4.2 Transmitter

The transmitter for the experimental FO-CDMA network consists of the following subunits: a pulse generator, also referred to as the system clock generator, a P-code generator, an encoder, a pseudo-random data generator, a laser modulator, a laser driver cooler and a semiconductor laser. A discussion of the functions of each of the above subunits along with their operation is made in the following section.

4.2.1 Clock generator

A HP-8116 A Pulse / Function generator is used as the clock generator. It is adjusted in order to generate a square wave at a frequency of 49.4 MHz, which is very close to the theoretically required frequency of 49.408 MHz for transmitting a 32 chip CDMA encoded DS1 signal.(1.544 Mb/s) This clock signal is fed to the two transmitters, and, in the experimental work of this thesis, also to the receiver. In an actual local area network, it would be necessary to use a clock recovery circuit to generate the clock at the receiver.

4.2.2. Code generator

A code generator capable of generating a set of P-codes, each of length $N=31$ chips, was designed and constructed. Individual code generators were constructed for both transmitters. A block diagram of the code generator is shown in Figure 4.2. The code generator circuit consists of two main sub-circuits; the counter and the P-code generator. The counter provides certain fixed delays to the system clock in order to generate the 32nd and the i th pulses. It also generates the data clock at a rate $1/32$ times that of the system clock. The P-code generator, generates the preferred m-sequence, with a delay $i = 31-n$. Since the code is cyclic, a delay of $31-n$ is equivalent to a left shift of n where n is the number of the P-code sequence being generated.

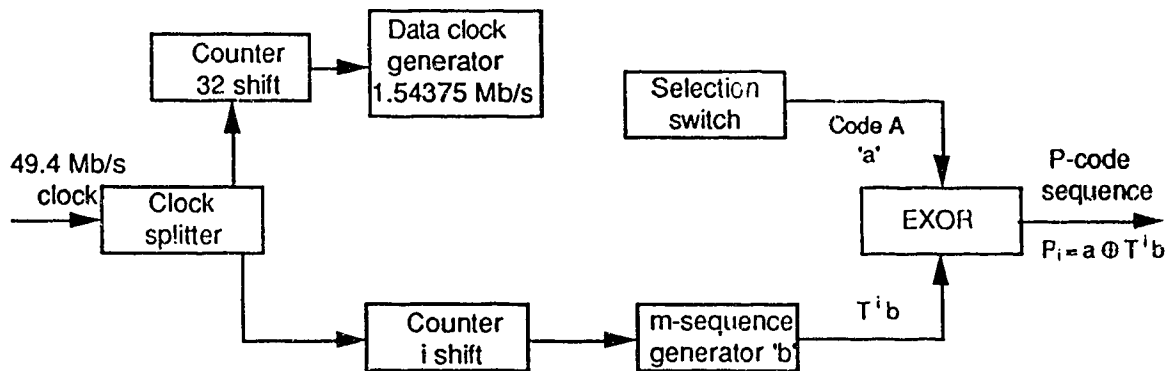


Fig. 4.2 Block diagram of the code generator

A schematic circuit for the code generator is shown in Figure 4.3. It is designed using both high speed TTL and ECL components. The generator consists of three main blocks. The schematics for these blocks, i.e., the 32 counter, the i counter and the $[5,4,3,2]$ m-sequence, are discussed later. A 32nd pulse is also generated by the counter and is used to generate the dumped clock.

It is important that the system be reset when it is switched 'ON'. The code generator has a push button switch, SW1, which is used to reset the D flip-flops (IC 74F74) in the circuit. When the switch is depressed, the capacitor C1 is shorted and the potential at the reset pins of the D flip-flops, D1A and D1B, makes a transition to a logic low. A direct consequence of this operation is that the output (pin 5) of the flip-flop D1A goes low and thus resets the D flip-flops, D2A and D2B. This prompts the input to the counter circuit to go to a logic low state. The output of the counter goes low and consequently the output of the code generator makes a transition to a logic low. On releasing the reset switch SW1, the capacitor starts charging and attains a logic high voltage. The two D

flip-flops D1A and D1B, damp the transients that occur when the reset switch is released and provide a trigger pulse (rising edge) to the system.

The system clock, at a rate of 49.4 Mb/s, drives all the circuits. The clock is distributed in the system using TTL inverters, IC 74F04, as fixed delays of around 1.5 nsec. The 32 chip counter and the i counter are both triggered at the same time by the rising edge of the trigger pulse and generate the 32nd and the i^{th} trigger pulse respectively. The 32nd trigger pulse is also referred to as the 0th pulse since it is generated by a modulo-32 counter. It is in the 32 chip counter that the system clock is divided by 32 to generate the data clock. Hence, the 32 chip counter is sometimes referred to as the data clock generator.

The counter circuit in Figure 4.4 consists of two modulo-32 counters, the 32 counter and i counter. Each modulo-32 counter is made up of a series combination of two modulo-16 counters U1, U2 and U3, U4 respectively. The intended receiver's number n is selected using the 5 bit DIP switch, SW DIP-5. The code for the receiver is $i = 32 - n$ and is generated by shifting the generating m-sequence code i bits to the left or $31 - i$ bits to the right. Figure 4.5 illustrates the fact that in a cyclic code of length 31, a n chip shift of the code to the left is equivalent to a $31 - n$ chip shift of the code to the right and vice versa. Since in the generator circuit used the code is shifted to the right, the switch is set to a binary value $31 - n$ in order to generate the code for the receiver n . The counters, U3 and U4, are controlled by the switch and provide the i^{th} trigger pulse (i is any integer value between 0 and 30). A series of AND gates, 74F08, are used to synchronize the trigger pulse with the rising edge of the clock. The 32nd trigger pulse or the 0th trigger pulse is produced by the counters, U1 and U2. The data clock waveform is obtained at pin 3 of the counter U2. This is a square wave

with a rate $1/32$ that of the system clock. (Figure 4.6) Thus the i^{th} and the 0^{th} pulses, and the data clock are the output waveforms of the counter circuits.

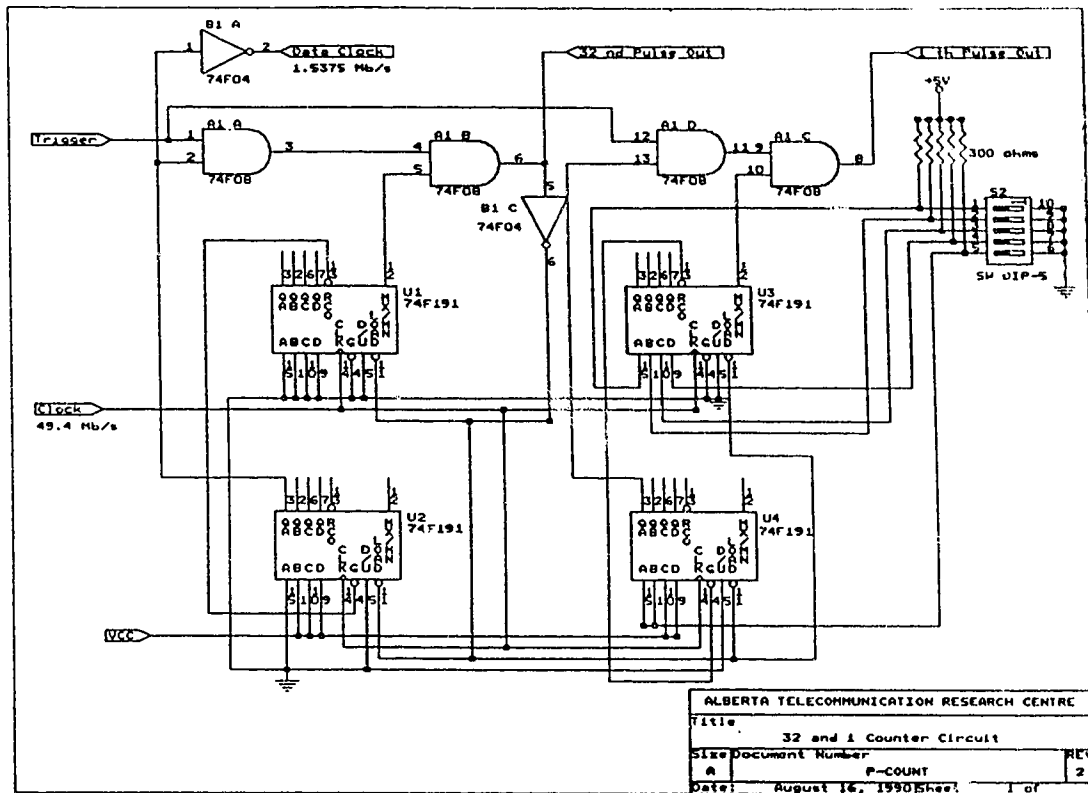


Fig. 4.4 Circuit schematic for the counter

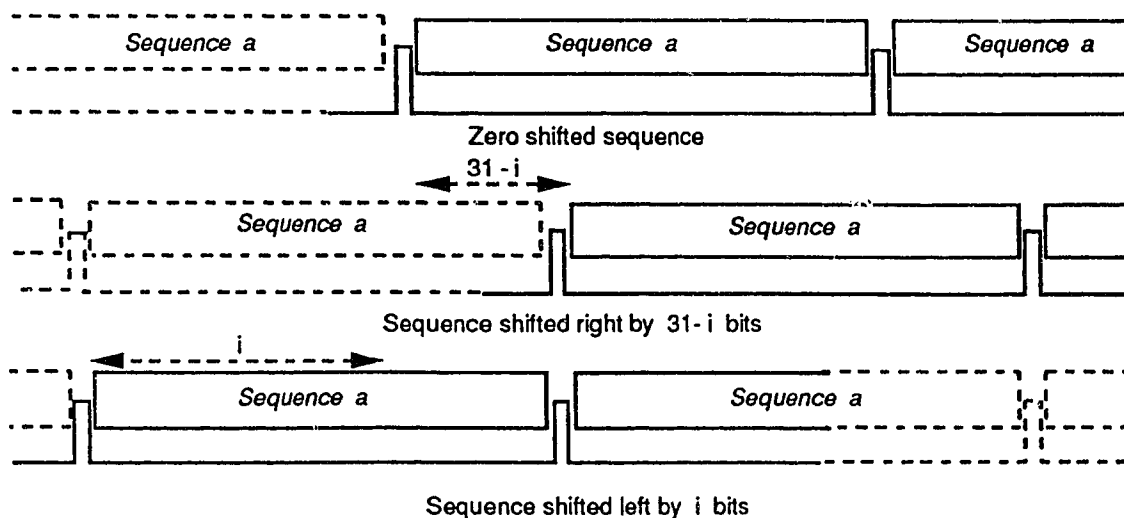


Fig. 4.5 Cyclic shifting of codes

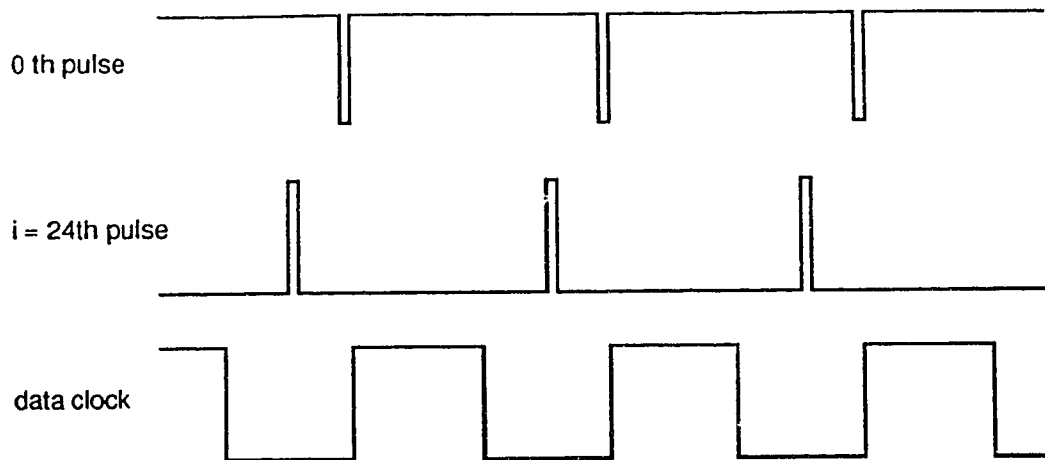


Fig. 4.6 Illustration of the 0th, $i = 24^{\text{th}}$ and the data clock

Delays are incurred in the counter proportional to the magnitude of the number being counted. As the value of n (the intended receiver number) changes, so does the value of the shift i . Thus the system delays vary according to the address of the intended receiver. In order to avoid system errors due to delay, the system has to be made insensitive to such variations by synchronizing the clock pulses to the system clock. Synchronization of the i^{th} pulse with the rising edge of the system clock is achieved by using the flip-flop D2B. The 0th pulse is synchronized with the rising edge of the system clock by using the D flip-flop D2A and TTL signal inverters as delays. Figure 4.6 shows the 0th pulse, the i equal to 24th pulse and the data clock generated from the counter circuitry. It is apparent that the data clock is in synchronism with the 0th pulse.

In Figure 4.3 the synchronized 32nd pulse, which is the output signal from the flip-flop D2B, is applied to the input of two ICs A2B and A2C. The output from these two AND gates is fed to the IC O1A to produce a dumped clock which is at the system rate of 49.4 Mb/s but has the 0th, 32nd, 2·32nd . . . $n \cdot 32^{\text{nd}}$ chips in the clock sequence dumped. The dumped wave at the output of

O1A is shown in Figure 4.7. The ICs B2A, B2B, B2C, A2D and B3A produce the i^{th} trigger pulse at the output of B3B, in synchronism with the dumped clock, at the output of O1A. The dumped clock along with the i^{th} clock is coupled into the P-code generator, which generates the P-code of the intended receiver.

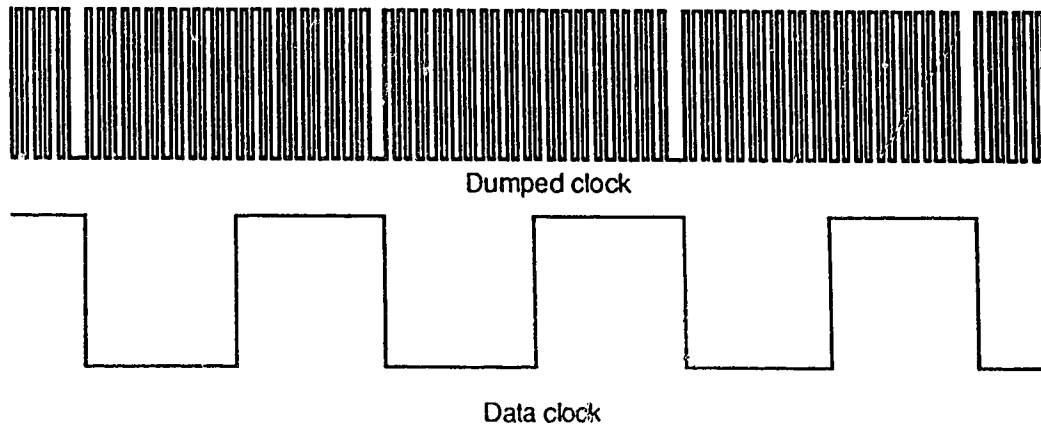


Fig. 4.7 Illustration of the dumped clock

P-codes are generated from two preferred m-sequences, the [5,3] and the [5,4,3,2] m-sequences. The [5,3] sequence are referred to as code A and the [5,4,3,2] sequence as code B. In order to experimentally generate the i^{th} P-code a modulo-2 addition of the i^{th} chip of code A with the i left shifted version of code B, T_i^b , is performed. The value of the i^{th} chip of code A is predetermined and this binary value, referred to as code A 'a', can be set by the switch SW-SPST in Figure 4.3. Meanwhile, code B is generated by a shift register with the feedback taken from the 2nd, 3rd, 4th and 5th stages of the shift register as shown in Figure 4.8.

The circuit for the generation of the code B and the P-code is shown in Figure 4.9. As is seen from Figure 4.3, the TTL signal is converted to an ECL signal before being coupled into the transmitter code generator. This is done

due to the fact that the code generator is constructed using all ECL devices. The reason for using ECL components is that the gate delays associated with ECL modulo-2 adders [35] [36] are very small, on the order of 1.5 nsec, as compared to the delay using TTL modulo-2 adders [37]. TTL shift register have a much larger delay time and thus cannot be used to produce a cyclical sequence at the 49.4 Mb/s chip rate.

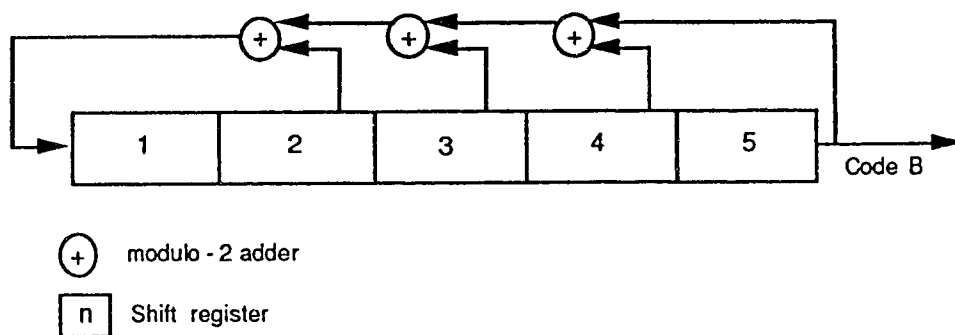


Fig. 4.8 Block diagram of the code B generator

The code generator circuit comprises two four-bit universal shift registers, U1 and U2, and three modulo-2 adders E1, E2 and E3. The shift registers are initialized to an all one state and the dumped clock is used to drive the system. When the i^{th} trigger pulse goes low, S2 goes low and enables the data to shift left for every clock pulse. At the i^{th} , $32+i^{\text{th}}$, $2 \cdot 32+i^{\text{th}}$. . . $n \cdot 32+i^{\text{th}}$ time slots, S2 is a logic high and this stops the shifting process. Thus an i chip shift of code B, T^{ib} , is achieved which is modulo-2 added with the code A to generate the P-code of length 31. The generated P-code sequence is in an ECL signal and is changed to a TTL format using a ECL to TTL converter.

The P-code generated for the intended receiver is coupled to an encoder where it modulates the incoming data to generate the coded data stream.

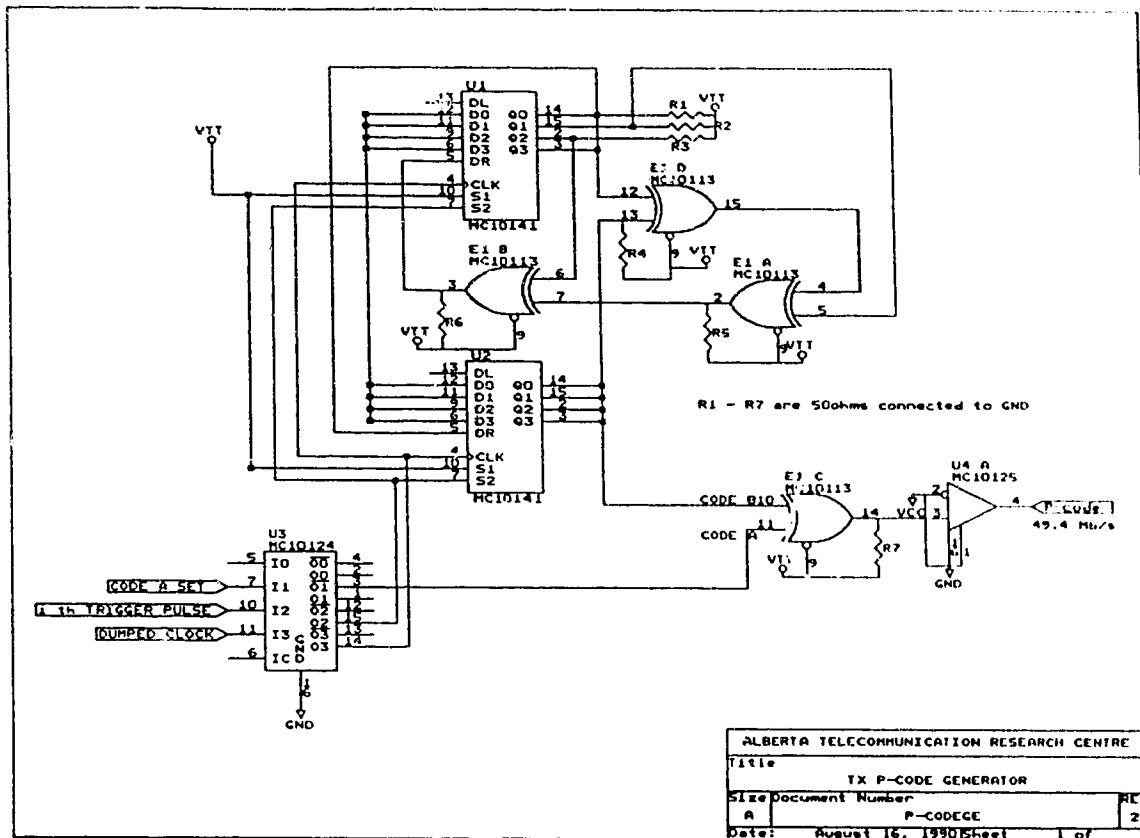


Fig. 4.9 Circuit schematic for the transmitter P-code generator

4.2.3. Encoder

As stated earlier, sequences from the pseudo-random data generator are modulated by the P-code from the code generator in the encoder. Figure 4.10 shows the diagram of the encoder. The D flip-flops D1A, D1B and D2A are used to synchronize the signals to the system clock at the chip rate of 49.4 Mb/s. The preset pulse, also referred to as the trigger pulse, is the output of the D flip-flop D1B in the code generator circuit of Figure 4.3 and is used to enable the D flip-flops.

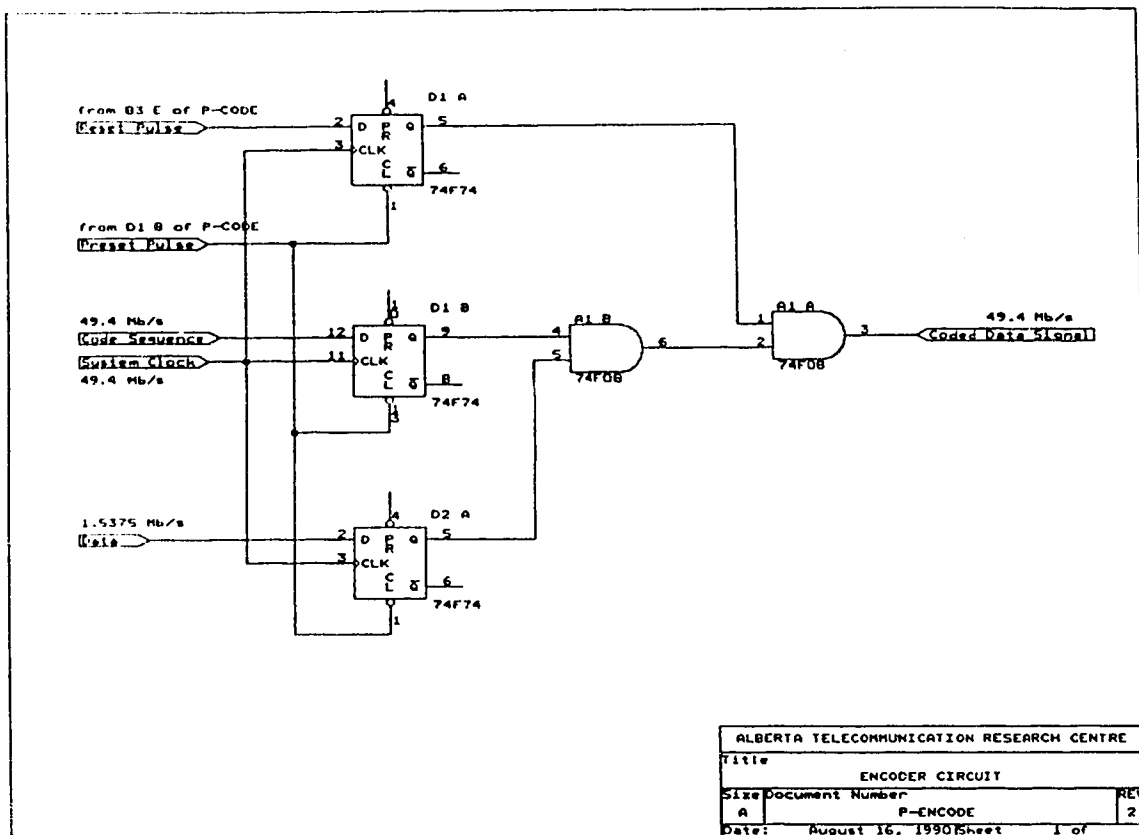


Fig. 4.10 Circuit diagram of the encoder

The P-code sequence at the output of the D flip-flop D1B is coupled to an AND gate A1 along with the pseudo-random data, the output of the D flip-flop D2A to generate the coded data sequence. Thus a data bit of '1' is coded with the P-code of the intended receiver; a data bit of '0' remains a zero. This coded signal is sent as an input to the AND gate A2 where it is synchronized with the reset pulse which is the inverted 32nd pulse. Figure 4.11 shows a '1010' input data sequence to the encoder, the coded output and along the synchronizing reset pulse. This coded data output is coupled into the laser driver circuit to modulate the current flowing through the laser diode.

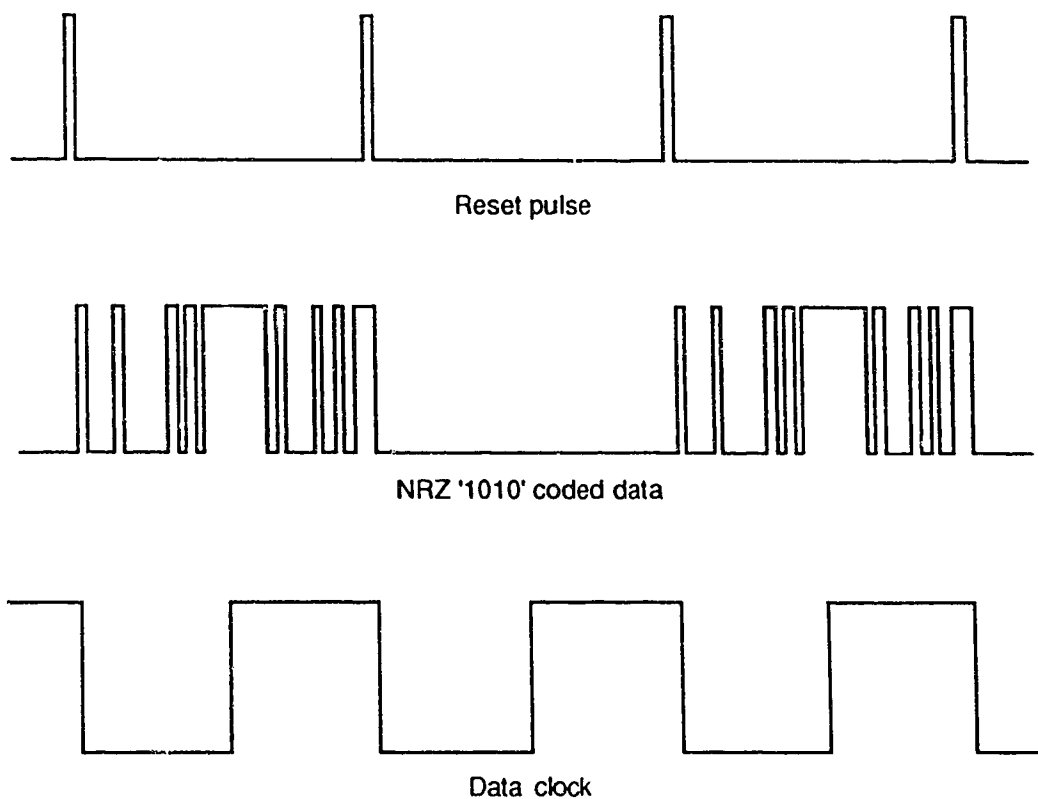


Fig. 4.11 Illustration of a '1010' coded data sequence and the reset pulse

4.2.4 Laser driver and modulator circuit

In the system used for FO-CDMA the laser driver consists of two main circuits, the laser diode modulation circuit and the laser diode temperature control circuit. In order to explain the operation of the above circuits a brief description of the laser packages used in the system is made.

The system has two transmitters with a dedicated laser for each transmitter. The two packaged lasers have a laser diode (LD) chip, a thermoelectric (TE) cooler, a thermistor, a monitoring photodiode and confocal coupling to a fibre pigtail. A LASER DIODE INC. 1300-09632 LD having a wavelength of 1309 nm is used by the first station. It has a threshold current of

15.2 mA and can produce a maximum output power of 0.6 mW, at the fibre. The second station has a NORTHERN TELECOM PBH-4317-32 LD with a wavelength of 1309 nm, a threshold current of 39.2 mA and a maximum output power of 0.6 mW, at the fibre.(APPENDIX F) Both laser diodes can be modulated to a speed of 800 Mb/s and have single mode fibre pigtail outputs.

The two LDs are intensity modulated (IM) by the variation of the current flowing through the laser diode which is proportional to the 49.4 Mb/s coded NRZ data signal. Extreme care is taken to ensure that the instantaneous LD driver current never exceeded the maximum safe operating current. There are two situations when the current in a driver circuit might exceed the safe limit, namely, when the modulator itself is overdriven or when the driver breaks into oscillations [38]. The LD modulation circuits in our system are designed using constant current sources, thus limiting the maximum possible current to a safe value. The circuits are shown in Figure 4.12 and 4.13 and are slightly different due to the different laser package specifications for the laser bias voltage and current.

The laser modulation circuit comprises a differential amplifier which is supplied with constant current sources. The output current (I_{out}) in the mirror can be adjusted, in terms of the reference current (I_{ref}) by employing a resistor-ratioed (Widlar) current source [39]. The advantage of using a Widlar current source is that a large number of low-value constant-current stages can be driven from a single current reference [40]. Another advantage of using such a configuration is that it has an output resistance R_{out} approximately β times that of an ordinary current mirror. The Widlar current mirror is shown in Figure 4.14.

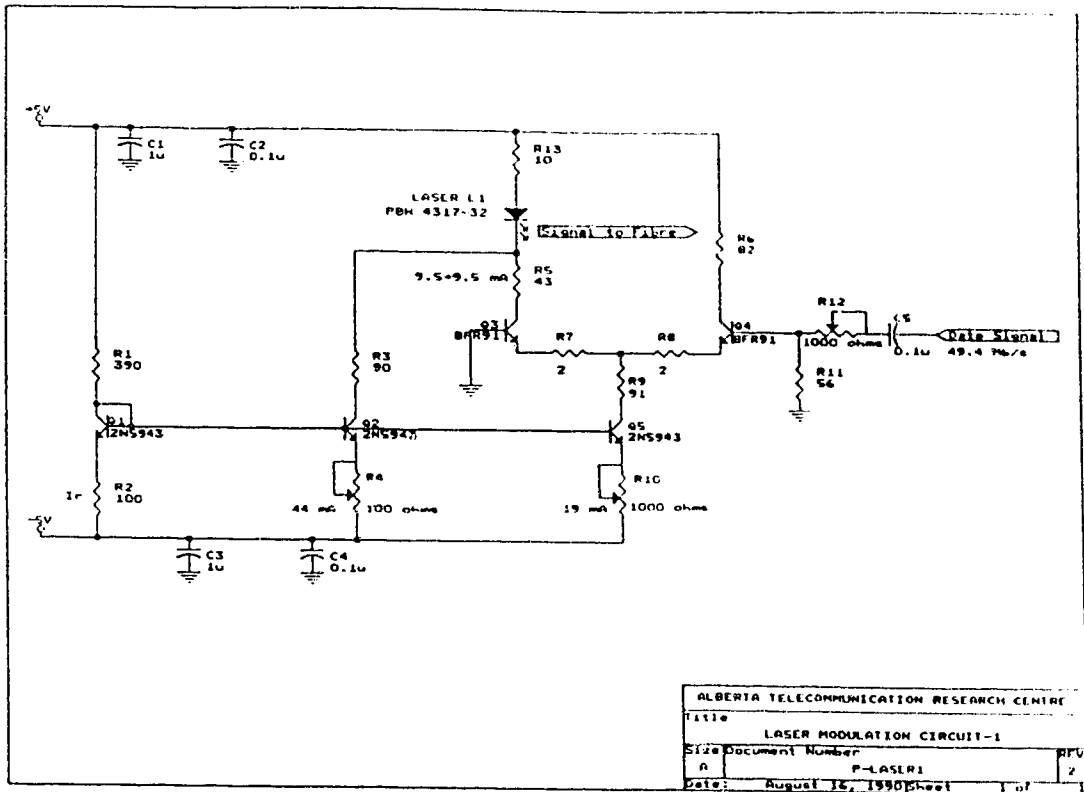


Fig. 4.12 Laser diode modulation circuit for transmitter #1.

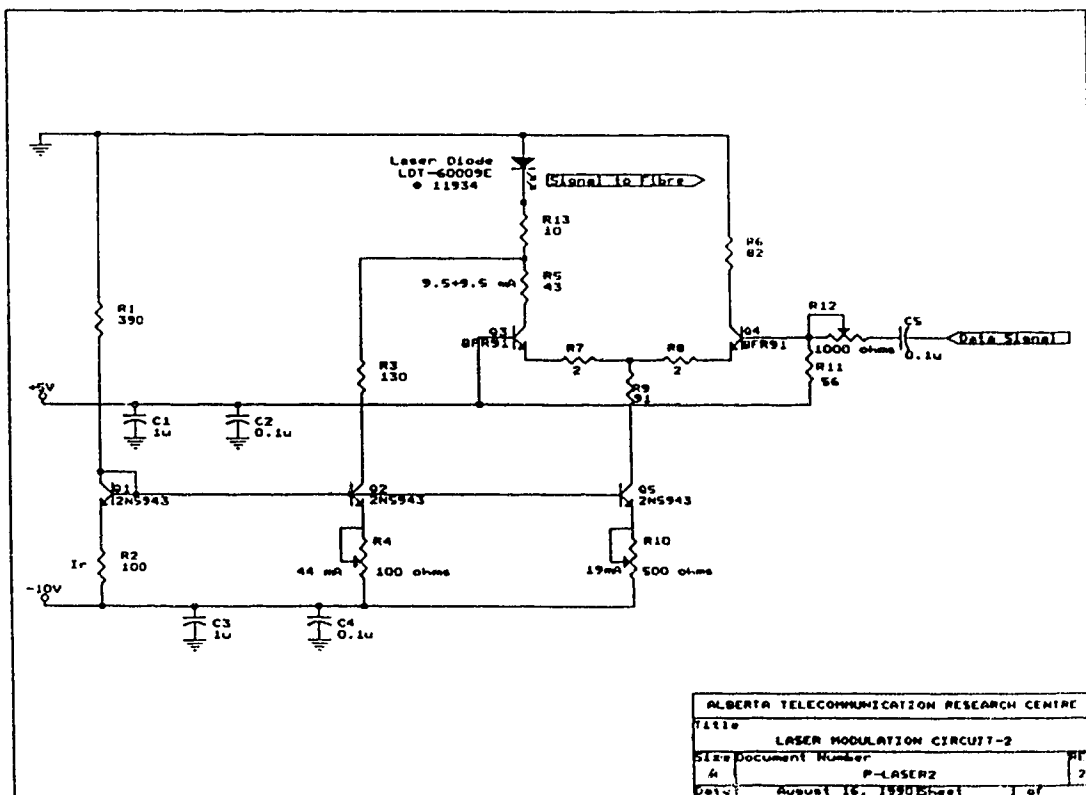


Fig. 4.13 Laser diode modulation circuit for transmitter #2.

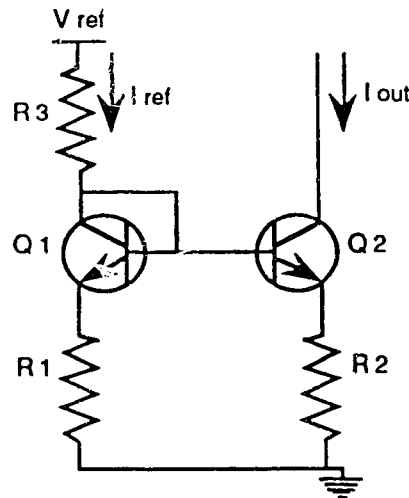


Fig. 4.14 Widlar current mirror circuit.

The two low-value current sources are driven from a single reference and allow precise control of the laser bias current and the modulation depth of the laser diode. The output current at the collector of Q2 and Q5 is given by [41]

$$I_{C2} \equiv I_{ref} R_2 / R_4 \quad (4.1)$$

$$I_{C5} \equiv I_{ref} R_2 / R_{10} \quad (4.2)$$

The collector current I_{C2} , flows through the resistor R_3 and the LD and is used to set the bias current for the laser. When R_1 and R_2 are fixed, changing R_4 changes the bias current of the LD's. At the same time changing R_{10} causes a change in the modulating current. Thus varying R_4 and R_{10} , the output optical power of the LD's can be adjusted. The value of R_4 and R_{10} for the two circuits are different due to the different laser bias and modulation current required to produce the same output optical power from the two LD circuits.

Meanwhile the transistor Q5 acts as a constant current source for the matched differential pair Q3 and Q4. Under quiescent conditions ($V_{i3} = V_{i4} = 0$) the collector currents of both Q3 and Q4 are equal to $I_{C5}/2$. When an input high

signal is applied to V_{i4} , Q4 goes 'ON' and the collector current I_{C4} increases thus decreasing I_{C3} . However, when an input low signal is applied, Q4 is at cutoff and all the current I_{C5} flows through the collector of Q3.

The emitter resistors (R7 and R8) of Q3 and Q4 are included in series with the emitters of the transistors in order to increase the range of input voltage over which the emitter coupled pair behaves approximately as a linear-amplifier. These resistors known as emitter degeneration resistors improve the distortion performance of the LD transmitters [42]. The collector resistor of Q2, Q3, Q4, and Q5 are used to decrease the collector emitter voltages, and hence reduce the power dissipation in these transistors to a permissible level. However, the values are such that none of the transistors is driven into saturation, even under conditions of maximum modulation of the differential amplifier. The peak-to-peak current modulation of the LD is limited by the current variation through the collector of Q5 and is equal to the maximum swing in the current I_{C5} .

The laser diode temperature control circuit makes up part of the laser diode circuit and is shown in Figure 4.15. When the laser is cool, the bridge circuit comprising of resistors R1 to R5 is balanced and the two output voltages (V_2 and V_3) to the operational amplifier U2 are equal. As the laser is modulated it starts to heat up and the resistance R_{T1} of the thermistor decreases causing the bridge to become unbalanced. The differential amplifier, U2, amplifies the difference between V_2 and V_3 , to generate the output V_6 which is fed as the input voltage to a base-current compensated voltage controlled current source. The output current I_c at the collector of transistor Q2 flows through the peltier cooler and cools the laser and the thermistor. This cooling causes an increase in the thermistor resistance (APPENDIX F), thus increasing V_2 , and in turn

decreasing V_6 and I_c . Therefore, the voltage V_3 is set by the adjusting the resistance R_2 in such a way that the the current I_c flowing through the cooler is sufficient enough to maintain the laser at its proper operating temperature.

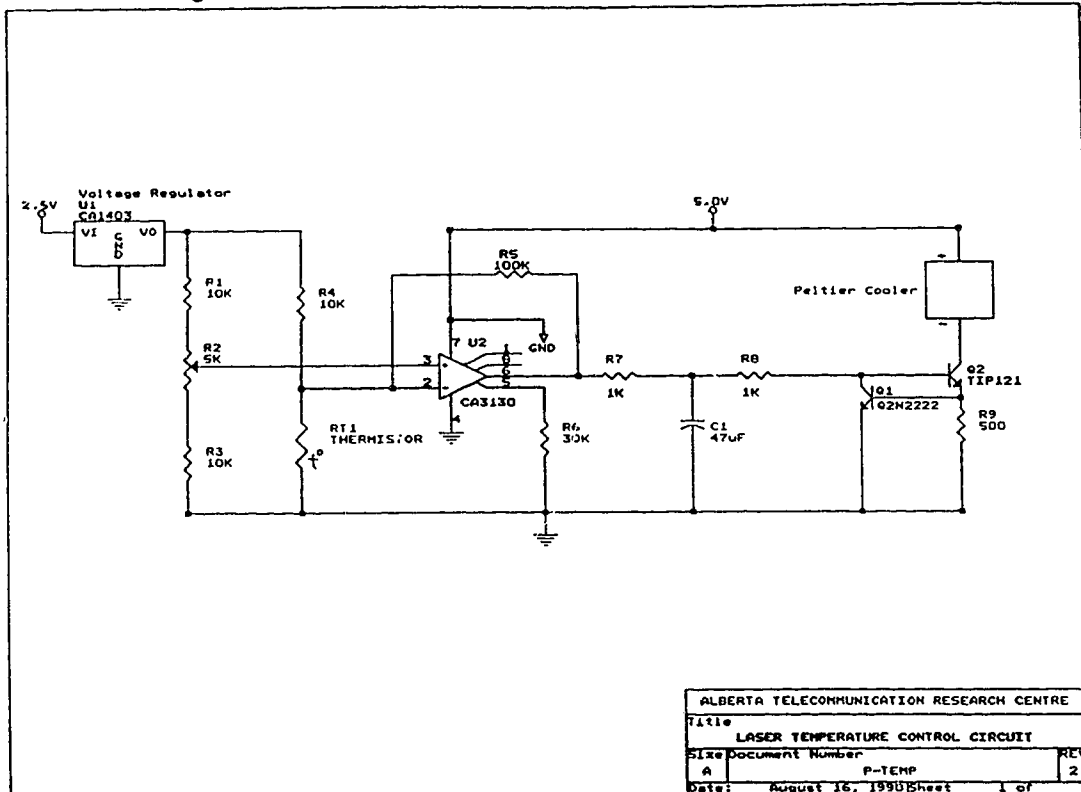


Fig. 4.15 Laser diode temperature control circuit.

4.3 Optical fibre couplers, links, attenuators and connections

4.3.1 Optical couplers, fibres and attenuators

A 2X2 optical coupler is used in the system to couple the optical outputs of the two transmitters into a single fibre. The 2X2 coupler used is a GOULD, S/N 1300-BA-100039, 3 db coupler with a coupling ratio of 63% at 1309 nm and an excess loss of 0.83 db. It is a single mode coupler of the fused biconical type.

One of the outputs of the coupler is spliced to the optical fibre which is used as the data channel in the FO-CDMA system. The fibre used is a $1.3\mu\text{m}$

Northern Telecom single mode step index fibre with a length of about 1.5 km and a fibre loss of about 0.2 db/km.

Since the transmission channel is limited to a length of 1.5 km due to the non-availability of a bigger length of fibre the optical power received at the detector is large enough to saturate it. The power transmitted from the laser could not be decreased below a certain level because this would make the laser operate in the non-linear region. Thus in order to have a higher optical power loss in the channel an optical attenuator is introduced in the system. This avoids saturation of the PIN detector and thus prevents distortion of the received signal.

Since no commercial single mode attenuator operating at 1300 nm was available, power attenuation had to be introduced by other means. An optical attenuator was constructed by winding 8 turns of fibre around a 0.8 cm diameter cylinder [43]. This introduces microbends in the fibre and thus there is a leakage of power from the core to the cladding. A portion of the fibre, after the microbend, is dipped into a glycerine bath in order to provide a medium for the cladding modes leak out of the fibre. An optical power attenuation of about 10 db is obtained using this procedure thus bringing the incident optical power level low enough to prevent saturation of the photodetector. In an actual local area network there is a $1/N$ (N is the total number of users supported by the system) splitting of the transmitted power at the $N \times N$ star coupler and attenuation of the signal along the length of the fibre. Thus, the received signal power is well within the linear operating range of the photodetector, and no attenuator is required.

4.3.2 Fibre connections

An important concern while making the fibre connections in a system, is to obtain the smallest optical power loss and minimum signal distortion at the connection. There are a number of methods that are being used to connect fibres together. However, the usual method for connecting optical fibres to form a strong joint is the butt-joint connection. The methods often used for butt-joint coupling are : fusion splicing, micro-positioner joining and V-groove joining.

In our system fusion splicing has been used. For a single mode fibre fusion splice, one needs to take care of two kinds of losses. They are the extrinsic loss and the intrinsic loss. Extrinsic loss is caused by the external parameters such as the quality of the connection while intrinsic loss is caused by differences in the two fibres being connected. Although extrinsic losses can be minimized by proper cleaving, alignment and cleanliness, intrinsic losses cannot be easily eliminated. Usually the fusion splice provides the smallest insertion loss and the most stable coupling. Losses of about 4.2 to 4.4 db per splice were obtained in the splices made in the FO-CDMA system.

Figure 4.16 shows the different fibre-to-fibre connections made in the system. Splice S1 and S2 connect the pigtails of the two lasers to the input pigtails of the 3 db coupler and have a total loss of 4.2 db and 4.4 db respectively. The splice S3 has a loss of 4.3 db and is used to connect one of the output fibres from the 3 db coupler to the 1.5 km length of the 1.3 μm single mode fibre. The other end of the 1.5 km fibre is connected to the pigtail of the photodiode by the splice S4 and has a loss of 4.4 db.

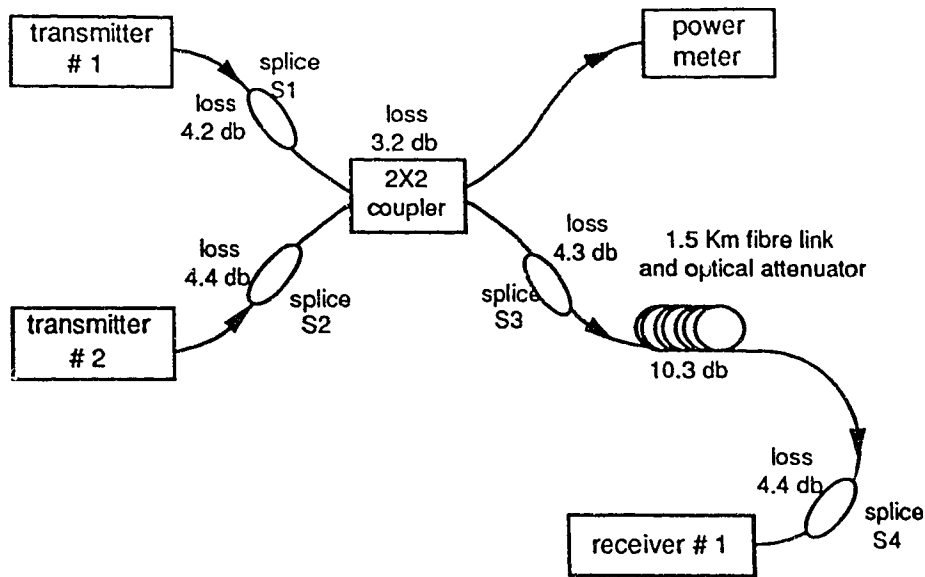


Fig. 4.16 Location of the fibre-to-fibre connections made in the experimental system.

4.4 Receiver

The receiver section in the experimental system is a modification of the proposed receiver stage (Section 2.2). In the experimental system, the optical signal is first converted to an electrical signal and then correlated. This is in contrast to the proposed correlation scheme of using an optical switch. The above modification was necessary due to the fact that the optical switch was not available. The block diagram of the new section is shown in Figure 4.17.

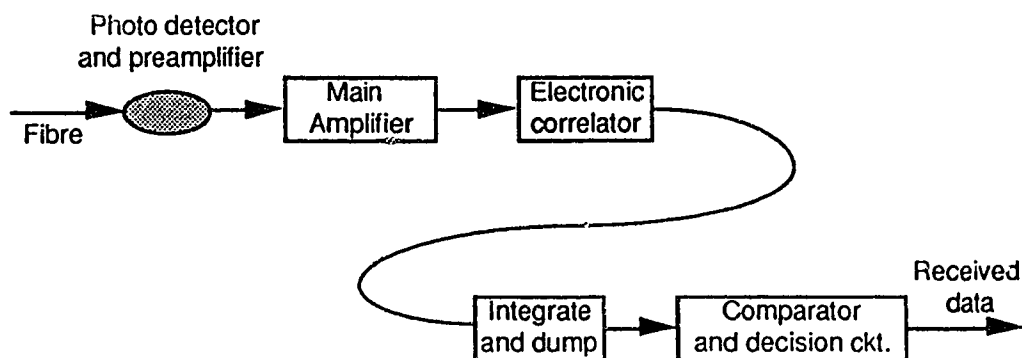


Fig. 4.17 Block diagram of the receiver section

4.4.1 Optical detector and preamplifier

After transmission over the single mode fibre and through the optical attenuator, the optical signal is detected by a PIN optical detector. The optical detector chosen for the system is a RCA type C30986-250 QC-02 with a bandwidth of 250 MHz. It is mounted in a hermetically-sealed 14 pin dual in-line package, and is provided with an integral single mode fibre pigtail having a core diameter of 50 μ m. (APPENDIX G) The detector is an Indium Gallium Arsenide photo-diode with an integrated hybrid amplifier, having a sensitivity of -35 dbm at a BER of 10^{-9} , a noise equivalent power (NEP) of 3.1 pW/(Hz)^{1/2} at 1.3 μ m and a responsivity of 7 kV/W.

The electrical output is terminated in a 500 ohm load, and AC (capacitively) coupled to the main amplifier. It is essential to have a precise value of the coupling capacitor in order to minimize the DC wander that might be generated by the reception of a 15 bit pseudo-random data sequence.

4.4.2 Main Amplifier

The electrical output from the detector preamplifier is AC coupled to a Keithley 105 Pulse Amplifier. The amplifier has a bandwidth of 500 MHz and an electrical gain of 10 or 100. The amplifier is set for a gain of 100 during the course of the experiments; this value of the gain produced a voltage of 500 mV (0 - 500 mV) when one user accessed the channel.

4.4.3 Local code generator

In order to detect a message sent for the receiver under test, the received signal must be correlated with the code sequence of the receiver.

Thus, it is important to have a dedicated code generator in each receiver which generates the code sequence for that receiver.

The receiver local code sequence generator is shown in Figure 4.18. The address or the P-code sequence of the receiver can be set by manually changing the parity on the array of switches SW1 to SW4, according to the binary value of the receiver code. In order to decode the data correctly the received signal must be synchronized with the local key sequence; a phase shift of even one chip may cause a false detection. Thus, the delay encountered by the data while travelling through the channel and the amplifier block has to be compensated.

In conventional systems synchronization is achieved by employing clock recovery and frame synchronization. Since the main objective of this project is the generation and verification of the properties of a new set of codes and the operation of a new correlation scheme, the design and implementation of a phase locked loop for synchronization of the receiver with the transmitter has not been looked into. In this system synchronization between the transmitter and the receiver is achieved by using a delayed data clock from the transmitter to trigger the local code generator at the receiver.

The data clock from the P-code generator in the transmitter is distributed to the receiver local code generator using a coaxial link. This signal is coupled to the input pin of the two mono-stable multivibrators that are connected in series. In the first mono-stable multivibrator the resistor R2 is adjusted in order to impart a phase shift to the data clock so as to synchronize it with the received data signal. The phase shifted data clock is aligned to the rising edge of the system clock using the D flip-flop.

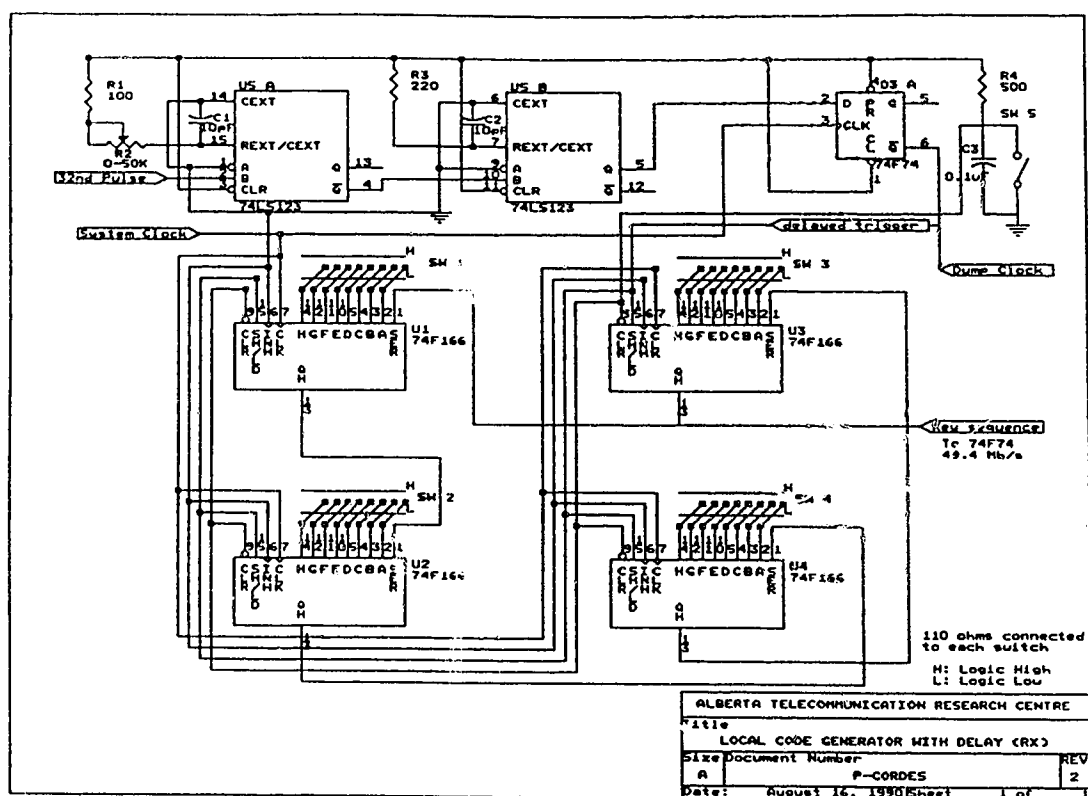


Fig. 4.18 Circuit for the receiver local code generator.

Another set of monostable multivibrators, U5A and U5B, and a D flip-flop D3A is used to provide synchronization and pulse broadening to the 32nd trigger pulse from the receiver. The output from the D flip-flop D3A is used to trigger the four 8-bit parallel load shift registers, 74F166's, which are connected in series to form a 32 bit shift register. Figure 4.19 shows the block diagram of such a series connection of shift registers. Another output is taken from the D flip-flop and termed the dump clock. The dump clock, which is the spread 32nd pulse, has a pulse width of about 33 nsec. and is used to dump the signal at the output of the integrate and dump filter.

When the trigger pulse goes high, which occurs once every 32 chip interval, the output from pin 6 of the D flip-flop D3A goes low. This causes the

shift registers to be loaded in parallel with the binary values selected in the switches SW1 to SW4. When the trigger pulse goes low, the output of pin 6 of the D flip-flop goes high and the registers start the shift operation. The sequence generated at the output of pin 1 of the register U1, of the 32 bit shift register, is the P-code sequence of the receiver.

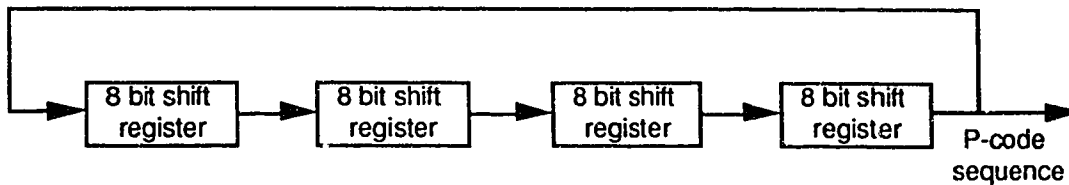


Fig. 4.19 A 32 bit P-code sequence generator using four 8 bit shift registers.

4.4.4 Correlator and the integrate and dump filter

The received signal, at the output of the amplifier, is a multilevel signal due to the combination of the coded signals that are being sent to different stations. To obtain the data signal sent to a certain station, the received signal is correlated with the local keyword and, depending on the output of the correlator, a decision is made as to whether a '1' or '0' has been received.

A new concept of correlation using optical switches has been introduced in this thesis (Section 2.2). This method, however, could not be implemented practically in our system, due to the un-availability of an optical switch. Instead, an electronic correlator was designed and used in the FO-CDMA system. The electronic correlator has the same truth table as that defined in Table 2.1 for a correlator using an optical switch.

The circuit for the electronic correlator is shown in Figure 4.20. It consists of a differential amplifier (Q4&Q5) with a modified active load (Q6&Q7),

with the amplifier current using a current source (Q1,Q2&Q3). The current from the current source is modulated by the received data signal; output from the main amplifier. The differential amplifier has a single ended input and a single ended output with the input signal to the differential amplifier being the P-code sequence generated by the local sequence generator.

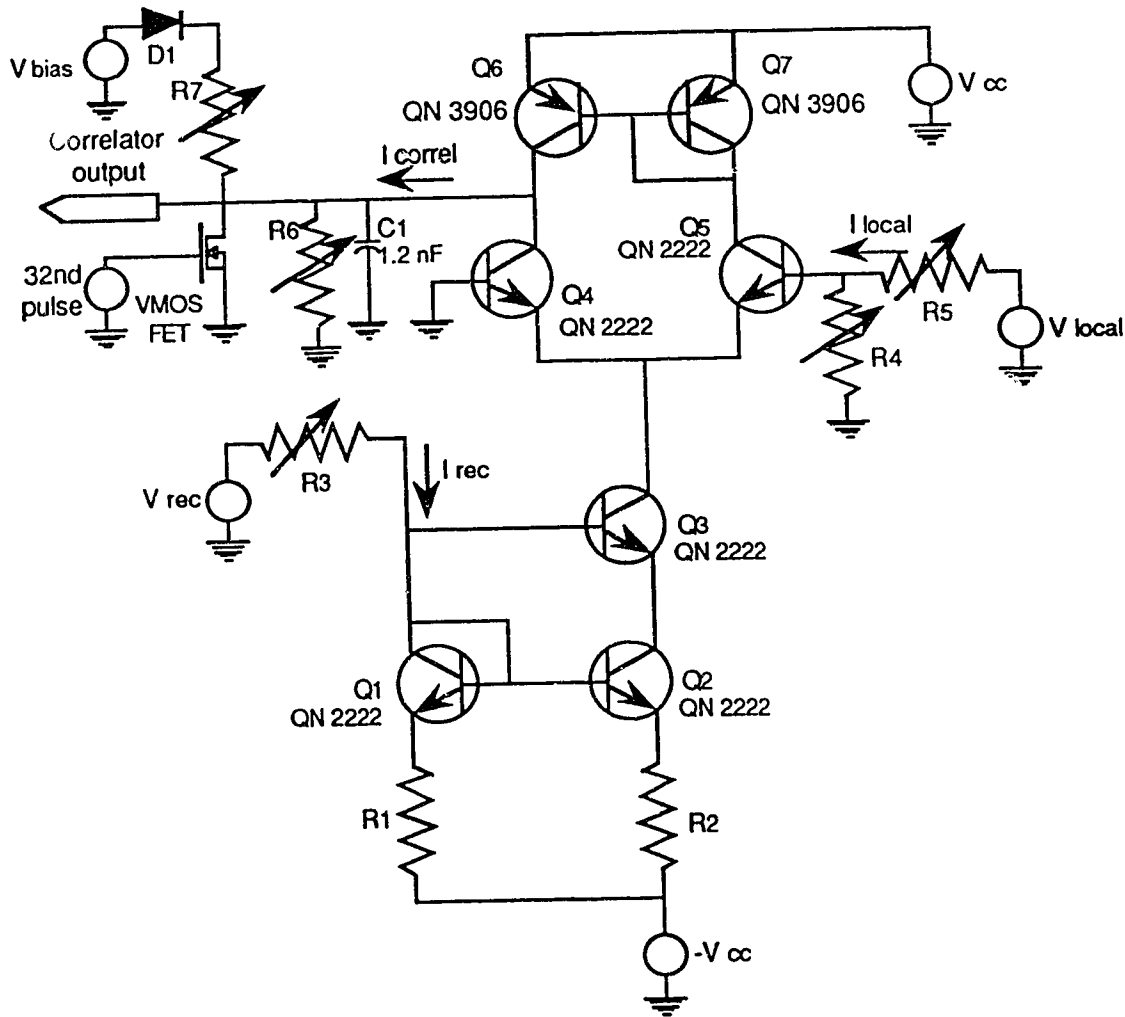


Fig. 4.20 Circuit diagram of the electronic correlator.

The above circuit with an active load provides a single output with much better rejection of common-mode input signals than a standard resistively loaded emitter-coupled pair with the output taken from the collector [42]. However, the circuit is very sensitive to the input offset voltage caused by the

variation of I_S between the two transistors Q_4 and Q_5 . The input offset voltage due to the difference in the I_S of the transistors Q_4 and Q_5 is given by

$$V_{os} = V_T \ln (I_{S4} / I_{S5}) \quad (4.3)$$

and can be regarded as a dc voltage source in series with the input. Thus, in order to minimize the offset voltage, V_o , and hence the effective differential voltage, $V_{id(eff)} = V_{id} + V_o$, the two transistors Q_4 and Q_5 must be very closely matched.

The received data drives the Wilson current source, which generates a current I_{det} flowing through the collector of Q_3 . The current source is adjusted to produce almost zero current when the received signal V_{in} is a zero. Thus when the received data is a zero, there is no current flowing in the differential pair. However, when a positive signal is received, the current flowing in the differential pair is proportional to the received voltage. As has been shown earlier, when the number of users increases the total power in the channel increases. This causes an increase in the received output voltage from the amplifier and hence an increase in the current flowing through the current source. Thus, the circuit had to be designed for a wide range of input voltage.

When the received signal is a '1', the current I_{det} flows in the differential amplifier according to the local code sequence. If the local code chip is a '1', Q_5 goes 'ON' and a current I_{on} flows through the collector of Q_5 and Q_7 . The current I_{on} is mirrored as I_{mir} by the current mirror formed by the transistors Q_6 and Q_7 . Since Q_5 is 'ON', Q_4 goes 'OFF' and the current I_{mir} flowing through the collector of Q_6 cannot flow through Q_4 . Thus the current I_{mir} flows into the capacitor C_1 .

When the received code is a '1' and the local code chip is a '0', Q_5 is 'OFF' and Q_4 is conducting. All the current I_{det} flows through the collector of Q_4

as I_{off} . However, since Q_5 is 'OFF', $I_{mir} = 0$ and thus the current I_{off} is supplied by the charge on the capacitor $C1$ and the capacitor discharges.

The circuit is designed so as to have a large RC discharge time. When the received signal is a zero, very little current flows from the capacitor and the capacitor voltage remains almost unchanged. However, when the received signal is a '1' and the local code has a stream of zeros at the beginning of the sequence, the capacitor keeps on discharging. Since a maximum of five consecutive 0's can occur in the codes and each '0' causes the capacitor voltage to drop by 20 millivolts, the capacitor should be able to supply a minimum potential of 100 millivolts. This is achieved by biasing the capacitor with a fixed voltage V_{bias} as shown in the figure.

It is required to discharge the capacitor completely within one chip interval, otherwise the correlator will not be properly reset for the next data period. This puts the following constraints on the basic requirements for the integrate and dump filter: a slow integration time and a quick dumping time. The slow integration time can be obtained by having a large RC constant and a short discharge time by a small RC constant. This can be achieved by having a switch with a high "off resistance" and a low "on resistance" in parallel with the capacitor. A VMOS FET in parallel having an effective "on resistance" of 5 ohms and a turn-ON and turn-OFF time of 5 nsec is used as a switch [48]. A discharge time of about 30 nsec, which is 1.5 times the chip rate, is required to completely discharge the capacitor. This is achieved by using the dump clock which has a pulse width of 33 nsec and is generated in the local code generator. The dumped output from the correlator is coupled to a comparator and decision circuit.

4.4.5 Comparator and decision circuit

Figure 4.21 shows the comparator and decision circuit used in the system. In the comparator and decision circuit, a differential voltage comparator, MC 3430, is used to compare the dumped output of the integrate and dump filter with a threshold. The threshold voltage is set to 1.2 volts and a comparator with an input sensitivity of ± 7 mV and a response time of about 40 msec. is used. Corresponding to the dumped voltage being greater or less than the threshold a comparator output of a logic '1' or '0' is obtained, which is coupled to a D flip-flop. The D flip-flop performs the operation of sample and hold. Hence, it is essential that the D flip-flop is well synchronized with the dump clock and the 1.54375 Mb/s data clock. According to whether the signal is a '1' or '0' at the sampling instant the output of the D flip-flop is held to a '1' or '0' for the next data period. Thus the output of the D flip-flop is the regenerated data after the decision of a data bit '1' or '0' is made.

4.4.6 Error detector

When an error is made, the regenerated waveform differs from the transmitted waveform. In order to measure the degree of correspondence between the transmitted and the regenerated (received) data, a measurement of the bit error rate has to be done. The regenerated waveform is sent to the HP-3780 A Pattern generator / Error detector where a comparison of the received data with the original transmitted data pattern is made.

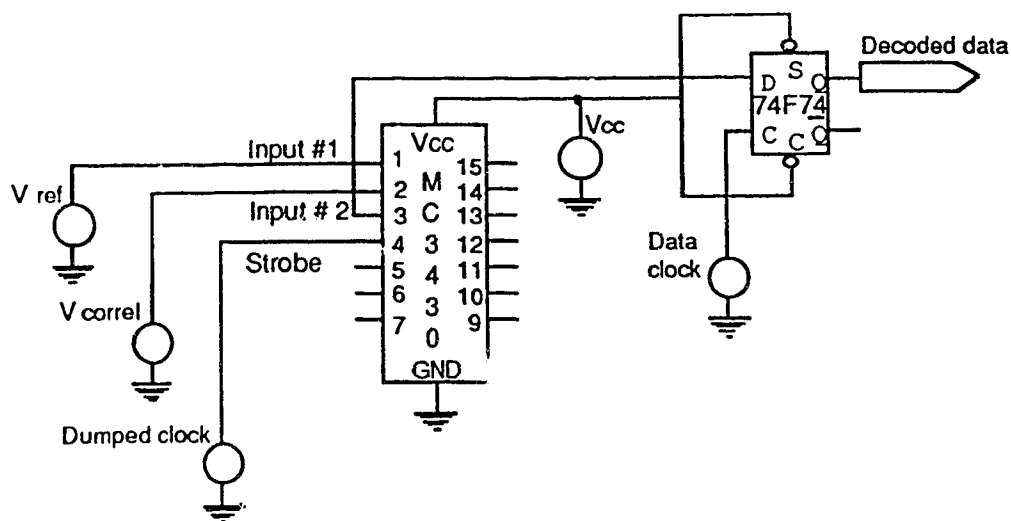


Fig. 4.21 Schematic of the comparator and hold circuit

The pattern generator used is capable of generating 9, 15 and 20 bit word and pseudo-random sequences along with the standard 1000, 1100, 1010 and 1111 sequences. In our system, 15 bit word sequences were used to align the system and necessary adjustments in the circuit were made in order to minimize the DC wander. Once the system was running at the data rate of 1.5375 Mb/s, $2^{15}-1$ bit pseudo-random sequences were used to test the performance of the system.

Bit error rate measurements were made using the internal BER counter of the error detector for measuring $\text{BER} > 10^{-8}$. The method of manual count of the number of errors was used to measure the BER when the number of errors are low ($< 10^{-8}$). Although it is desirable to wait for a larger number of errors to occur [45], the 10 error method (waiting for 10 errors to occur) was used since it would take many hours to record 100 errors. This was done because the system parameters are likely to change if the system is 'ON' for a long time and then the measured results will be wrong. Measurements were made for various system conditions: one station transmitting, two stations transmitting with equal power,

two stations transmitting with unequal power, two stations transmitting with detection threshold adjusted once for an increase in the number of users from one to two and two stations transmitting with dynamic detection employed at the receiver.

CHAPTER 5

EXPERIMENTAL RESULTS

In this chapter the various measurements made using the experimental system described in the previous chapter are presented and discussed. The first section presents the performance of the various building blocks of the system. This is followed by a discussion of the BER measurements made under various conditions. The variation of BER for a change in the power of the received signal, the power of an interfering user and the number of simultaneous users is presented. The variation of the BER for a change in the number of simultaneous users when dynamic detection is used is also given. Finally, the spectra of the uncoded and coded data sequences are shown, in order to illustrate the spreading of the spectrum that is obtained when P-codes are used for DS-CDMA.

5.1 System performance

5.1.1 Code generator

In the system one of the transmitters was selected to transmit the P-code, P8, for receiver #8, a Group 2 type receiver. Thus the switch SW1, in Figure 4.3, for the selection of the receiver code was set to a binary equivalent of $32 - 8 = 24$, i.e., 11000. Figure 5.1 illustrates the 32nd pulse, the $i = 24^{\text{th}}$ pulse and the data clock generated in the code generator. Another signal of interest, which is generated in the code generator, is the dumped clock. The dumped clock which is generated, at the output of IC 01A in Figure 4.3, from the system clock by dumping every 32nd bit of the system clock is shown in Figure 5.2.

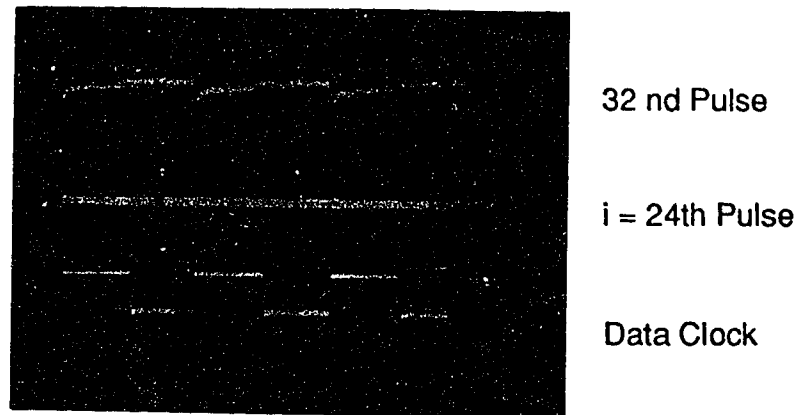


Fig. 5.1 Illustration of the 32nd pulse, the $i=24^{\text{th}}$ pulse and the data clock

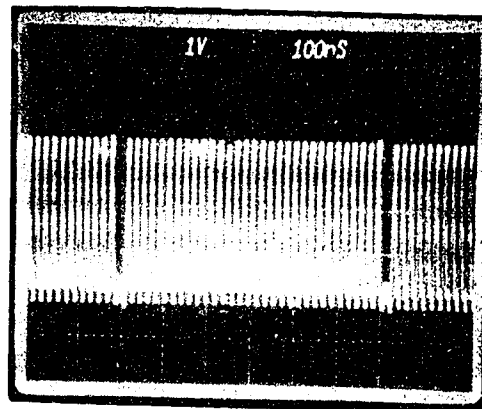


Fig. 5.2 Illustration of the dumped clock obtained at the output of the P-code generator

The dumped clock and the i^{th} trigger pulse are converted to an ECL format and coupled into the transmitter P-code generator (Figure 4.8). The P-code generated at the output of IC E1C in Figure 4.8 is converted back to a TTL signal using IC U4A, an ECL to TTL converter, before being multiplied by the data sequence in the encoder. The P-code sequence generated at the output of the transmitter P-code generator (Figure 4.8) is shown in Figure 5.3.

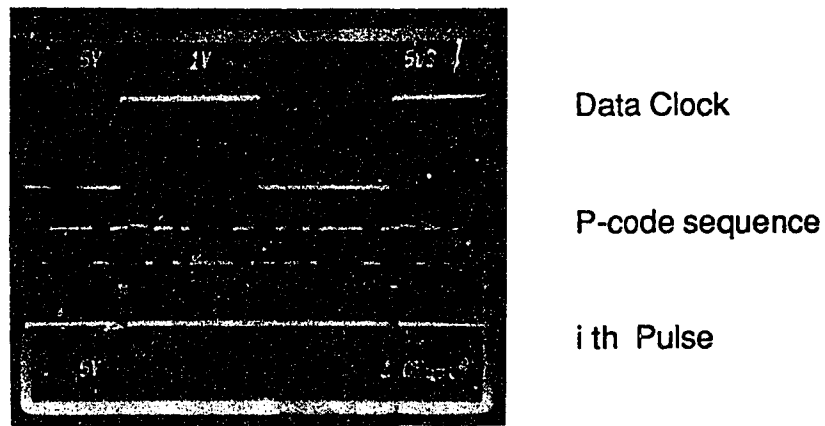


Fig. 5.3 Illustration of the P-code sequence, the data clock and the i^{th} pulse

Each station generates the P-code sequence corresponding to the address of the intended receiver. Since one receiver should be addressed by only one transmitter at a particular time, each transmitter addresses different receivers and hence generates a different P-code sequence. The two different P-code sequences that were generated in the system are shown in Figure 5.4.

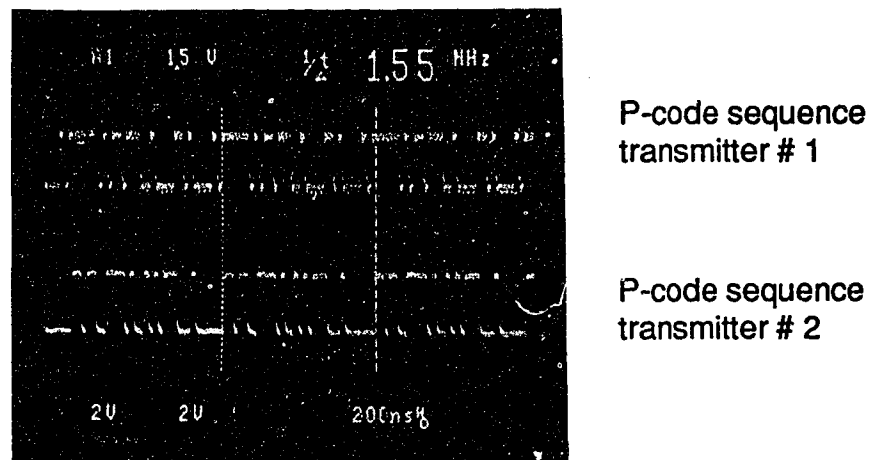


Fig. 5.4 P-code sequences for transmitter #1 and transmitter #2

5.1.2 Encoder

The encoder takes the data from the pseudo-random data generator and encodes it according to the P-code of the intended receiver. The encoder performs the chip-by-chip multiplication of the two signals and is also referred to as the modulator. The output of the encoder is a coded data sequence at a rate of 49.4 Mb/s. Figure 5.5 shows the NRZ '1010' data input to the encoder and the coded data output. To check for possible DC wander in the encoder circuit, a $2^{15}-1$ pseudo-random data bit sequence was transmitted. Figure 5.6 illustrates the waveform obtained at the output of the encoder for a $2^{15}-1$ pseudo-random bit sequence (PRBS). It is seen that the encoded waveform has a symmetrical and almost open eye indicating that there is very little jitter and noise in the system. The encoded waveform is found to be free from any DC wander.

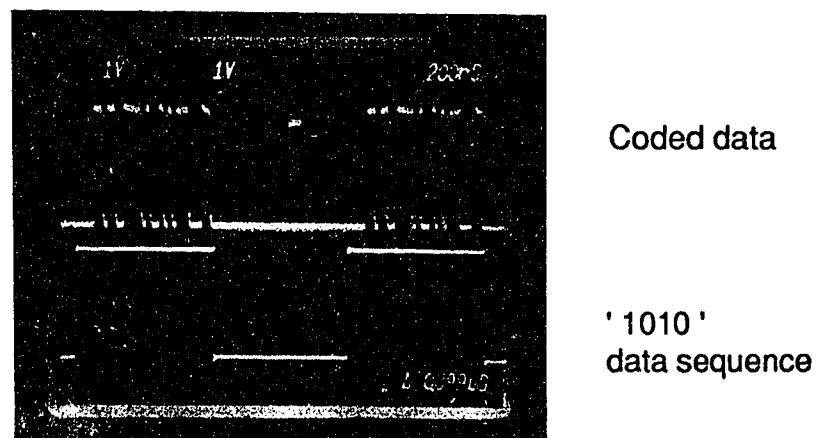


Fig. 5.5 NRZ '1010' data sequences and the coded data; output of the encoder

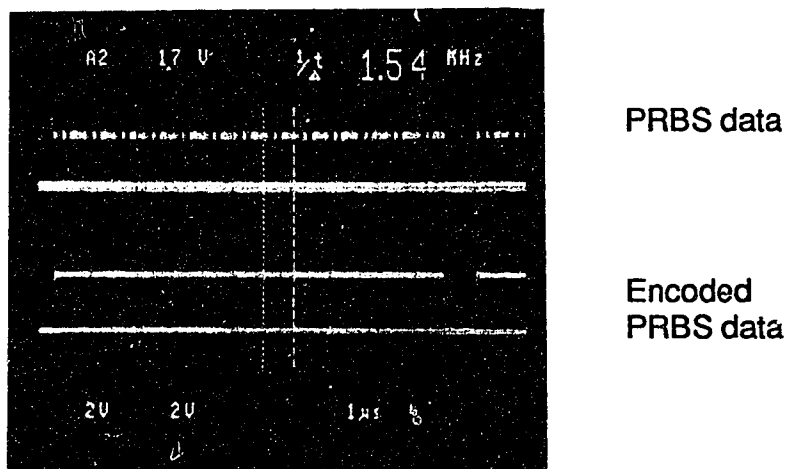


Fig. 5.6 Encoded output for a $2^{15}-1$ PRBS data signal

5.1.3 Laser drive circuit

The encoded data is coupled to one of the inputs to the differential amplifier of the laser modulator. This input voltage modulates the current flowing through the laser, thus generating the optical signal. Figures 5.7 and 5.8 show the voltage developed across a 10Ω resistor in series with the laser for transmitter #1 and transmitter #2, respectively.

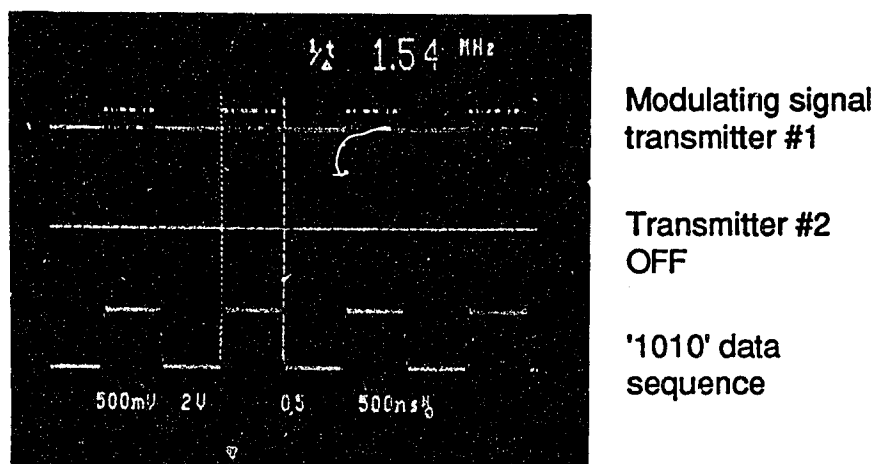


Fig. 5.7 Modulating signal at the laser driver for Tx #1

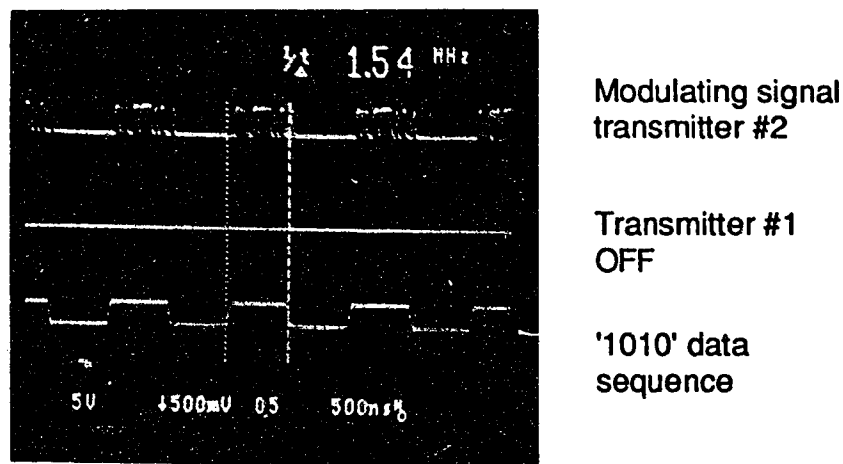


Fig. 5.8 Modulating signal at the laser driver for Tx #2

5.1.4 Detector output

The optical outputs from both the transmitters are coupled using a 2X2 coupler. One output of the coupler is connected to a power meter while the other output of the coupler is spliced to a 1.5 km length of single mode fibre whose other end is spliced to the photodetector.

The detected output is sent to the Keithley pulse amplifier which is set to a gain of 20 db. Figure 5.9 depicts the coded NRZ '11011110' data sequence received at the detector when only one transmitter is operating. As is seen in figure there is a small propagation delay in the system. It is seen that the detected output is noisy when a chip '0' is received. The main source of this noise is traced to the Keithley pulse amplifier which generated a noise of 60 mV at the "zero input" state, i.e., when the laser was off. Other sources of noise, resulting in the degradation of the received signal are the thermal noise of the laser driver circuit and the shot noise in the preamplifier.

Figure 5.10 shows the amplifier output when both the transmitters are 'ON' and one of the transmitters is sending a continuous stream of '1's while the other transmitter sends a 9 bit word pattern. As is seen in the figure, the amplitude of the received signal per chip interval is proportional to the sum of the transmitted signal.

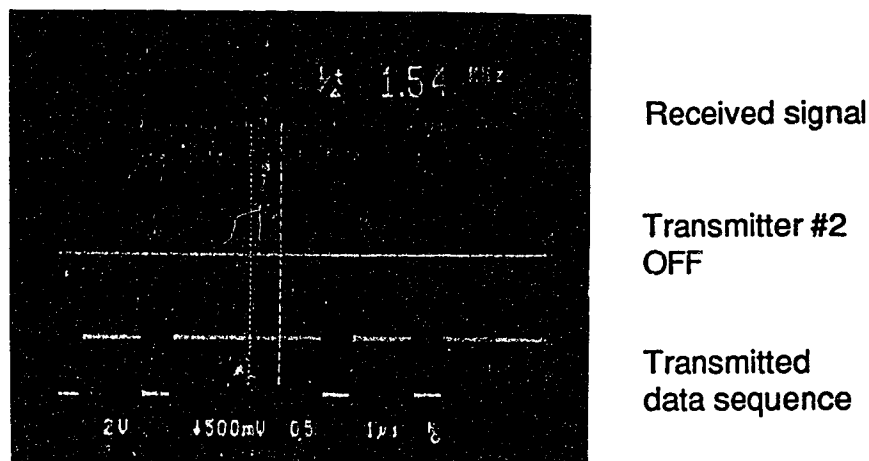


Fig. 5.9 NRZ '11011110' sequence received at the output of the main amplifier with only one transmitter 'ON'

5.1.1.5 Local code generator

The local code generator generates the P-code sequence of the receiver. It is essential that the sequence generated is in synchronism with the received signal. This synchronism is achieved by using a set of mono-stable multivibrators to shift the phase of the 32nd pulse in order to generate the framing pulse. The local code generator is triggered by this framing pulse in order to synchronize the locally generated P-code sequence with the received signal. Figure 5.11 shows a local P-code sequence generated using the 32nd pulse and the system clock from the transmitter.

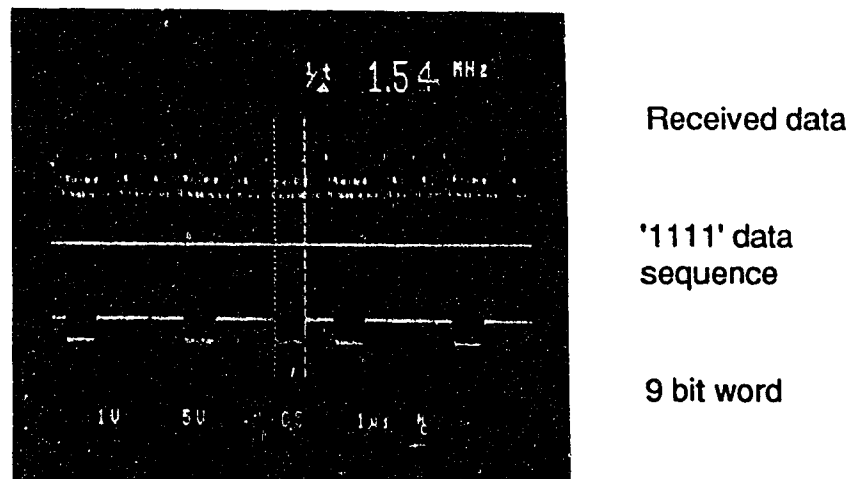


Fig. 5.10 Illustration of the signal received at the output of the main amplifier with both transmitters 'ON'; one transmitter sent a '1111' word while the other transmitted a 9 bit word pattern

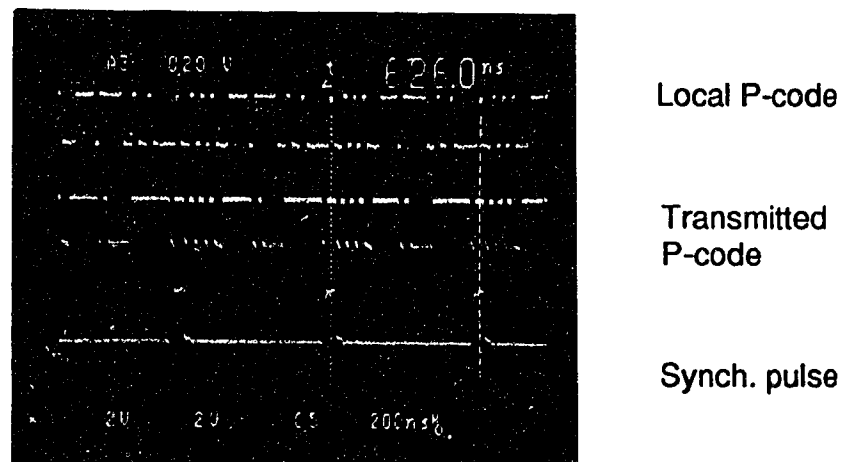


Fig. 5.11 Illustration of the P-code generated at the transmitter and the local code generator along with the synchronization pulse

5.1.6 Decoder correlator

The received signal is correlated with the local code sequence to retrieve the transmitted data. Since the receiver that we have chosen is a Type-2 receiver, we see that the correlator output goes negative when a data '1' is transmitted. This result complies with our theoretical calculations. The output of the correlator is fed to a decision circuit, where it is compared with a preset threshold voltage applied to a comparator. It is here that a decision is made as to whether a bit received is a '1' or a '0'. The receiver used in this thesis being a Type-2 unit, generates a '1' when the received voltage is below the threshold and a '0' when the voltage is higher than the threshold. The reverse case was seen to be true for a Type-1 receiver unit.

Figure 5.12 shows an illustration of two different codes that were generated to check the cross-correlation properties of the codes. The waveform at the top of the figure is for the transmitted P-code while the bottom one is the local P-code sequence which is different from the transmitted code. These codes were used as the V_{rec} and V_{local} inputs to the correlator shown in Figure 4.19. The correlator output, for the above codes and the integrating capacitor C1 removed from the circuit, is shown in Figure 5.13. From this illustration it can be observed that the received unipolar signal has been converted into a bipolar signal. From Figure 5.13 we see that, at a particular time slot, when the chips in both codes are a '1', the output of the correlator is equal to +0.5V. At the same time, when the local code is a '0' and the received signal is a '1', the output of the correlator is -0.5V. It is also observed that the output is 0V when the received signal is a '0'. Thus it can be said that the correlator works according to the table presented in Section 2.2. The correlator output is coupled to the

integrate-and-dump filter, where it is integrated and then dumped at the data rate of 1.5375 Mb/s. Figure 5.14 shows the integrated and dumped output for a 15 bit word pattern.

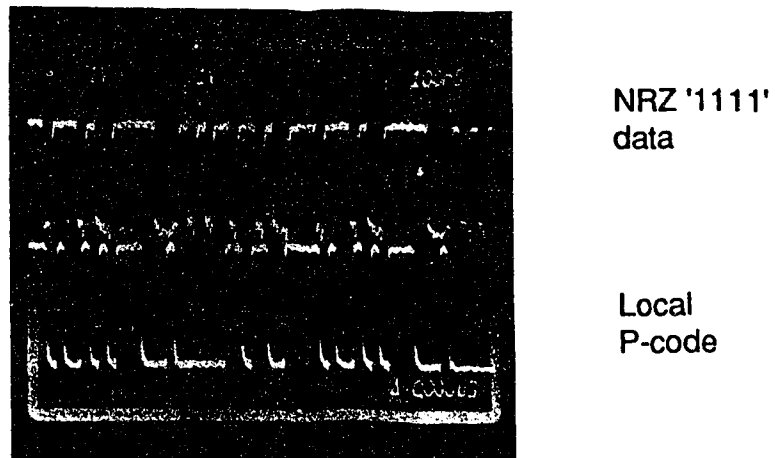


Fig. 5.12 Illustration of the received '1111' NRZ data and the local P-code sequence

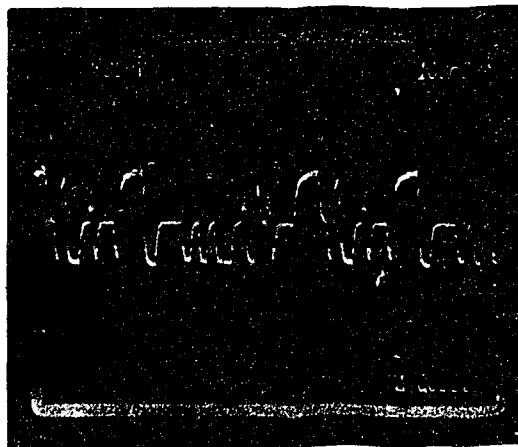


Fig. 5.13 Cross-correlated output for the signals in Fig. 5.12

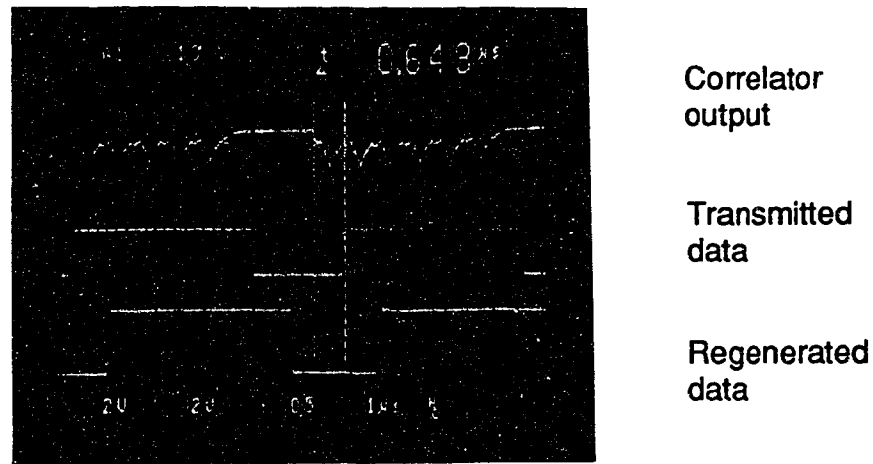


Fig. 5.14 Integrated and dumped waveform for a 15 bit word

5.1.7 Decoder decision unit

The output signal from the correlator is coupled to the decision circuit. It consists of the comparator which is used to compare the received signal with a preset voltage and a D flip-flop which regenerates the signal. As has been explained earlier, for the receiver under test, the signal coupled into the integrate-and-dump filter is a negative-going signal when a '1' has been detected by the correlator. This signal is compared with the fixed threshold voltage at the sampling instant to generate a logic high output when the received voltage is lower than the threshold. This output of the comparator is stored in the D flip-flop till the next sampling, hence the output of the D flip-flop is held in a high or a low state for a bit period of 1.5375 Mb/s. The regenerated data at the output of the D flip-flop, the correlator output and the transmitted signal, for a 20 bit pseudo-random data sequence, are shown in Figure 5.15

The above measurement was made to check auto-correlation, i.e., when the local code sequence is the same as the P-code of the coded data

being transmitted. Measurements were also made to study the cross-correlation performance of the system. It is seen that the voltage generated at the correlator of a Type-2 receiver when the local code and the transmitted code are different is well above the threshold voltage and thus the regenerated signal is always a zero. For a Type-2 receiver, the voltage is found to be well below the threshold and the regenerated signal is always a zero.

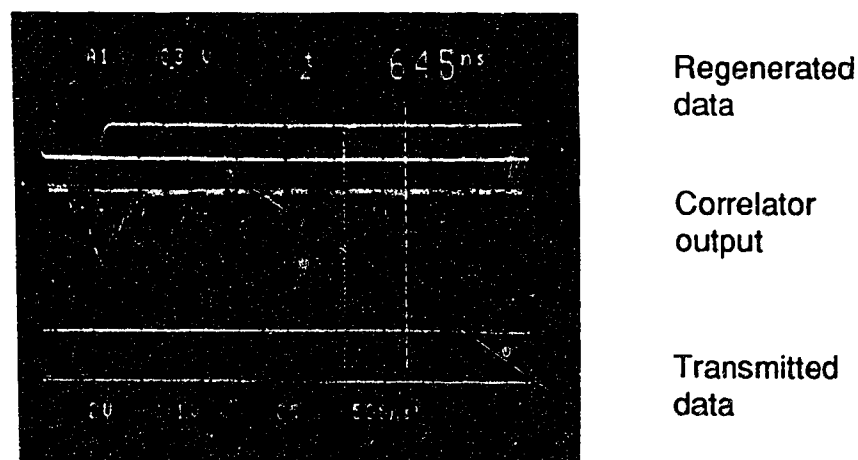


Fig. 5.15 Eye pattern obtained for a 20 bit PRBS

Figure 5.16 shows the transmitted data sequence, the correlator output and the regenerated output signal when the transmitted signal was not intended for the receiver under test. It is seen that, when the power of the interfering signal increases, the cross-correlation products increase and this can cause decoding errors. Figure 5.17 shows the output for the system when the P-code of the received signal is different from the local code and there is heavy interference in the channel. As can be seen in Figure 5.17, few errors are detected in such an operating scenario. These errors can however be minimized by adjusting the threshold, i.e., using a dynamic detection circuit.

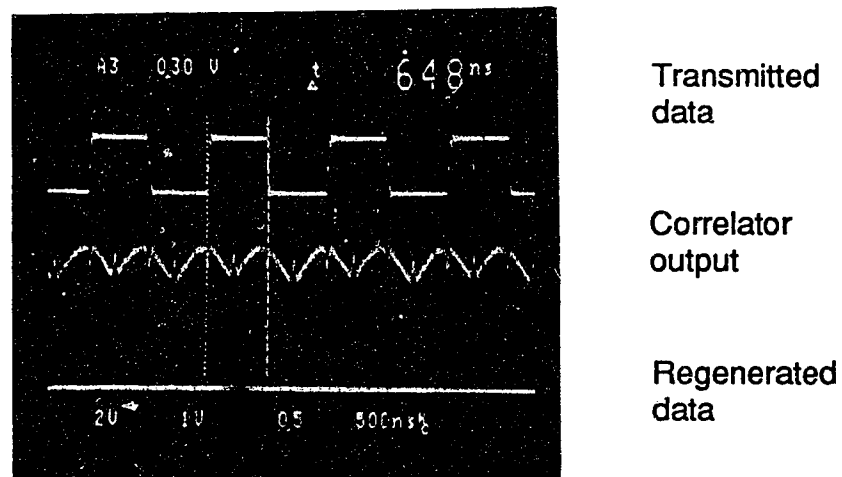


Fig. 5.16 Regenerated output for cross-correlation (at low power)

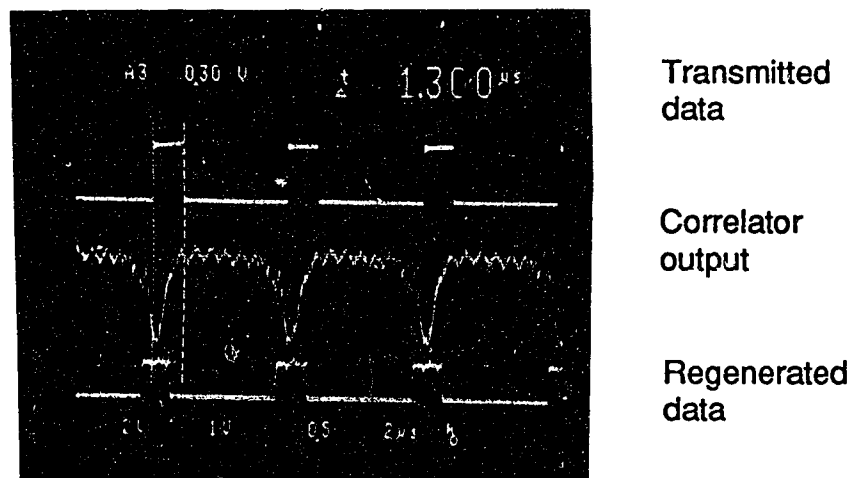


Fig. 5.17 Regenerated output for cross-correlation (at high power)

5.2 Bit error rate measurements

BER measurements were performed in order to identify the number of simultaneous users supported by the system for a particular value of the transmitted power. The variation of BER with reference to the near-far problem was also considered and some measurements were made.

5.2.1 BER variation with the number of simultaneous users.

The fibre optic CDMA system was designed to support two transmitters and a receiver. Thus it was possible in our experiment to test only up to two simultaneous users. However, in order to have a good test on the system, one of the transmitters could be triggered with a code sequence that is a combination of a couple of codes.

BER measurements for the case of varying number of users show that a 1.8 dB to 2.5 dB power penalty is incurred when an additional user gains access to the channel and starts transmitting. At the same time it is worth mentioning that using dynamic detection the power penalty was decreased to about 0.3 dB. The average received power was calculated from the average power transmitted from the transmitters. System calculations have shown that the total signal loss in the system, between the transmitter and the receiver, is about 26.4 dB. Figure 5.18 shows the plot for the variation of BER with the average received power and the number of users supported in the system. Referring to the index in Figure 5.18, case (i) defines the BER when only transmitter #1 is 'ON' while case (ii) is the measurement when both transmitters are 'ON' and transmitter #2 is transmitting at a constant power of -10 dBm. Case (iii) lists the BER measurements made when both the transmitters are 'ON' and the detection threshold is initially adjusted for minimum errors. Case (iv) is the same as case (iii) except that the detection threshold is continually adjusted for minimum errors. As is seen in the plot, a $BER < 10^{-9}$ can be achieved using the system.

Measurements to check the change in the BER for the near-far problem show that there is, at the maximum, one order of magnitude change in the BER

when the interfering user gains access to the channel and transmits with an optical power about 10 dB more than that from the receiver's intended transmitter. The curve for the variation of the BER with a change in the power of the interfering user, for a fixed power of the receiver's intended transmitter, is shown in Figure 5.19. It is seen that, by employing dynamic detection, the change in the BER for a near-far case can be minimized.

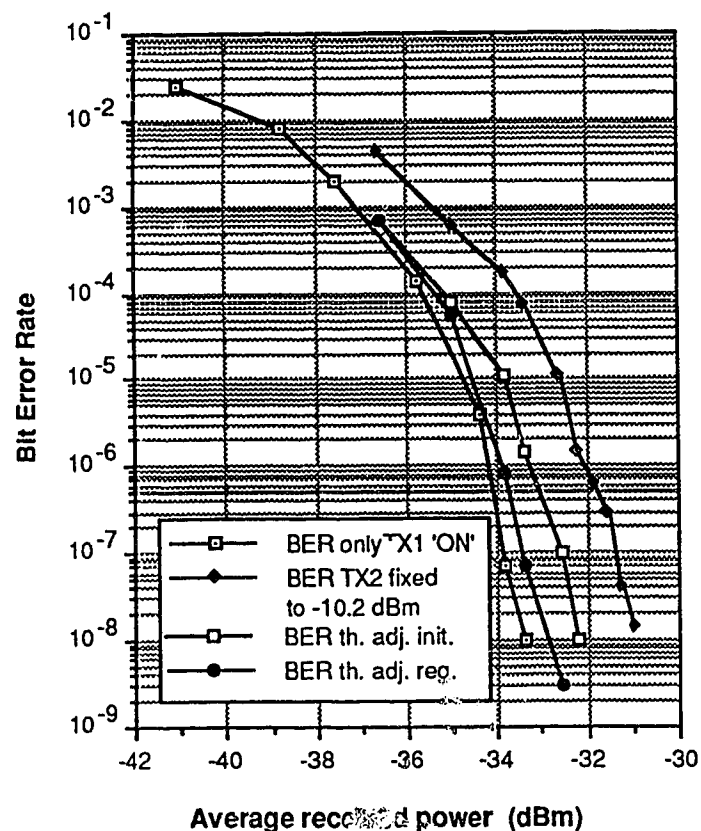


Fig 5.18 BER measurements for P-codes for the following cases :

- i. only TX1 'ON'
- ii. both transmitters 'ON' and TX2 transmitting -10 dBm
- iii. Case ii with the threshold adjusted initially at a received power of -36.6 dBm
- iv. Case ii with the threshold optimally adjusted, at each step

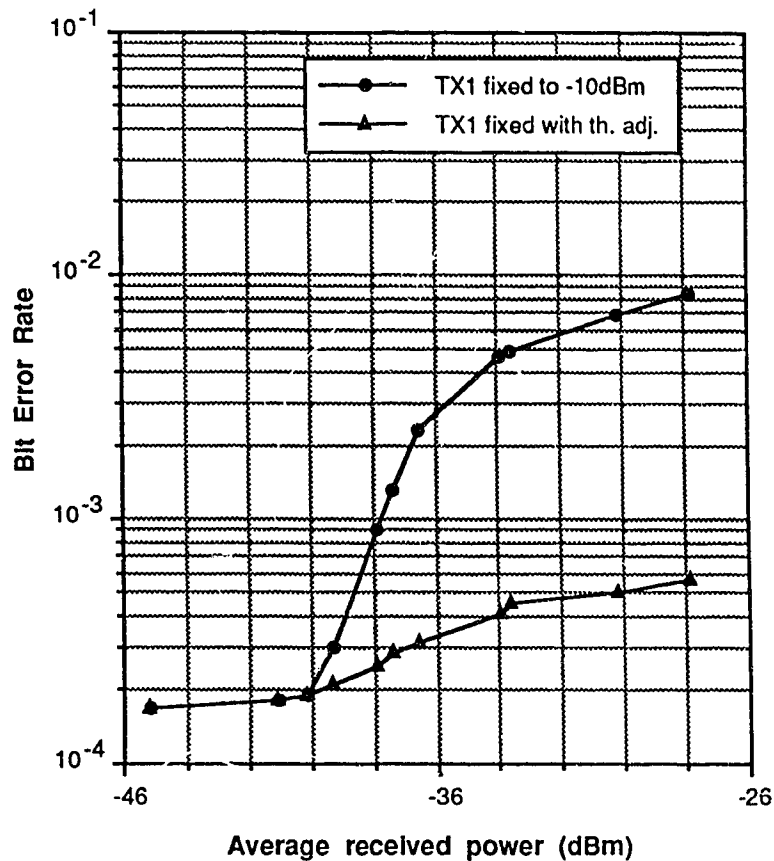


Fig. 5.19 Variation of BER with the power of the jamming transmitter

5.3 Power Spectra

Spread spectrum communication derives its name from the fact that at the transmitter the data is modulated in such a way that the bandwidth of the spectrum of the output data signal is much higher than the original data, i.e., the spectrum of the signal has been spread. Thus, in order to check the performance of the FO-CDMA system, it is important to study the spectrum of the data sequence at various stages of the system.

The power spectra for a 1.544 Mb/s, $2^{15}-1$ PRBS, data signal is shown in Figure 5.20. This is a NRZ data signal which is modulated with the P-code of

the intended receiver in the coder. Figure 5.21 shows the power spectrum for the encoded $2^{15}-1$ PRBS at the output of the coder. The spread in the spectrum is clearly visible and the power spectrum is uniform for a long range of frequencies as compared with the spectrum in Figure 5.20. It is seen from Figure 5.21 that the spread-spectrum nulls occur at the chip rate of 49.4 Mb/s and that the spectrum has a bandwidth of about 98.8 MHz.

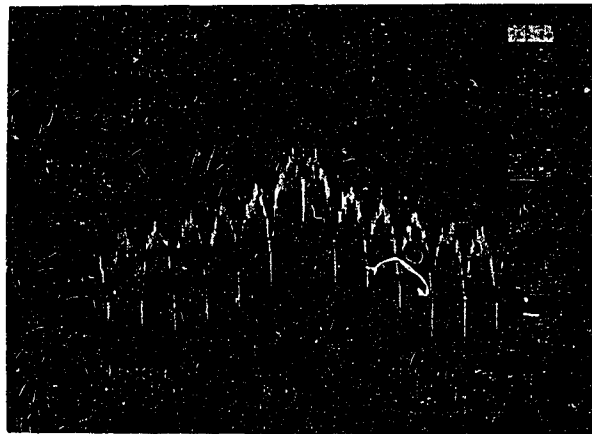


Fig. 5.20 Spectra of the 1.544 Mb/s PRBS transmitted data
Horizontal : 2 MHz / div Vertical : 10 dB / div

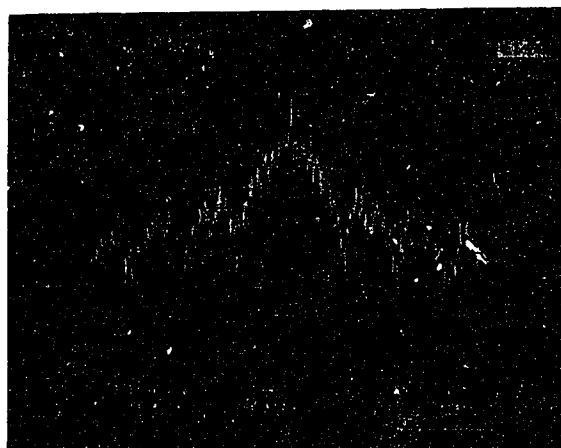


Fig. 5.21 Spectrum of the 49.408 Mb/s $2^{15}-1$ PRBS coded data
Horizontal : 40 MHz / div Vertical : 10 dB / div

It is important that the bandwidth of the all the components in the receiver section, till the correlator, have a bandwidth greater than the bandwidth of the spectrum. Thus, the signal is detected at the pin photodetector having a bandwidth of 250 MHz and amplified using the Keithley pulse amplifier which has a signal bandwidth of 500 MHz.

Figure 5.22 shows the spectrum for the signal received at the output of the amplifier. The spectrum is similar to that at the output of the encoder. The amplified signal, from the amplifier, is coupled to the correlator where it is correlated with the local keyword. Figure 5.23 shows the power spectrum for the $2^{15}-1$ PRBS at the output of the correlator while Figure 5.24 shows the spectrum of the signal at the output of the decision circuit. It is seen by comparing Figure 5.20 and Figure 5.24 that as would be expected both the power spectra are almost similar.

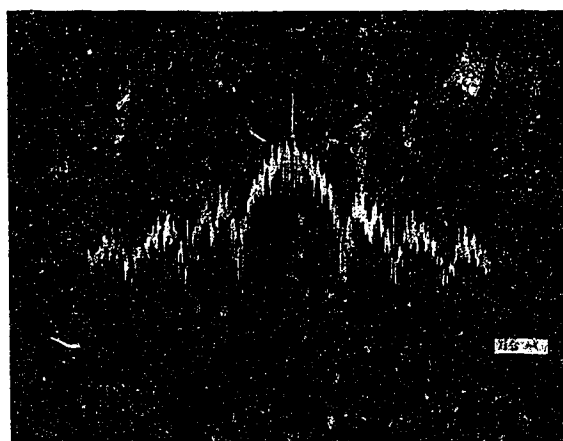


Fig. 5.22 Spectrum of the data at the output of the amplifier
Horizontal : 40 MHz / div **Vertical : 10 dB / div**

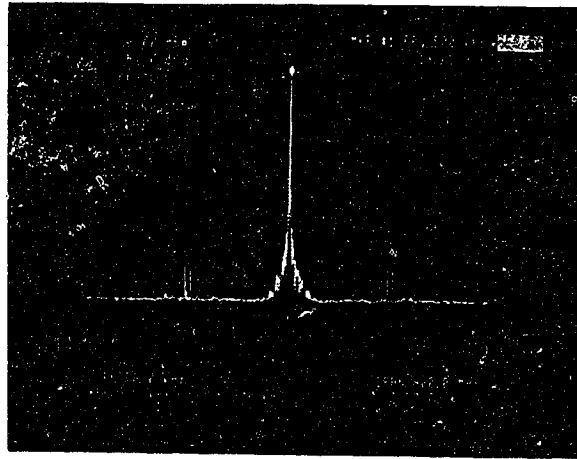


Fig. 5.23 Spectrum of the data at the output of the correlator
 Horizontal : 40 MHz / div Vertical : 10 dB / div

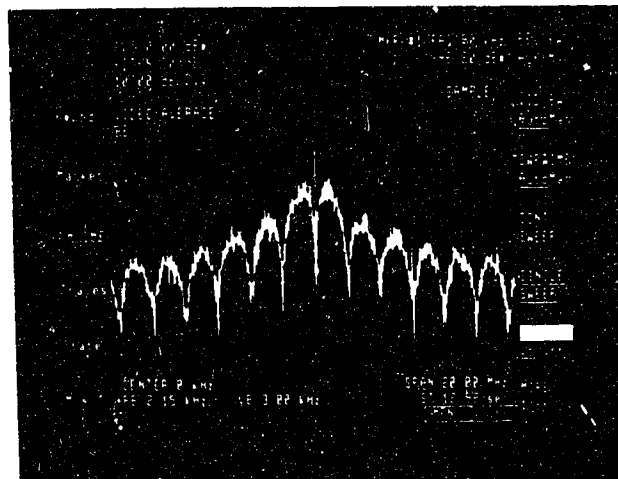


Fig. 5.24 Spectrum of the data at the output of the decision circuit
 Horizontal : 2 MHz / div Vertical : 10 dB / div

CHAPTER 6

DISCUSSION AND CONCLUSION

Spread spectrum systems require a large bandwidth and hence spread spectrum modulation is not widely used in most conventional systems. In optical fibre systems the available bandwidth is large, which makes the use of CDMA in local area networks a very attractive approach. This thesis work has investigated and demonstrated a new set of codes and a new correlation scheme for FO-CDMA in local area networks. Various sets of codes exist for spread spectrum communication. However, these codes are defined mainly for electrical systems and thus do not work well for optical systems. In this thesis the possibility of using a more efficient code for CDMA in an optical system has been explored. A new set of codes, called P-codes, has been defined in this thesis and some of the code properties have been studied using computer simulation. The codes that have been proposed have a bandwidth expansion factor (i.e., the ratio of the number of chips in the code to the number of simultaneous users supported) of one, and are thus viewed to be bandwidth efficient.

A number of systems for FO-CDMA have been defined [12-16]. Researchers have employed either electrical processing [17,18] or optical processing [19-26, 49-57] for detecting the signals. The two most common correlation techniques, which are used in both electrical and optical CDMA schemes, are serial processing and parallel processing. In this thesis a new correlation format, complementary correlation with an optical switch, has been discussed and applied in an FO-CDMA system. Simulations have been performed to check the performance of such a system. Using this approach, an

effective reduction in the effect of noise due to multiuser interference has been achieved. The use of an optical switch for correlation has been proposed. However, since an optical switch was not available, an electronic correlator has been designed and constructed to replace the switch. Ideally, the electronic correlator serves the same function as the optical switch; however, the electronic correlator cannot operate at very high data rates (> 70 Mb/s) and the switching operation also causes a certain amount of electrical interference or noise.

Computer simulations have been performed to check the system performance of P-codes and a mathematical equation for the representation of P-codes has been derived. The system capacity, probability density function for the interfering signals and the BER caused by interference from other signals, for the newly derived P-codes, were calculated. The detection threshold and signal required for correct detection of data as a function of the number of simultaneous users has also been calculated. Simulation results have shown that an n chip/bit code can support n simultaneous users provided that the system is synchronous, and that dynamic detection techniques are used. The simulation results indicate that CDMA using P-codes is a suitable method for achieving multi-user access in an optical fibre communication system.

An experimental CDMA communication system was designed and fabricated, consisting of two transmitters and a receiver. Each transmitter was made up of a code generator, encoder, laser driver and laser, while the receiver housed a PIN photo-detector, amplifier, correlator and decision circuit. A 3 dB coupler and single mode fibre were used to connect the transmitters to the receiver. The system operated at a data rate close to the DS1 rate of 1.544 Mb/s and a chip rate of 49.4 Mb/s. P-code sequences for the address of the intended

receiver were generated at the transmitters by selecting the receiver number. The receiver code generator was designed to be able to generate any P-code sequence; i.e., it was able to function as the receiver for any one of the 31 possible users. Although a commercial system would have a fixed receiver code, the experimental receiver was so designed so that it would be able to test all the code sequences.

The decoder circuitry used to perform the de-correlation is similar to that used in an analog multiplier; an integrate-and-dump filter was used for storing the correlated output. The decoder had a comparator whose output depends on the threshold setting of the comparator and the dumped signal. The correlator, designed using quad transistor packages, operated at a speed of 49.4 Mb/s, which is higher than the one achieved by Tamura [17] and Chen [27] for electrical processing. A point worth mentioning is that, although electrical processing was used at the receiver in the experimental system, the codes and correlation scheme have been defined for optical processing. Data rates much higher than those used in this thesis could be obtained if an optical switch were used.

Experimental measurements for the BER were taken for various system conditions. The experimental results show that a 1.8 to 2.5 dB power penalty is incurred when the number of users is doubled, when a fixed detection threshold is used. This penalty drops to about 0.3 dB when dynamic detection is used. Thus, the influence of interference from other users on the desired signal is minimal when dynamic detection is used. The near-far problem was also considered and it was seen that for a 3 dB difference of power the BER changed considerably. However, when dynamic detection was used, the BER changed

only slightly. Thus the system performance in a near-far situation improves when dynamic detection is used.

A BER of 10^{-9} was achieved for a transmitted power of -6.7 dBm when one user was transmitting; this corresponds to a received power of about -33.1 dBm. For two users transmitting equal amounts of power, the same BER could be obtained for transmitted powers of -6.4 dBm, when dynamic detection was used.

Summing up, it can be said that a new set of codes and a new correlation scheme for FO-CDMA has been presented in this thesis. An experimental FO-CDMA system employing the new codes, and correlation scheme, has been successfully developed and tested proving that the codes and the correlation scheme do indeed work. Using dynamic detection, a bandwidth expansion factor of one and a process gain of 31 have been achieved for P-codes of length 31. The immunity to interference, i.e., small power penalty and the unity bandwidth expansion factor makes the use of FO-CDMA using P-codes an attractive option for local area networks.

The following topics could be investigated further in order to fully realize the advantages of the new set of codes and the correlation scheme :

- (i) Investigation of the performance of the system when using an optical switch and a pair of photo-detectors at the correlator, is necessary to better evaluate the potential of proposed correlation scheme.
- (ii) In this thesis, a potentiometer was used to manually vary the detection threshold when the number of users increased. A dynamic

detection circuit can be designed and constructed to replace the potentiometer.

(iii) This project has experimentally investigated the system performance for only two simultaneous users. Further investigation of the system performance should be made by introducing more users.

(iv) Another avenue of potential study is an investigation into the possibility of integrating the electronic correlator. Although the correlator would not be required in a system using an optical switch for correlation, the use of the circuit as a correlator in other electrical CDMA systems is a possibility. Integration of the unit would improve the system performance and operation of the system at higher bit rates, greater than 500 Mb/s, would be possible.

(v) A study of the application of P-codes as a spreading sequence, and the correlation scheme, using the electronic correlator, to mobile communication is an interesting topic for further research.

(vi) A study can be made of the performance of other codes using the new correlation scheme. This could lead to new codes that may be easier to synchronize or those that could operate in an asynchronous system.

It is hoped that this work will lead to new CDMA codes and new methods for implementing fibre-optic local area networks.

BIBLIOGRAPHY

1. G.R.Cooper and R.W.Nettleton, "A spread spectrum technique for high capacity mobile communication", *IEEE Trans. Vehic. Technol.*, Vol.VT-27, pp. 264-75, Nov. 1978.
2. H.J.Kochnar, "Spread spectrum multiple access communication experiment through satellite", *IEEE Trans. Commn.*, Vol 27, pp. 853-56, Aug. 1979.
3. C.T.Sprackles and C.Smythe, "Communication protocols for a spread spectrum local area network", *Proc. of 8th Exposition FOC/LAN* , Las Vegas, NV, pp. 70-74, 1984.
4. R.A Mayers, Editor , *Encyclopedia of Telecommunications*, Academic Press, Inc., SanDiego, pp. 257, 1988.
5. E.A.Lee and D.G.Messerschmitt, *Digital Communication*, Kluwer Academic Publishers, U.S.A. , pp. 464, 1988.
6. R.L.Pickholtz, D.L.Schilling and L.B.Milstein, "Theory of spread spectrum communication - a tutorial", *IEEE Trans. Commun.*, COM-30(5), pp. 855-884, May 1982.
7. R.A.Scholtz, "The origin of spread-spectrum communication", *IEEE Trans. Comm.*, COM - 30(5), pp. 822, May 1982.
8. R.C.Dixon, *Spread Spectrum Systems, 2nd Ed* , John Wiley & Sons, Inc., New York, pp. 214-248, 1984.
9. C.E.Cook, F.W.Ellersick, L.B.Milstein and D.L.Schilling, Eds., "Special issue on spread-spectrum communication", *IEEE Trans. Commun.*, Vol. COM-25, May 1982.
10. H.M.Hafez, A.K.El-Hakeem and S.A.Mahmoud, "Spread spectrum access in two-hop CATV data networks", *IEEE J. Select. Areas Commun.*, Vol.SAC-3, pp. 312-322, March 1985.

11. K.G.Johannsen, "CDMA versus FDMA channel capacity in mobile satellite communication", *International J. of Satellite Commun.*, Vol. 6, pp. 29-39, 1988.
12. P.W.Smith, "Digital optical signal processing", *Proc. of Int. Conf. on Lasers'84*, pp. 34-43, Nov.1984.
13. M.A.Santoro and P.R.Prucnal, "Asynchronous fibre optic local area networks using CDMA and optical correlation", *Proc. IEEE*, Vol 75, No 9, pp. 1336 -38, Sept. 1987.
14. K.P.Jackson, S.A.Newton, B.Mosehi, M.Tur, C.C.Cutler, J.W.Goodman and H.J.Shaw, "Optical fibre delay line signal processing", *IEEE Trans. Microwave Theory and Techniques*, Vol MTT-33, No. 3, pp. 193 -210, March 1985.
15. F.R.K.Chung, J.A.Salehi and V.K.Wei, "Optical orthogonal codes: design, analysis, and applications", *IEEE Trans. Inf. Theory* , Vol 37, May 1989.
16. R.I.MacDonald, "Fully orthogonal optical-code multiplex for broadcasting", *Optics Letters*, Vol.13, pp. 539 - 41, June 1988.
17. S.Tamura, S.Nakano and K.Okazaki, "Optical code-multiplex transmission by Gold sequences", *J. Lightwave Technol.*, Vol. LT-3, No. 1, pp. 121-127, Feb. 1985.
18. Z.Chen, P.A.Goud and C.G.Englefield, "Fibre optic multi-user access using spread spectrum techniques", *Proc. Canadian Conf. on Electrical and Computer Eng.* , Vancouver, pp. B. 3.5-3.8, Nov.1988.
19. P.R.Prucnal and M.A.Santoro, "Spread spectrum fibre-optic local area network using optical processing", *J. Lightwave Technol.*, Vol. LT-4, No.5, pp. 547-554, May 1987.
20. D.J.Blumenthal and P.R.Prucnal, "Performance of an 8X8 LiNbO₃ switch matrix as a giga-hertz self-routing switch node", *Electron. Lett.*, Vol.23, pp. 1359 -60, 1987.

21. P.R.Prucnal, "Ultra fast fibre-optic networks using all-optical processing", *Proc. ICC'88*, pp. 1485-89, 1988.
22. M.A.Santoro and P.R.Prucnal, "Asynchronous fibre optic local area network using CDMA and Optical Correlation", *Proc. IEEE*, Vol 75, No 9, pp. 1336 - 38, Sept. 1987.
23. J.A.Salehi and C.A.Brackett, "Fundamental principles of FO-CDMA", *IEEE Int. Conf. in Commun.* , Seattle, Washington, pp. 1601-09, 1987.
24. R.I.MacDonald, and G.D.Fraser, "Optical code-division multiplex for high speed transmission", *Proc. 14th Biennial Symposium on Commun.*, Kingston, pp. A.4.1-4.3 , May 1988.
25. P.R.Prucnal et. al., "Ultrafast all optical synchronous multiple access fibre network", *IEEE J. Selected areas in Commun.*, SAC -4(9), pp. 1484 - 93, 1986.
26. A.D.German et. al., "A fibre optic CDMA network for real time communication", *IEEE INFOCOM'88*, New Orleans, pp. 62-69, Mar. 1988.
27. Z.C.Chen, A study of CDMA using Gold codes for an optical fibre communication system, M.Sc thesis, Electrical Engineering Department, University of Alberta, Spring 90.
28. P.R.Prucnal et. al., "Self routing photonic switching demonstration with optical control", *Optical Engg.*, Vol 26, No 5, pp. 473 - 77, May 1987.
29. P.R.Prucnal, "All-optical ultra-fast networks", *SPIE Vol.715*, pp. 42 -47, *Fibre Telecommunications and Computer Networks* (1986).
30. I.M.Habbab, K.Kavehrad and C.Sundery, "Protocols for very high speed fibre local area networks using a passive star topology", *J.Lightwave Technol.*, LT-5, pp 1782 - 94, Dec. 1987.
31. Z.A.Abbasi and F.Ghani, "Multi-level sequences with good auto-correlation properties", *Electron. Lett.*, Vol.24, No.24, No.7, pp. 393 - 394, Mar. 1988.

32. J.R.Lee et. al., "A code division multiple access local area network", *IEEE Trans. Commun.*, Vol. Com-35, No.6, pp. 667-671, June 1987.
33. William G. Chambers, *Basics of Communication and Coding*, Oxford Science Publications, Oxford, pp. 32, 1985.
34. T.W.Madron, *Local Area Networks: The second generation*, Wiley, New York, pp. 11-12, 1988.
35. MECL databook, Motorola Inc. , 1987.
36. W.R.Blood, MECL design handbook, Motorola Inc., 1983.
37. Schottky TTL Databook, Motorola Inc., 1983.
38. Technical staff of CSELT, *Optical fibre communication*, McGraw-Hill Inc., Torino, Italy, pp. 780-783, 1981.
39. P.R.Grey and R.G.Mayer, *Analysis and design of analog integrated circuits*, John Wiley & Sons, New York, pp. 202, 1977.
40. A.B.Grebene, *Bipolar and MOS analog integrated circuit design*, John Wiley & Sons, New York, pp. 177, 1984.
41. P.R.Grey and R.G.Mayer, *Analysis and design of analog integrated circuits*, John Wiley & Sons, New York, pp. 13, 1977.
42. P.R.Grey and R.G.Mayer, *Analysis and design of analog integrated circuits*, John Wiley & Sons, New York, pp. 160, 1977.
43. J.Gower, *Optical communication systems*, Prentice-Hall Inc., London, pp. 78-80, 1981.
44. R.Skang and J.F.Hjelmstad, *Spread spectrum in communication*, I.E.E. Telecommunication series 12, pp. 10, 1985.

45. H.Taub and D.C.Schilling, *Principles of communication systems*, McGraw Hill Inc. , New York, pp. 89-91, 1986.
46. M.Kawai et. al., "Smart optical receiver with automatic decision threshold setting and retiming phase alignment", *J. Lightwave Technol.*, Vol. 7, No. 11, pp. 121-127, Nov. 1989.
47. I.N.Gibra, *Probability and statistical inference for scientists and engineers*, Prentice-Hall, Inc., Englewood Cliffs, New York, pp.141, 1973.
48. VMOS Power FETs Design Catalog, Siliconix, Inc., Dec. 1980.
49. J.A.Salehi, "Emerging optical code-division multiple access communication systems", *IEEE Networks*, 31-39, March 1989.
50. A.M.Weiner, J.P.Heritage and J.A.Salehi, "Encoding and decoding of femtosecond pulses", *Optics letters*, Vol. 13, pp. 300-303, 1988.
51. G.J.Foschini and G.Vanucci, "Using spread spectrum in a high capacity fibre-optic, local area network", *IEEE J. Lightwave Technol.*, No. 3, Vol. 6, pp. 370, 1988.
52. J.A.Salehi and C.A.Brackett, "Principle and application of nonlinear optical elements in Fibre Optic Code Division Multiple Access networks (FO-CDMA)", *IEEE Military Commun. Conf.*, McLean, Virginia, pp. 848-855, 1987.
53. A.M.Weiner, J.P.Heritage and J.A.Salehi, "Frequency domian coding of femtosecond pulses for spread spectrum communication", *Conf. on Lasers and Electro-optics*, Post deadline paper, Baltimore, pp. 294-296, April 1987.
54. J.A.Salehi, "Code division multiple access technology in optical fibre networks - Part I, Fundamental principles", *IEEE Trans. Commun.*, Vol. 37, No. 8, pp. 824-833, August 1989.

55. J.A.Salehi and C.A.Brackett, "Code division multiple access technology in optical fibre networks - Part II, System performance analysis", *IEEE Trans. Commun.*, Vol. 37, No. 8, pp. 834-842, August 1989.
56. J.R.Lee and C.K.Un, "A code division multiple access LAN", *IEEE Trans. Commun.*, Vol. Com 35, No. 6, pp. 667-671, June 1987.
57. R.Petrovic and S.Holmes, "Orthogonal codes for CDMA optical fibre LANs with variable bit interval", *Electronics Letters*, Vol. 26, No. 10, 662-663, 10 May 1990.

APPENDIX A - ASYNCHRONOUS CORRELATION OF GOLD CODES

Program name “Ascroxxx”. This program finds the asynchronous correlation of the Gold codes when the codes access the network synchronously. While doing the asynchronous correlation of the code with itself, the auto-correlation peak is also calculated.

```
REM  PROGRAM CALULATES THE CORRELATION VALUES OBTAINED FOR GOLD
REM  CODES WHEN THE TRANSMISSION IS IDEAL CHIP ASYNCHRONOUS.
REM
REM  IN THIS PROGRAM WE READ THE GOLD CODE SEQUENCES FOR THE [5,3] AND
REM  [5,4,3,2] M-SEQUENCES FROM THE FILES ASYNCDAT1 AND ASYNCDAT2
REM
DIM   X1(35,35), Y1(35,35)
DIM   X2(70,35), Y2(70,35)
DIM   ASYNCOR1(70,35), ASYNCOR2(70,35)
REM
REM  THIS IS TO READ THE VALUES FOR X1(T,I) AND Y1(T,I) FROM THE FILES
REM  ASYNCDAT1 AND ASYNCDAT2
REM
OPEN "I", #1, "ASYNCDAT1"
OPEN "I", #2, "ASYNCDAT2"
FOR T=1 TO 33
FOR I=1 TO 31
INPUT #1, X1(T,I)
INPUT #2, Y1(T,I)
NEXT I
NEXT T
CLOSE #1
CLOSE #2
REM
REM  THIS IS THE INITIALIZATION PROCESS FOR FINDING THE CORRELATION IN THE
REM  CASE OF ASYNCHRONOUS TRANSMISION
REM
FOR T=1 TO 33
FOR I=1 TO 31
```

```

X2(T,I)=0 : Y2(T,I)=0
NEXT I
NEXT T
FOR T=34 TO 66
FOR I=1 TO 31
X2(T,I) = X1(T-33,I)
Y2(T,I) = Y2(T-33,I)
NEXT I
NEXT T
REM
REM  OPEN THE FILES ASCROCO1 AND ASCROCO2 TO STORE THE CORRELATION
REM  VALUES IN A 31 X 66 MATRIX
REM
OPEN "O", #1, "ASCROCO1"
OPEN "O", #2, "ASCROCO2"
FOR I=1 TO 31
FOR X=1 TO 31
FOR S=1 TO 66
ASYNCOR1(S,X) = 0
ASYNCOR2(S,X) = 0
NEXT S
NEXT X
FOR X=1 TO 31
FOR S=1 TO 66
Q = 0: R = 0
FOR T=1 TO 22
IF X1(T,I) = X2(T,X) AND X1(T,I) <> 0 THEN Q=Q+1
IF Y1(T,I) = Y2(T,X) AND Y1(T,I) <> 0 THEN R=R+1
ANEXT T
ASYNCOR1(S,X) = Q
ASYNCOR2(S,X) = R
Q1 = X2(1,X)
Q2 = Y2(1,X)
FOR B=1 TO 65
X2(B,X) = X2(B+1,X)
Y2(B,X) = Y2(B+1,X)

```

```
NEXT B
X2(66,X) = Q1
Y2(66,X) = Q2
PRINT #1, ASYNCOR(S,X);
PRINT #2, ASYNCOR(S,X);
NEXT S
PRINT #1, "ASYNCHRONOUS CORRELATION FOR CODE#";I; "WITH CODE"; X
PRINT #2, "ASYNCHRONOUS CORRELATION FOR CODE#";I; "WITH CODE"; X
NEXT X
NEXT I
CLOSE #1
CLOSE #2
END
```

APPENDIX B - PROGRAM TO CALCULATE AUTO-CORRELATION

Program name "Allcor31p". This program finds the correlator output when all the 31 users are accessing the network synchronously and the intended receiver code is also transmitted by one of the users.

```
#include <stdio.h>

#define value 34
#define iteration 67

/* PROGRAM FINDS THE CORRELATION OUTPUT FOR 31 USERS */

/* THE CODES ARE ASSUMED TO BE REACHING THE RECEIVER AT THE */
/* SAME TIME AND HENCE CAN BE CONSIDERED SYNCHRONIZED */

/* .      dt. July 24, 1989  */

/* THE INTENDED RECEIVER CODE IS ALSO TRANSMITTED */

main()
{
    FILE *fname;
    FILE *fname1;
    FILE *fname2;

    char readin[6];
    int X[iteration],Z[iteration],XP[value][value],X1[value][value];
    int X2[value][value],CORSWIT2[35];

    register int A,B,C1,E,F,I,J,K,N,Q,S,T;
    int count;

    X[1]=X[2]=X[3]=X[4]=X[5]=1;
    Z[1]=Z[2]=Z[3]=Z[4]=Z[5]=1;
/* CALCULATE FEEDBACK */

    for (l=5;l<=61;l++){
        A=FNF(X[3],X[5]);
        B=FNF(Z[2],Z[3]);
        F=FNF(B,Z[4]);
        E=FNF(F,Z[5]);

/* SHIFT DATA */

        for (N=l;N>=1;N--){
            X[N+1]=X[N];
```

```

        Z[N+1]=Z[N];
    }

/* FEEDBACK VALUE FOR FIRST BIT */

    X[1]=A;
    Z[1]=E;
} /* LOOP ENDS FOR I */

fname=fopen("D:/PANDE/msequen","wt+");
for (l=1;l<=31;l++){
    X[l]=X[63-l];
    fprintf(fname,"%d ",X[l]);
}
fprintf(fname,"\n");
for (l=1;l<=31;l++){
    Z[l]=Z[63-l];
    fprintf(fname,"%d ",Z[l]);
}
fclose(fname);

for (T=1;T<=31;T++){

    for (l=1;l<=31;l++)
        X1[T][l]=FNF(X[l],Z[l]);

    C1=Z[1];

    for (l=1;l<=30;l++)
        Z[l]=Z[l+1];

    Z[31]=C1;
}

fname1=fopen("D:/PANDE/SWITDAT","wt+");
for (l=1;l<=31;l++){
    for (T=1;T<=31;T++){
        fprintf(fname1,"%d ",X1[T][l]);
        X2[T][l]=0;
    }
    fprintf(fname1,"\n");
}

fclose(fname1);

fname2=fopen("D:/PANDE/CORSWIT2","a");

for(l=1;l<=31;l++){

```

```

        J=K=0;
        for(T=1;T<=31;T++){
            for(S=1;S<=31;S++){
                X2[T][I]=X1[T][S]+X2[T][I];
            }
        }
    }
    for(I=1;I<=31;I++){
        J=K=0;CORSWIT2[I]=0;
        for(T=1;T<=31;T++){
            if (X1[T][I]!=0)
                J=J+X2[T][I];
            else
                K=K+X2[T][I];
        } /* CLOSE LOOP FOR T */
        CORSWIT2[I]=J-K;
        fprintf(fname2,"%d ",CORSWIT2[I]);
    } /* close loop I */
    fprintf(fname2,"RX code PRESENT,users=1 to");
    fprintf(fname2,"%d",S-1);
    fprintf(fname2,"\n");
    fclose(fname2);
}

int FNF(C,D)
int C,D;
{
    return(C*(1-D)+D*(1-C));
}

```


APPENDIX C - PROGRAM TO CALCULATE CROSS-CORRELATION

Program name Allcor31". This program finds the correlator output when 30 users are accessing the network synchronously and the intended receiver code is not transmitted by any of the users.

```
#include <stdio.h>

#define value 34
#define iteration 67

/* FILE DOES THE SYNCHRONOUS CORRELATION OF 30 USERS */
/* WITH THE CODE. THE CODES ARE ASSUMED TO BE TRANSMITTED */
/* SIMULTANEOUSLY AND THUS REACH THE RECEIVER AT THE */
/* SAME TIME AND HENCE CAN BE CONSIDERED SYNCHRONIZED */
/* .      dt. July 24, 1989 */
/* THE INTENDED RECEIVER CODE IS NOT TRANSMITTED */

main()
{
    FILE *fname;
    FILE *fname1;
    FILE *fname2;

    char readin[6];
    int X[iteration],Z[iteration],XP[value][value],X1[value][value];
    int X2[value][value],CORSWIT2[35];

    register int A,B,C1,E,F,I,J,K,N,Q,S,T;
    int count;

    X[1]=X[2]=X[3]=X[4]=X[5]=1;
    Z[1]=Z[2]=Z[3]=Z[4]=Z[5]=1;

    /* CALCULATE FEEDBACK */

    for (l=5;l<=61;l++){
        A=FNF(X[3],X[5]);
        B=FNF(Z[2],Z[3]);
        F=FNF(B,Z[4]);
        E=FNF(F,Z[5]);

        /* SHIFT DATA */
```

```

        for (N=I;N>=1;N--){
            X[N+1]=X[N];
            Z[N+1]=Z[N];
        }

/* FEEDBACK VALUE FOR FIRST BIT */

        X[1]=A;
        Z[1]=E;
    } /* LOOP ENDS FOR I */

fname=fopen("D:/PANDE/msequen","wt+");
for (l=1;l<=31;l++){
    X[l]=X[63-l];
    fprintf(fname,"%d ",X[l]);
}
fprintf(fname,"\n");
for (l=1;l<=31;l++){
    Z[l]=Z[63-l];
    fprintf(fname,"%d ",Z[l]);
}
fclose(fname);

for (T=1;T<=31;T++){
    for (l=1;l<=31;l++){
        X1[T][l]=FNF(X[l],Z[l]);

        C1=Z[1];

        for (l=1;l<=30;l++){
            Z[l]=Z[l+1];

            Z[31]=C1;
        }

        fname1=fopen("D:/PANDE/SWITDAT","wt+");
        for (l=1;l<=31;l++){
            for (T=1;T<=31;T++){
                fprintf(fname1,"%d ",X1[T][l]);
                X2[T][l]=0;
            }
            fprintf(fname1,"\n");
        }

        fclose(fname1);

```

```

fname2=fopen("D:/PANDE/CORSWIT1","a");

for(l=1;l<=31;l++){
    J=K=0;
    for(T=1;T<=31;T++){
        for(S=1;S<=31;S++){
            if(S!=l)
                X2[T][l]=X1[T][S]+X2[T][l];
            else
                X2[T][l]=X2[T][l];
        }
    }
}

for(l=1;l<=31;l++){
    J=K=0;CORSWIT2[l]=0;
    for(T=1;T<=31;T++){
        if (X1[T][l]!=0)
            J=J+X2[T][l];
        else
            K=K+X2[T][l];
    } /* CLOSE LOOP FOR T */
    CORSWIT2[l]=J-K;
    fprintf(fname2,"%d ",CORSWIT2[l]);
} /* close loop l */
fprintf(fname2,"RX code not present,users=");
fprintf(fname2,"%d",S-1);
fprintf(fname2,"\n");
fclose(fname2);

}

int FNF(C,D)
int C,D;
{
    return(C*(1-D)+D*(1-C));
}

```

APPENDIX D - PROGRAM TO CALCULATE AUTO-CORRELATION FOR AN ASYNCHRONOUS TRANSMISSION MODE

Program name "As31co1". This program finds the correlator output when all the 31 users are accessing the network asynchronously. The intended receiver code is also transmitted by one of the users. The output is simulated for all asynchronous situations; varying from 1 chip asynchronous to 30 chip asynchronous.

```
#include <stdio.h>

main()
{
    FILE *fname;
    FILE *fname1;

    int X1[32][32],X2[64][32],ASYNCOR1[32][32], help;
    register int B,I,Q,Q1,R,S,T,X;

/* READ DATA FROM SWITDAT */
    fname=fopen("D:/PANDE/SWITDAT","r");
    if ( fname==NULL){
        printf("Cannot open file SWITDAT \n");
        exit();
    }
    for (I=1;I<=31;I++){
        for (T=1;T<=31;T++){
            fscanf(fname,"%d",&help);
            X1[T][I]=help;
        }
        fscanf(fname,"\n");
    }
    fclose(fname);

/* INITIALIZE THE VALUE TO FIND CORRELATION */

    fname1=fopen("D:/PANDE/ASCROCO1","wt+");
    if (fname1==NULL){
        printf("Cannot open input file ASCROCO1\n");
        exit ();
    }

    for(T=1;T<=31;T++){
        for(I=1;I<=31;I++){
            X2[T][I]=X1[T][I];
        }
    }
}
```

```

for(l=1;l<=31;l++){
    for(S=1;S<=31;S++){
        for(X=1;X<=31;X++){
            ASYNCOR1[X][S]=0;
            Q=R=0;

            for(T=1;T<=31;T++){
                if (X1[T][l]!=0)
                    Q=Q+X2[T][S];
                else
                    R=R+X2[T][S];
            } /* CLOSE T LOOP */
            ASYNCOR1[X][S]=Q-R;

            Q1=X2[1][S];
            for(B=1;B<=30;B++)
                X2[B][S]=X2[B+1][S];

            X2[31][S]=Q1;

            fprintf(fname1,"%d ",ASYNCOR1[X][S]);
        } /* CLOSE X LOOP */

        fprintf(fname1,"\n");
    } /* CLOSE S LOOP */

    fprintf(fname1,"\n","\n");
} /* CLOSE I LOOP */

fclose(fname1);
}

```

APPENDIX E - PROGRAM TO CALCULATE THE CORRELATOR OUTPUT FOR ANY NUMBER OF USERS

Program name "Mathgen1". This is a generalized program to find the correlator output given the total number of users and the intended receiver code.

```
/* PROGRAM TO FIND THE CORRELATION OF ANY NUMBER OF USERS */
```

```
/* In this program one has to set the following values */
```

```
/* K ( K defines the receiver code number ) */
```

```
/* USERS ( USERS defines the total number of users in the line ) */
```

```
/* RECTXD (RECTXD defines whether code for receiver is transmitted) */
```

```
/* U[1] to U[31] ( They define whether that user code is on line or not)*/
```

```
/* Value of RECTXD is got from U[K] */
```

```
/* Value of USERS is got from all the 1's from U[1] to U[31] */
```

```
#include <stdio.h>
```

```
#include <math.h>
```

```
#define K 6 /* receiver number */
```

```
#define USER 31
```

```
#define RECTXD 0 /* 1 DEFINES receiver code is transmitted */
```

```
/* 0 DEFINES user code is not transmitted */
```

```
main ()
```

```
{
```

```
FILE *fname;
```

```
FILE *fname1;
```

```
int INT[33],S[33][33],A[33],B[33],RX[33][33],X1[3][33],run;
```

```
int PRO[33],S1[33],FK1[33],RKB1[33],U[33];
```

```
register int L,N,J,I;
```

```
U[1]= 1;U[2]= 1; U[3]= 1; U[4]= 1; U[5]= 1; U[6]= 0; U[7]= 1;
```

```
U[8]= 1;U[9]= 1;U[10]= 1;U[11]= 1;U[12]= 1;U[13]= 1;
```

```
U[14]= 1;U[15]= 1;U[16]= 1; U[17]= 1;U[18]= 1;U[19]= 1;
```

```
U[20]= 1;U[21]= 1;U[22]= 1; U[23]= 1;U[24]= 1;U[25]= 1;
```

```
U[26]= 1;U[27]= 1;U[28]= 1; U[29]= 1;U[30]= 1;U[31]= 1;
```

```
fname=fopen("D:/PANDE/msequen","r");
```

```
for (L=1;L<=2;L++){
```

```
for (I=1;I<=31;I++){
```

```

        fscanf(fname,"%d",&run);
        X1[L][I]=run;
    }
    fscanf(fname,"\n");
}
/* Define whether user is in line or not */
for (L=1;L<=2;L++){
    for (I=1;I<=31;I++){
        if(L==1)
            B[I-1]=X1[L][I];
        else
            A[I-1]=X1[L][I];
    }
}
fclose(fname);

for(N=1;N<=31;N++){
    if(U[N]!=0){
        if(RECTXD==0){
            for(J=0;J<=30;J++){
                if(N!=K){
                    S[J][N]=fmod(A[fmod(N-1+J,31)]+B[N-1],2); /*ALL THE USERS POWER*/
                }
                else{
                    S[J][N]=0;
                } /* close N!=K loop */
            } /* close J loop */
        } /* if.. else for RECTXD */
        else{
            for(J=0;J<=30;J++){
                S[J][N]=fmod(A[fmod(N-1+J,31)]+B[N-1],2); /* ALL THE USERS POWER
*/
            } /* close RECTXD loop */
        }
        else{
            for ( J=0;J<=30;J++){
                S[J][N]=0;
            } /* close J loop for U[N] */
        } /* close U[N] loop */
    }
    printf("\n"); /*
} /* close N loop */

for(J=0;J<=30;J++){
    RK1[J]=fmod(A[fmod(K-1+J,31)]+B[K-1],2); /* RECEIVER CODE */
    RKB1[J]=fmod(A[fmod(K-1+J,31)]+B[K-1]+1,2); /* COMPLEMENT

```

OF rx */

```

        S1[J]=0;
/*  printf("%d ",S1[J]); */
/*  printf("%d ",RK1[J]); */
/*  printf("%d ",RKB1[J]); */
    }

    for(J=0;J<=30;J++){
        for(N=1;N<=31;N++){
            S1[J]=S1[J]+S[J][N];
        }
/*  printf("%d ",S1[J]); */
    }

    RX[USER][K]=0;
    for(J=0;J<=30;J++){
        INT[J]=RK1[J]-RKB1[J];
/*  printf("%d ",INT[J]); */
        PRO[J]=S1[J]*INT[J];
/*  printf("%d ",PRO[J]); */
        RX[USER][K]=RX[USER][K]+PRO[J];
    }

    fname1=fopen("D:/pande/rxdata","a");
    fprintf(fname1,"%d ",RX[USER][K]);
    printf("%d ",RX[USER][K]);
    fclose(fname1);

}

```


APPENDIX F - PROGRAM TO FIND THE ORDER OF A SEQUENCE

Program name "Iter2". This program does the polynomial division to find the order of a given sequence.

```
#include    <stdio.h>

main ()
{
    /* array of five(5) values */
    char readin[5];
    int a[5], a1[5], b[5], q[5] ;
    register int x, y, length, stepup, stepdown, count, subcount;
    register int borrowcnt, try, iteration , power;

    printf("-----\n");
    printf("Polynomial Division\n");
    printf("-----\n");
    printf("(C) A. Pande 1989  \n\n");

    /* Input the values in a serial order */
    printf("Please Input Dividend : ");

    /* Writes the buffered O/P from a stream to associated file */
    fflush(stdout);

    /* Reads character from stdin into readin. Stops reading when it */
    /* reads n-1 characters */
    fgets(readin, 6, stdin);

    /* The carriage return i.e. \n is taken as a value after the data */
    /* so we subtract 1 for that and a 1 for the value going from 0 */
    length = strlen(readin);

    printf("%d", length );
    printf("\n");

    /* (int)readin[count] gives the ASCII value so we delete ASCII 0 */

    for (count = length - 1 ; count >= 0; count --)
        a[length - count] = (int)readin[count] - '0';

    for ( stepup = 0 ; stepup <= 4 ; stepup ++ )
        b[stepup] = 0 ;
    b[1] = b[length] = 1 ;

    stepdown = length;
    while ( a[stepdown] == 0 )
```

```

        stepdown -- ;

printf("%d",stepdown);
printf("\n");

for ( iteration = length ; iteration >= stepdown ; iteration -- ) {

    if ( b[iteration] == 1 ) {
        power = iteration - stepdown ;
        q[power] = 1;

printf("%d",power);
printf("\n");

        for( x=0 ; x <= stepdown ; ++x ) {
            try = x + power ;
            a1[try] = a[x];
        }

        for( y=1; y <= power; ++y) {
            a1[y] = 0;
        }
        for ( subcount = 1 ; subcount <= iteration; subcount ++ ) {
            b[subcount] -= a1[subcount] ;

                if ( b[subcount] < 0 ) {
                    b[subcount] = 1 ;
                } else {
                    b[subcount]=b[subcount];
                }
        }
    } else {
        power = iteration - stepdown;
        q[power] = 0;
    }
}
/* Iteration steps end */

printf("Result = ");
for (power = length - stepdown ; power >=0; power -- ){
printf("%d", q[power]);
}
printf("Remainder=");
printf("%d",b[subcount]);
}
printf("\n");
}

```

**APPENDIX G - CALIBRATION CURVES FOR THE LASER DIODES
AND THE THERMISTOR AND THE DATA SHEET
FOR THE PHOTODIODE MODULE**

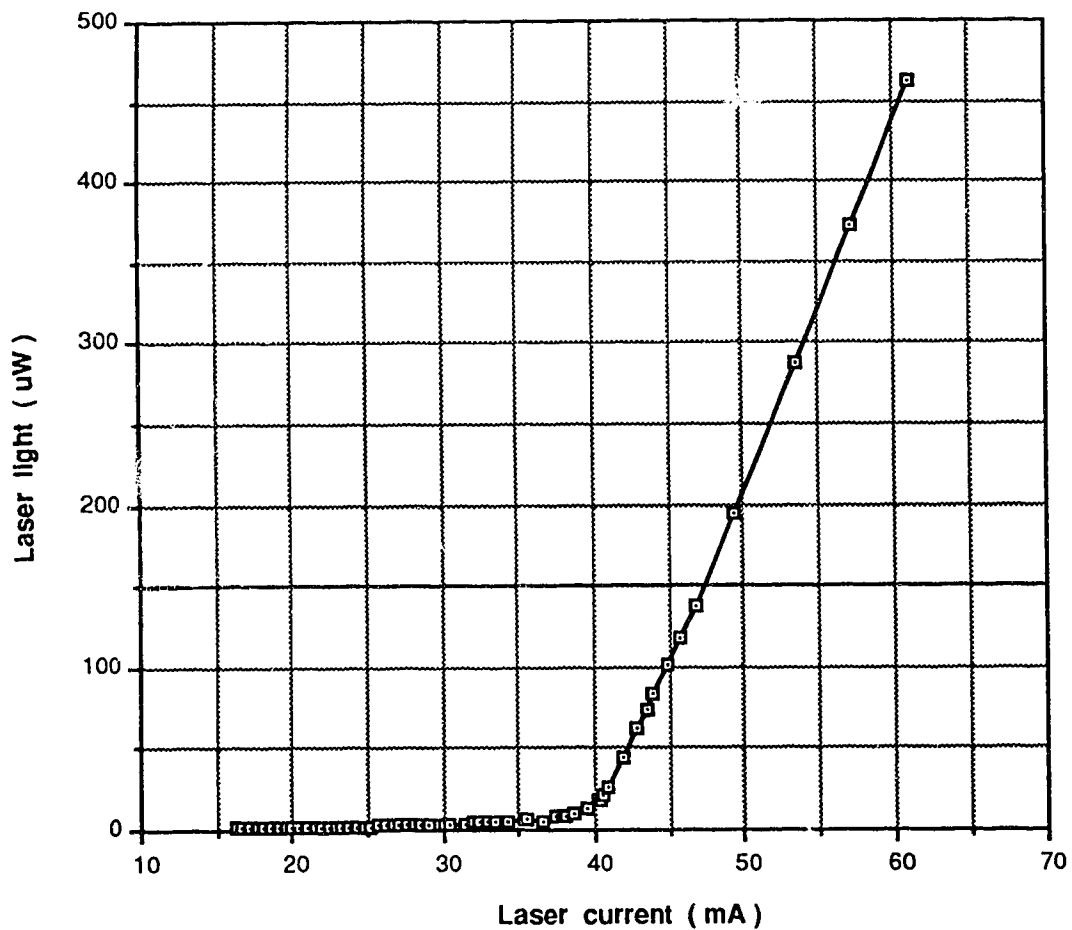


Fig. F.1 Laser output power characteristics, as a function of the bias current, for NORTHERN TELECOM PBH-4317-32 LD

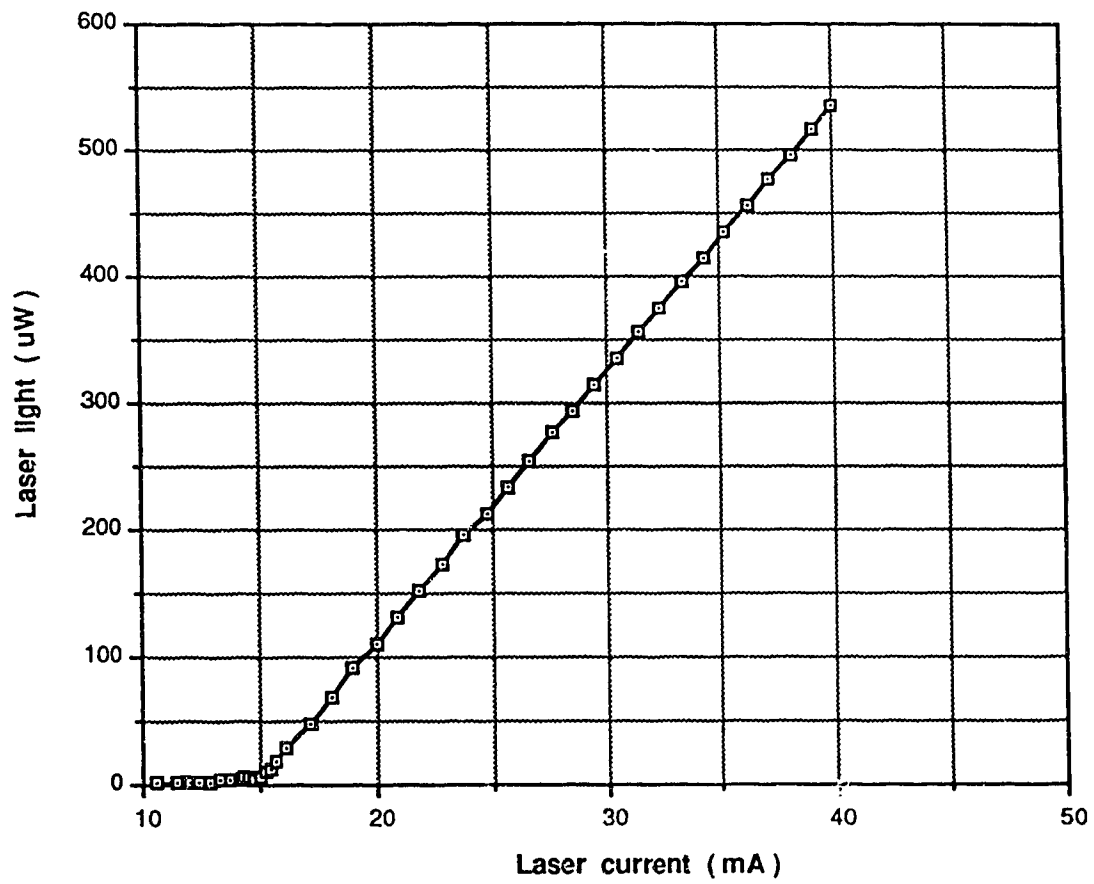


Fig. F.2 Laser output power characteristics, as a function of the bias current, for LASER DIODE INC. 1300-09632 LD

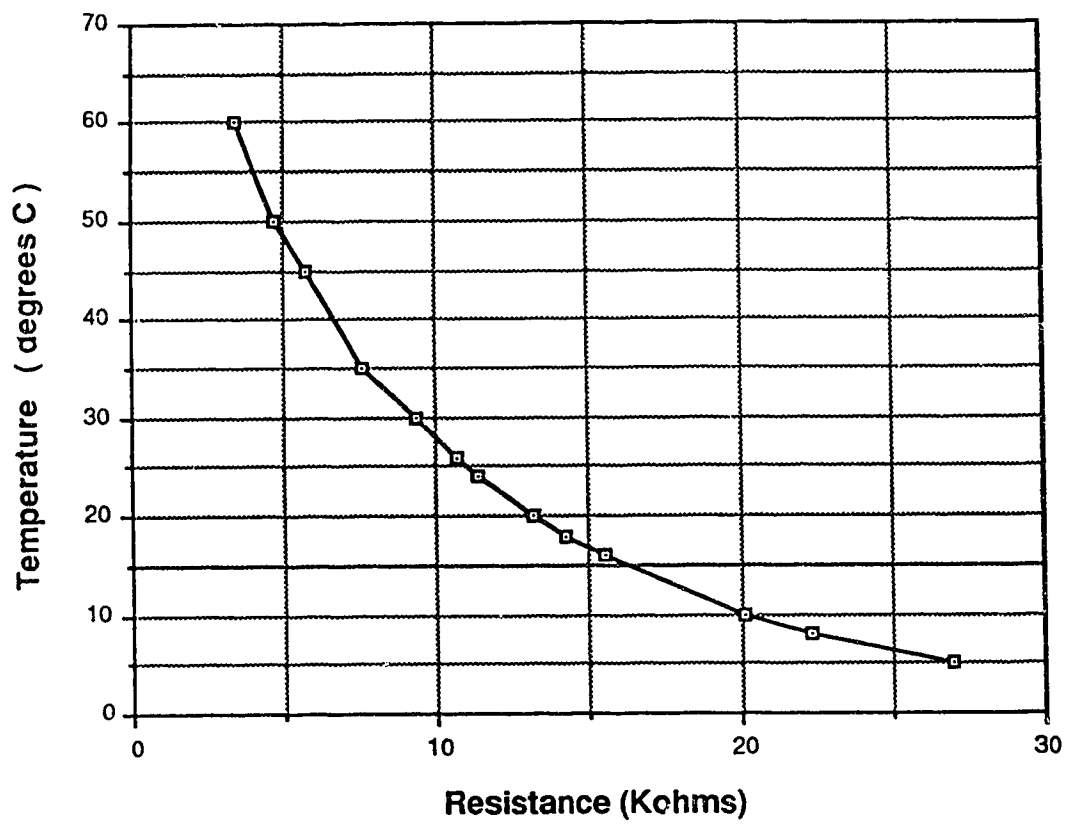


Fig. F.3 Temperature vs. resistance curves obtained for the thermistor

Table F.1 Data sheet for the RCA type C30986QC-02 photo-detector module

	C30986-030 C30986-030QC-YY			C30986-090 C30986-090QC-YY			C30986-250 C30986-250QC-YY			C30986-350 C30986-350QC-YY			Units
	Min.	Typ.	Max.	Min.	Typ.	Max.	Min.	Typ.	Max.	Min.	Typ.	Max.	
Responsivity:													
At 1.3 μm	1.8x10 ³	2.2x10 ³	—	4.0x10 ⁴	5.0x10 ⁴	—	5.5x10 ³	7.3x10 ³	—	3.3x10 ³	4.1x10 ³	—	V/W
At 1.55 μm	2.2x10 ³	2.6x10 ³	—	4.8x10 ⁴	6.0x10 ⁴	—	6.7x10 ³	8.4x10 ³	—	4.0x10 ³	5.0x10 ³	—	V/W
Noise Equivalent Power (NEP): 100 kHz $\triangleleft \triangleleft_0/2$													
At 1.3 μm	—	0.7	1.1	—	1.3	2.1	—	3.1	5.4	—	3.7	6.1	pW/Hz ^{1/2}
At 1.55 μm	—	0.6	0.9	—	1.1	1.8	—	2.6	4.5	—	3.0	5.0	pW/Hz ^{1/2}
Output Spectral Noise Voltage Density:													
$f = 100 \text{ kHz} - f_0$													
$\Delta f = 1.0 \text{ Hz}$	—	150	200	—	65	85	—	22	30	—	15	20	nV/Hz ^{1/2}
Output Impedance	—	20	40	—	20	40	—	20	40	—	20	40	Ω
System Bandwidth, f_0 (3 dB point)	24	30	—	70	90	—	200	250	—	280	350	—	MHz
Rise Time, t_r :													
$\lambda = 1.3 \mu\text{m} \text{ \& } 1.55 \mu\text{m}$ 10% to 90% points ...	—	12	15	—	4	5	—	1.5	2	—	1.0	1.3	ns
Fall Time:													
$\lambda = 1.3 \mu\text{m} \text{ \& } 1.55 \mu\text{m}$ 90% to 10% points ...	—	12	15	—	4	5	—	1.5	2	—	1.0	1.3	ns
Dynamic Range	21	24	—	21	24	—	21	24	—	21	24	—	dB
Output Offset Voltage	-0.7	-1.5	-3.0	-0.7	-1.5	-3.0	-0.7	-1.5	-3.0	-0.7	-1.5	-3.0	V
Supply Current:													
+5.2 V	—	25	35	—	25	35	—	25	35	—	25	35	mA
-5.2 V	—	10	15	—	10	15	—	10	15	—	10	15	mA
Projected Sensitivity @ 10 ⁻⁹ B.E.R.													
[NRZ, avg power, Data Rate $\approx 2x$ Bandwidth at 1.3 μm	-45	-47	—	-39	-41	—	-33	-35	—	-31	-33	—	dBm